Anders Sand

Microscopic Simulation of Pigment Coating Consolidation

Microscopic Simulation of Pigment Coating Consolidation

Anders Sand

2010

ISBN 978-952-12-2412-6

UNIPRINT
Åbo 2010

Mats Anders Sand

Born 1979 in Vaasa

Mr. Sand obtained his M. Sc. degree in Chemical Engineering at Åbo Akademi University in 2003. He started his D. Sc. work at the Laboratory of Paper Coating and Converting in 2004.

MICROSCOPIC SIMULATION OF PIGMENT COATING CONSOLIDATION

Anders Sand

Laboratory of Paper Coating and Converting
Centre for Functional Materials

Department of Chemical Engineering
Åbo Akademi University

Åbo 2010

To family and friends

"Piled Higher and Deeper" by Jorge Cham (2009), http://www.phdcomics.com.
Reproduced with permission.

PREFACE

This thesis is a summary of the following publications, referred to in the text with their corresponding Roman numerals:

I. Sand, A., Nopola, T., Hjelt, T. and Toivakka, M. (2009): A Particle Motion Model for the Study of Consolidation Phenomena, Computers & Chemical Engineering 33: 1227-1239.

II. Sand, A., Toivakka, M. and Hjelt, T. (2008): Investigation of Filter Cake Stability using Numerical Simulation Technique, TAPPI Journal 7(2):4-10.

III. Sand, A., Toivakka, M. and Hjelt, T. (2008): Influence of Drying Strategy on Coating Layer Structure Formation, Nordic Pulp and Paper Research Journal 23(1):46-51.

IV. Sand, A., Toivakka, M. and Hjelt, T. (2008): Small Particle Mobility in Consolidating Coating Layers, Nordic Pulp and Paper Research Journal 23(1):52-56.

V. Sand, A., Toivakka, M. and Hjelt, T. (2009), Influence of Colloidal Interactions on Pigment Coating Layer Structure Formation, Journal of Colloid and Interface Science 332: 394-401.

VI. Sand, A., Kniivilä, J., Toivakka, M. and Hjelt, T., Structure Formation Mechanisms in Consolidating Pigment Coatings – Simulation and Visualisation, Chemical Engineering and Processing, submitted 2010.

The work was carried out during the period 2004-2010 at the Laboratory of Paper Coating and Converting, and Centre for Functional Materials under the supervision of Professor Martti Toivakka and Dr. Tuomo Hjelt at VTT, Espoo (previously KCL). The work was financed by a KCL-coordinated 3-year consortium project and the International Doctoral Programme for Pulp and Paper Science and Technology in Finland (PaPSaT). The National Technology Agency of Finland (Tekes) and the Academy of Finland are also acknowledged for financial support. The foundation of Åbo Akademi, through Stiftelsen för Åbo Akademis Forskningsinstitut, is acknowledged for providing travel grants.

SUPPORTING PUBLICATIONS

I. Sand, A., Toivakka, M. and Hjelt, T. (2006): Investigation of Filter Cake Stability using Numerical Simulation Technique, Proceedings of TAPPI Advanced Coating Fundamentals Symposium, February 8-10, Turku, Finland, 279-289.

II. Sand, A., Toivakka, M. and Hjelt, T. (2007): The Application of Modified Stokesian Dynamics to 3D Particle Motion Simulations of Pigment Coating Colours, Proceedings of the International Conference on Computational Methods, April 4-6, Hiroshima, Japan, 97 (full manuscript on conference CD).

III. Sand, A., Toivakka, M. and Hjelt, T. (2008): Coating Layer Consolidation and the Influence of Drying Strategy – A Numerical Study, Proceedings of Progress in Paper Physics Seminar, June 2-5, Espoo, Finland, 65-67.

IV. Sand, A., Toivakka, M. and Hjelt, T. (2008): Small Particle Migration Mechanisms in Consolidating Pigment Coating Layers, Proceedings of TAPPI Advanced Coating Fundamentals Symposium, June 11-13, Montreal, Canada, 289-298.

V. Sand, A., Toivakka, M. and Hjelt, T. (2009): Colloidal Interactions and Particle Clustering in Consolidating Pigment Coating Layers, Proceedings of Papermaking Research Symposium, June 1-4, Kuopio, Finland, 39 (full manuscript on conference CD).

VI. Sand, A., Kniivilä, J., Toivakka, M. and Hjelt, T. (2009): Microstructure Development in Consolidating Pigment Coatings Studied by Numerical Simulation, Proceedings of European Coating Symposium, September 7-9, Karlsruhe, Germany, 69-72.

TABLE OF CONTENTS

ABSTRACT

The control of coating layer properties is becoming increasingly important as a result of an emerging demand for novel coated paper-based products and an increasing popularity of new coating application methods. The governing mechanisms of microstructure formation dynamics during consolidation and drying are nevertheless, still poorly understood. Some of the difficulties encountered by experimental methods can be overcome by the utilisation of numerical modelling and simulation-based studies of the consolidation process.

The objective of this study was to improve the fundamental understanding of pigment coating consolidation and structure formation mechanisms taking place on the microscopic level. Furthermore, it is aimed to relate the impact of process and suspension properties to the microstructure of the coating layer.

A mathematical model based on a modified Stokesian dynamics particle simulation technique was developed and applied in several studies of consolidation-related phenomena. The model includes particle-particle and particle-boundary hydrodynamics, colloidal interactions, Born repulsion, and a steric repulsion model. The Brownian motion and a free surface model were incorporated to enable the specific investigation of consolidation and drying.

Filter cake stability was simulated in various particle systems, and subjected to a range of base substrate absorption rates and system temperatures. The stability of the filter cake was primarily affected by the absorption rate and size of particles. Temperature was also shown to have an influence. The consolidation of polydisperse systems, with varying wet coating thicknesses, was studied using imposed pilot trial and model-based drying conditions. The results show that drying methods have a clear influence on the microstructure development, on small particle distributions in the coating layer and also on the mobility of particles during consolidation. It is concluded that colloidal properties can significantly impact coating layer shrinkage as well as the internal solids concentration profile. Visualisations of particle system development in time and comparison of systems at different conditions are useful in illustrating coating layer structure formation mechanisms.

The results aid in understanding the underlying mechanisms of pigment coating layer consolidation. Guidance is given regarding the relationship between coating process conditions and internal coating slurry properties and their effects on the microstructure of the coating.

KEYWORDS

Pigment coating, consolidation, microstructure, hydrodynamics, colloidal interactions, particle motion, particle mobility, drying, modelling, simulation, Stokesian dynamics.

ABBREVIATIONS

ABS	Absorption
ASD	Accelerated Stokesian Dynamics
CD	Cross Direction
CC	Covercarb
CSC	Center for Scientific Computing (a.k.a. Finnish IT Center for Science)
DEM	Discrete Element Method
DLVO	Derjaguin, Landau, Verwey, Overbeek
DPD	Dissipative Particle Dynamics
EVA	Evaporation
FCC	First Critical Concentration
FEM	Finite Element Method
GCC	Ground Calcium Carbonate
HC	Hydrocarb
HLL	High-Low-Low
HND	Hiorns and Nesbitt's Deposition
ICC	Inter-Critical Concentration
KCL	Keskuslaboratorio-Centrallaboratorium
LB	Lattice-Boltzmann
LID	Lyons and Iyer's Deposition
LLH	Low-Low-High
LWC	Light Weight Coated
MCD	Monte-Carlo Deposition
MD	Machine Direction
MWC	Medium Weight Coated
OpenGL	Open Graphics Library
PiMP	Particle Mobility Program
RDF	Radial Distribution Function
SCC	Second Critical Concentration
SD	Stokesian Dynamics
SDD	Steepest Descent Deposition
SEM	Scanning Electron Microscopy
VTT	Technical Research Centre of Finland

NOMENCLATURE

Roman symbols

A_H	Hamaker constant
a	Particle radius
a_{char}	Characteristic particle size
c	Ion concentration
D	Diffusivity (Brownian motion) or particle diameter
d	Particle diameter
$f(h)$	Particle penetration length (Free surface model)
H	Characteristic length scale
h	Particle penetration height (Free surface model)
K	Boltzmann constant
K_1, K_2	Steric force model parameters
K_{Coll}	Hydrodynamic/ colloidal force ratio
K_{Brown}	Scaling constant in Brownian motion model
k_f	Filter cake permeability
N_A	Avogadro's constant
P_{cap}	Capillary pressure
P_{ext}	External pressure
Pe	Peclet number
$p(d)$	Probability of particle diameter in particle size distribution
R	Universal gas constant
Re_p	Particle Reynolds number
T	Temperature
t	Time
u	Velocity
u_{char}	Characteristic system velocity
u_{surf}	Velocity of surface approaching particle
V / A	Dewatered liquid volume per area
z	Valence of ions
$\overline{a^0}$	Randomly determined unit vector (Brownian motion model)
$\mathbf{m}$	Particle mass vector
$\overline{F}$	Force vector
$\mathbf{F}^B$	Force giving rise to the Brownian motion

$\mathbf{F}^H$ Hydrodynamic force and torque matrix
F^H_{p-fs} Hydrodynamic force between particle and free surface
F^H_{p-sb} Hydrodynamic force between particle and solid boundary
F_{ST} Surface tension force
$\mathbf{F}^P$ External or internal deterministic particle forces and torques
F^P_{coll} Particle force by colloidal interactions
F^P_{el} Electrostatic repulsive force (DLVO model)
F^P_{vdw} Van der Waals attractive force (DLVO model)
F^P_{st} Steric particle force
F^{st}_{el} Steric repulsion model elastic force component
F^{st}_{osm} Steric repulsion model osmotic force component
$\mathbf{M}^{\infty}$ Mobility matrix
$\mathbf{R}$ Resistance matrix
$\mathbf{U}$ Velocity vector
$\bar{x}$ Mean Brownian displacement vector

Greek symbols

β Boundary/ particle centre separation or particle pair size difference
Δ Surface separation distance
Δ_{surf} Increase in liquid surface length due to boundary penetration
δ_{ster} Thickness of adsorbed polymer layer
μ Viscosity of the liquid phase
μ_d Mean particle diameter
ρ_l Liquid phase density
σ Surface tension coefficient
ε_0 Permittivity of vacuum
ε_r Continuous phase dielectric constant (pure water at NTP)
ϕ Coating colour solids volume fraction
ϕ_f Filter cake solids volume fraction
$1/\kappa$ Double layer thickness
λ London characteristic wavelength
σ_d Standard deviation in particle diameter
ψ Particle surface potential
ζ Zeta potential

$\boldsymbol{\Omega}$	Rotational velocity of particle relative to surrounding medium

1. INTRODUCTION

The paper industry plays an important role in Finnish society. It provides, either directly or indirectly, employment for 200,000 people within Finland, and 100,000 in Finnish companies abroad. Its share of Finnish exports is about one-fifth (2004). The annual global consumption of paper in 2007 reached 400 million tonnes, or 59 kg per capita. The Finnish forest industry is currently the sixth-largest producer of paper and board, with exports reaching 15 % of the world market.

Currently, industry finds itself in a time of transition, facing ever increasing global competition and decreasing profit margins. Industry is attempting to offset the competition by improving product quality, increasing production process efficiency and by developing broader and more technologically advanced applications for paper products. In more recent times, attention has been directed towards novel applications in various fields such as intelligent packages including sensoring techniques, printed electronics and even biomedical applications. The utilisation of paper in such products puts greater demand both on the paper itself and on its surface treatment. Throughout the production chain, there is an increased need for tailoring the properties of the paper in order to obtain optimum performance. There is clearly a need for a deeper understanding of fundamental mechanisms taking place during the papermaking process and how these influence the properties of the end product.

The production speed and inherent properties of the pigment coating process make experimental studies extremely challenging and in many cases practically impossible. This is especially so when focusing on the dynamic behaviour of the coating suspension. The paper web speed in a modern coating process can be up to 2,000 m/min (≈ 30 m/s), the size scale of the pigment

coating layer is only a few µm. Furthermore the paper is subjected to extreme pressure pulses and temperatures during the very short time scale, typically less than one second, between coating application and immobilisation. Most experimental studies have therefore focused either on the properties of the wet pigment coating slurry, macroscopic-type runnability aspects of the process, or the end-use properties of the coated paper. Very few studies have been able to capture the dynamics of the pigment coating process at the microscopic scale, since such research is both complex and expensive. Microscopic mechanisms suggested to take place in the pigment slurry during consolidation, have mostly been based on theories which remain challenging to confirm empirically.

This work utilises a Stokesian dynamics-based modelling and simulation approach in studying pigment coating of paper. The focus is on simulating coating consolidation mechanisms at the particle level. This is done by linking deterministic particle interactions and the physical behaviour of particle systems to microstructural development of the coating layer. The objective was to identify possible microscopic structures that arise in pigment coating layers during consolidation. In this way, the fundamental understanding of pigment coating consolidation mechanisms taking place at the microscopic level can be improved. Furthermore, the impact of wet state structure, process and suspension properties, as well as the drying strategy on the consolidation and structure of the coating layer can be predicted.

2. BACKGROUND

2.1 Pigment Coating of Paper

Pigment coating is the surface treatment of paper by application of an aqueous suspension of pigments, binder and other additives to the surface of a base paper substrate. The intention behind surface treatment is to produce a paper with desirable properties given its end use. Depending on the application, the coating on the paper might influence its optical, mechanical, physical, barrier or printing properties (Santos, Velho 2004; Parpaillon et al. 1985; Lepoutre 1989; Prall et al. 2000).

Coating can be applied to the paper by a number of different methods, the most common being jet or roll application combined with blade, roll, rod or air-jet metering. The interest in novel methods of contact-free application, curtain or spray coating, has also increased (Lehtinen 2000; Mendez, Morita 2001; Hämäläinen 2003). Depending on the application and metering method, coating suspension properties and the coating process parameters, coating layers of different thickness can be obtained. Typical coat weights and coating layer thicknesses for different coated paper grades are shown in Table 1 (Linnonmaa, Trefz 2000). Although not mentioned by Linnonmaa and Trefz, the relationship between coat weight and coating layer thickness is not necessarily equivalent. The thickness may vary depending on the particle size distribution, additives and porosity.

Application and metering are followed by a drying system, which may include Infra Red (IR), air flotation or cylinder dryers. The drying strategy, i.e. the intensity, duration and number of drying steps, is known to significantly influence the microstructure and other properties of the coating layer and coated

paper (Rajala et al. 2002; Rajala 2004). A pilot coater system, including pre-heating of the paper web, applicators, IR and air foil dryers, is shown in Figure 1.

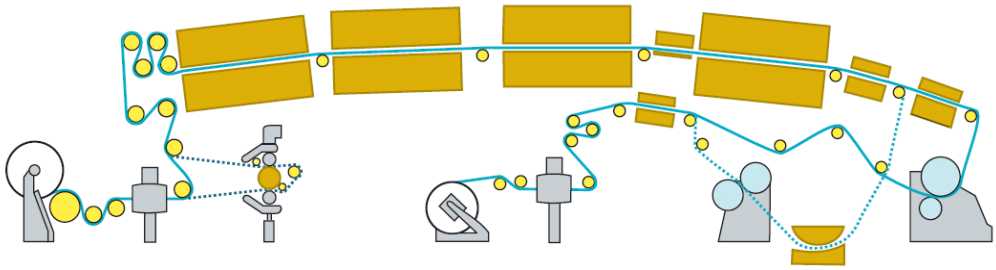

Figure 1. Pilot coater at VTT (formerly KCL) in Espoo, Finland. Reproduced with permission.

After drying, the coating layer is typically already immobilised. However, to further improve surface smoothness and other such properties, the coated paper can be run through a single- or multi-nip calender. The calender can be either online or offline and composed of hard and soft nips in a number of different configurations (Kilmartin 1990).

Table 1. Typical coat weights (per side) and coating layer thicknesses in manufactured coated paper

Paper grade	**Coat weight** [g/m^2] **or** **Coating layer thickness** [µm]
Lightweight coated (LWC)	5 - 10
Single-coated, medium weight (MWC)	8 – 16
Double-coated	14 - 26
Triple-coated	24 - 40

2.2 The Pigment Coating Suspension

A coating suspension is a complex system of minerals, organic and inorganic additives. The properties of the coating suspension and dry coating layer are determined by the components of the suspension, their interactions, processing

parameters and macroscopic properties such as the dry solids content. This chapter discusses the components and properties of the coating suspension, as well as the interactions between particles within the coating.

2.2.1 Components of the coating suspension

Coating suspensions are typically composed of pigment, binder, and additives in an aqueous medium. The most common pigments used are ground or precipitated calcium carbonate, kaolin, talcum, titanium dioxide, gypsum or combinations thereof. Pigment particles can, depending on the processing method and inherent mineral properties, be of a number of different shapes. These shapes can range from roundish to platy, rodlike, or cubic. Pigments can also be of different sizes and comprise broad or narrow size distributions. These may in turn also influence the maximum solids content in the dispersion. The coating suspension is typically prepared with as high solids concentration as possible, though pumping and coater runnability problems still need to be taken into consideration. By example, for ground calcium carbonate (GCC), which can be fairly broad in its size distribution, solids contents of between 65 and 78 wt-% are common. Depending on the type of mineral, the density is normally 2.3 to 4.0 kg/dm^3 and with most particles being of size 0.1 to 5 µm. Calcite, GCC, which is one of the most common pigments, are low aspect ratio roundish, cubic or prismatic-shaped with most particles being 0.5 to 2 µm in size and with a density of 2.7 kg/dm^3. A comprehensive summary of the physical properties of coating pigments is presented, e.g., by Lehtinen (2000) and Eiroma and Huuskonen (1983).

Binder is used for a number of different purposes, the most important of which is the binding of pigment particles to each other and to the base paper. Binder also influences the pore structure of the coating, as well as coating

suspension properties such as water retention and viscosity. The most common binders include latexes and starch. Latex particles can be considered relatively spherical in shape and are typically 100-200 nm in diameter. The density of latex binder is close to that of water, i.e. 1.0 kg/dm^3.

In addition to pigments and binder, a number of different additives can be used to improve the end properties of the coating layer, the runnability of the pigment system on the coater, or the properties of the coating suspension. Such additives include thickeners, dispersants, water retention agents, optical brighteners, lubricants and rheology modifiers (Heikkilä et al. 2000).

2.2.2 Coating particle interactions

Forces on particles in a coating suspension and the interactions between them originate from a multitude of physical and chemical phenomena. Such phenomena might be velocity or position dependent, but also vary with solids concentration or pH. In a suspension of moving particles, equilibrium between the repulsive and attractive interparticle, boundary-particle, and macroscopic forces and torques determines the individual as well as collective behaviour of the particles. Macroscopically measurable properties, such as viscosity, also relate to these interactions. For example, particle aggregation may result from the balance between repulsive and attractive colloidal forces. The dominant particle interactions are discussed below. They are selected in order to capture the essential physics of the system, including the movement and distribution of particles in a coating suspension.

Hydrodynamic interactions

Hydrodynamic forces on particles in suspension arise as a result of the macroscopic flow of the liquid, movement of nearby particles and the movement of particles relative to a solid boundary or to the liquid free surface. Due to the viscosity of the liquid phase, particles approaching each other experience a pressure build-up resulting in a flow of liquid away from the gap between the particles. Similarly, if particles are moving apart, liquid is required to flow into the developing gap. These hydrodynamic interactions can therefore generate either interparticle attraction or repulsion, depending on the movement of particles relative to each other. Due to friction between particle surfaces and the liquid, the relative motions of particles can also give rise to torques. The relative motion can be divided into 4 main types; squeezing, shearing, pumping and twisting (Nopola 2004). The hydrodynamic interactions are further described in section 3.

Colloidal interactions

A colloidal suspension is often defined as a liquid medium containing particles of 1 nm to 1-2 µm in size. Due to the size scale of the particles in the coating suspension, the surface properties of the particles and the properties of the liquid medium, the wet coating suspension can be considered a complex colloidal system (Grön 1998). The balance between the repulsive and attractive components of the colloidal forces will determine the behaviour of the suspension.

It is well known that uncharged colloidal particles in a suspending liquid with a different dielectric constant compared to the particles will aggregate. Particle aggregation is essentially due to van der Waals interaction forces. In the case of electrically charged particles, the interaction between them will be composed of an attractive van der Waals component and electrostatic repulsion.

The dominating theory for describing such systems is referred to as DLVO (from Derjaguin, Landau, Verwey, Overbeek), which simply combines the two contributing elements to net force or interaction energy between the particles. Due to differences in distance dependence between the repulsive and attractive components, a primary and secondary interaction energy minimum can be obtained. The minima are separated by energy barriers, which may vary in magnitude. This results in relatively complex behaviour of the particle-liquid system (Hiemenz 1986; Shaw 2003; Grön 1998). Some examples are given in Figure 2, which plots the interparticle potential energy versus particle surface separation.

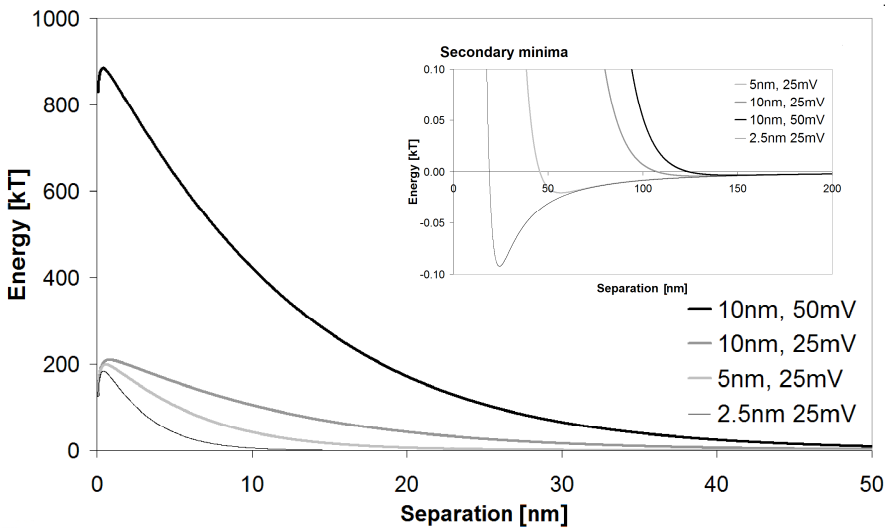

Figure 2. DLVO potential energy curve for a model suspension at a few different double layer thickness and particle surface charge settings (the radii of the interacting particles are 500 nm).

A third repulsion force, Born repulsion, comes into play when particles are in close contact. This strong repulsive force originates from overlap of electron clouds. Although Born repulsion is not considered an colloidal force, it causes a primary energy minimum when integrated into the DLVO interaction curve. If only taking into account the van der Waals attraction and electrostatic

repulsion; infinite attraction would result at a zero surface separation distance (Lyklema 2005a).

Steric stabilisation

Polymer can be added to the coating suspension as a stabiliser, since polymer adsorbed to the surfaces of pigment particles give rise to a steric barrier that counteracts particle agglomeration. There are two basic processes which may take place; interpenetration (overlapping of the polymer layers) and mixing (osmotic pressure) or compression of the polymer layers. The mechanisms depend on the segment density distribution as well as the dynamics of the adsorbed layers (Grön 1998). In general, a steep segment density distribution and high density of the adsorbed polymer layer can be expected to result in compression, while interpenetration and mixing is likely to occur in dilute layers. At high degrees of interpenetration, polymers adsorbed to one particle can reach the surface of another particle. Compression may also occur in dilute adsorbed layers. Figure 3 illustrates the steric repulsion force as function of interparticle separation, utilising both osmotic and elastic force components (Vincent et al. 1980, 1986; Einarson, Berg 1993; Toivakka et al. 1997).

The thermodynamics of two polymer layers mixing and overlapping is comparable to the mixing of polymer solutions. The increasing polymer concentration results in a loss of mixing entropy, which causes repulsion between the layers. The effect is also opposed, however, by favourable polymer-polymer contact interaction energies, as stated in the Flory-Higgins theory (Napper 1983).

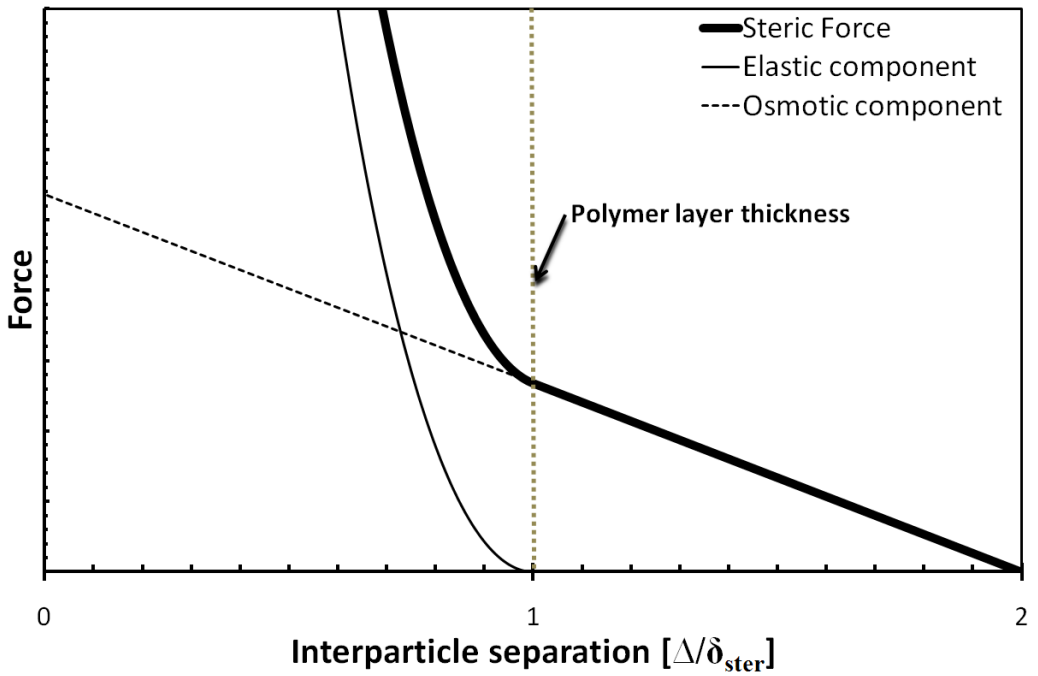

Figure 3. Steric repulsion force, as described by a combined osmotic and elastic repulsion component. The interparticle separation is normalised with the polymer layer thickness.

Bridging flocculation

Bridging flocculation results from the mutual attraction between coating particles with adsorbed polymer provided the same polymer chain or system of polymer chains attaches to more than one particle at the same time. It is considered that an optimum dosage of polymer should be present in the coating suspension for bridging flocculation to be effective. This effect is closely related to the saturation level and surface coverage of polymer adsorbed on pigments. At low coverage, adsorbed polymers lie relatively flat on the surfaces of particles, which reduces the probability of adsorption onto other particles. If particle surfaces are saturated with polymer, there is no further possibility for polymer tails to find free sites for adsorption onto adjacent pigment particles. It is estimated that around 50% surface coverage results in optimally high bridging flocculation (Napper 1983; Grön 1998; Shaw 2003).

Depletion flocculation

The addition of nonadsorbing polymer to a particle suspension is, under favourable circumstances, known to induce particle flocculation in the suspension. This is provided a critical volume fraction of polymer is exceeded. The critical volume depends on the molecular weight of the polymer and its volume fraction in the suspension. The mechanism is known as depletion flocculation and has been extensively studied since its discovery (Tadros 1987).

There are several theories describing the mechanism of depletion flocculation. It is believed to take place when two suspension particles move closer to each other than the diameter of the nonadsorbing polymer coil. The polymer is then excluded from the region between the particles. This results in an attractive force, related to the lower osmotic pressure in the region between the particles (Tadros 1987). Other approaches assume depletion of chain polymers near nonadsorbing particles, which produce osmotic attraction between the particles when two depletion layers overlap (Napper 1983).

Brownian motion

The Brownian motion is a perpetual irregular motion of small particles in a fluid, due to fluctuations in the mean force exerted on them by the molecules of the suspension liquid. A Brownian particle is believed to experience as many as 10^{21} collisions per second with molecules of the fluid. The influence of all these collisions will give rise to a random movement of the particle, as illustrated in Figure 4. The phenomenon owes its name to the botanist Robert Brown (1773-1858), who observed the motion to take place for pollen grains in water (Van de Ven 1989). Brownian motion is believed to be of importance mainly for small coating particles and additives, e.g. latex (100-300nm) and thickeners (5-10nm).

Brownian motion is also linked with particle sedimentation under the influence of gravity. Essentially, smaller particles sediment more slowly than

larger ones. Small particles might in fact not sediment at all if the system temperature is sufficiently high. In this context it is important to note that due to the path the paper web takes in industrial coating processes, the direction of the gravity component is not straight-forward. Moreover, due to the very short time scale of the process, the influence of gravity and sedimentation on the microstructure can be considered insignificant.

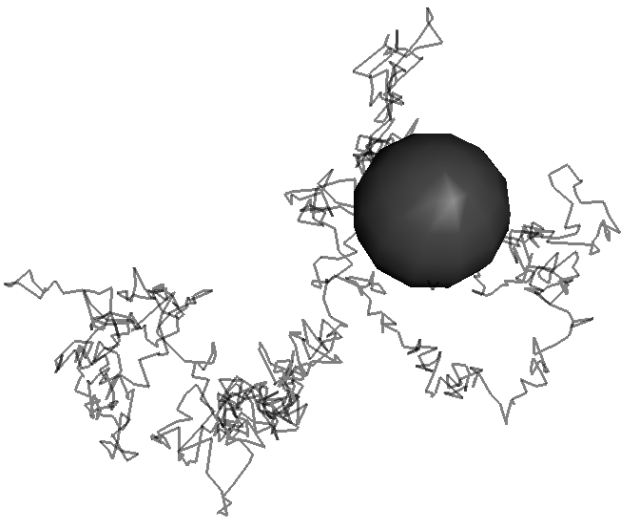

Figure 4. Brownian motion trajectory of a single particle.

2.3 Coating Layer Consolidation

The consolidation of a coating layer is defined as the gradual transition of the wet slurry applied onto the base substrate to a dry and immobilised structure. This results from the absorption of the liquid to the base substrate as well as evaporation from the top of the coating layer. The mechanisms of base paper absorption and evaporation can be considered as fundamentally different. The prerequisite for absorption is a flow of liquid from the coating layer into the

base substrate. Evaporation, on the other hand, can simply be comprehended as the expulsion of liquid from the surface of the wet coating. This expelling of liquid does not necessarily entail a flow of liquid phase to the surface of the coating.

The drying of pigment coating has been divided by Watanabe and Lepoutre (1982) into three phases, which are separated by a first and second critical concentration (FCC and SCC). The first critical concentration is reached as the loss of the liquid phase causes solid particles of the coating suspension to start to penetrate the liquid surface and initiate the formation of liquid menisci. This results in a sharp decrease in gloss. The second critical concentration defines the point when air starts to penetrate into the voids in the rigid particle network, giving rise to a sharp increase in reflectance. The first critical concentration is in industry often referred to as the immobilisation solids concentration (Salminen, Toivakka 2000; Lepoutre 1989). The applicability of this work ranges roughly from the start of consolidation until the point when particles begin to penetrate the liquid surface, i.e. some time between FCC and SCC. A third point, known as the inter-critical concentration (ICC), has also been suggested (Laudone et al. 2006). The inter-critical concentration is determined as the point when the porosity decrease is half-way between the FCC and SCC. This point is not as distinguishable as the FCC and SCC, but is argued to be relevant due to the importance for coating layer shrinkage taking place between these two points. The initiation of each of these phases is the starting point for different redistribution processes of the particles and liquid. These processes may influence the cross-structural solids concentrations and particle distributions (II; Sand et al. 2008a).

2.3.1 Filter cake formation

The accumulation of pigment particles on the base substrate has been the subject of several investigations over the years (Eklund and Salminen 1986; Letzelter and Eklund 1993a; Lohmander et al. 2001; Engström 1986; Salminen et al. 1995). The structure of the filter cake will have influence on the final structure of the dry immobilised layer and therefore determine physical and functional properties of the coated paper. For instance, the absorptive properties and binder distribution in the coating layer will influence printability and the mechanical properties of the layer. Additionally, filter cake formation has influence on the runnability of the coater. Filter cake formation is a result of pressure-induced liquid penetration or capillary absorption of the liquid phase into the base substrate.

Assuming at least some degree of coating holdout, a locally increased concentration of dispersed solids from the bulk coating suspension will form at the coating/ base substrate interface, Figure 5. The rate of solids accumulation will decrease as the flow of liquid becomes increasingly impeded by the high-concentration solids region. At some point, equilibrium can be expected to arise between particles accumulating and particles escaping from the filter cake due to their thermal motion.

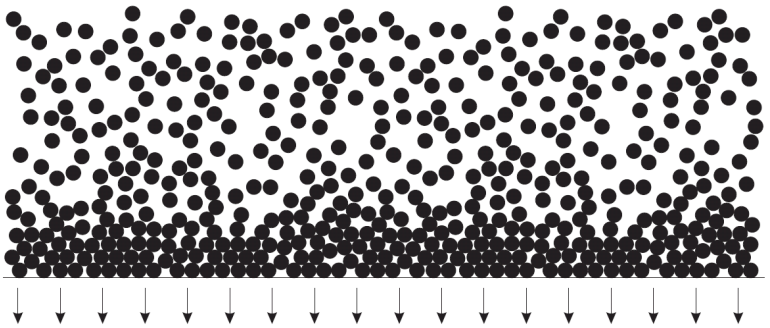

Figure 5. Filter cake formation as result of base substrate absorption (Toivakka 1997).

However, the mechanism by which filter cakes form is complex and has been a cause of controversy within the research community. Two dominating theories have been proposed for explaining the mechanism of filter cake formation. Immobilisation through filter cake formation assumes there is a sharp solids concentration difference between the filter cake and the bulk coating suspension. Immobilisation through thickening, however, suggests the existence of a concentration gradient throughout the filter cake structure. The mechanisms have been debated in several papers (e.g. Lohmander et al. 2001; Engström 1986; Salminen et al. 1995). An illustration of the two mechanisms is shown in Figure 6.

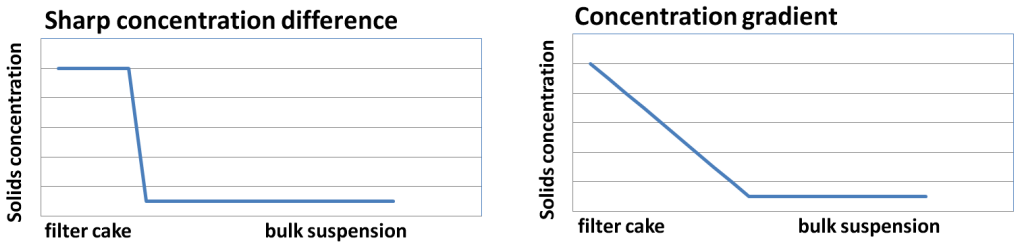

Figure 6. Comparison between the two filter cake formation mechanisms proposed in the literature.

Commonly, Darcy's law-type (Darcy 1856) absorption profiles are used as an estimate of macroscopic liquid absorption given the simultaneous formation of a filter cake. An equation by Usher et al. (2001)

$$\frac{V}{A} = \sqrt{\left(\frac{k_f}{\mu}\right)\frac{\phi_f - \phi}{\phi} 2t \sqrt{P_{cap} + P_{ext}}}, \quad (1)$$

states that the dewatered amount, (V/A), depends on the permeability of the filter cake, k_f, the viscosity of the liquid phase of the coating, μ, the filter cake and coating colour solids volume fractions, ϕ_f and ϕ, the capillary and

external pressures, P_{cap} and P_{ext} and time, t. Both theoretical and experimental results comparable to the equation can be found in the literature (e.g. Letzelter, Eklund 1993a,b; Heikkilä 1993).

2.3.2 Skinning

A region of increased concentration of solids at the coating/ air interface is formed as a result of the evaporation of liquid from the coating layer. The coating layer shrinks as liquid is expelled from the air/ coating interface. If the evaporation rate is faster than the ability of solids in the coating to rearrange and even out any solids concentration gradient that may arise, a denser layer of solids will accumulate at the surface of the coating. This process of solids concentration increase due to drying is commonly termed skinning (Salminen, Toivakka 2000). A 2D illustration of skinning is given in Figure 7. The effect is also believed to be intimately linked with binder migration (Luo et al. 2008), which will be described in more detail in section 2.3.3.

The mechanism of skinning has been studied numerically. The particle volume fraction in the skin depends on Peclet number. Furthermore, the formation of the skin at the top of a suspension film differs from conventional sedimentation, due to the domination of convection phenomena rather than diffusion (Routh, Zimmerman 2004). Particle deformation has also been found to be a factor in the formation of high solids concentration regions in particle systems. Such mechanisms have frequently been studied (e.g. Routh, Russel 1999), but their simulation is too complex to be handled by most particle-based computational techniques.

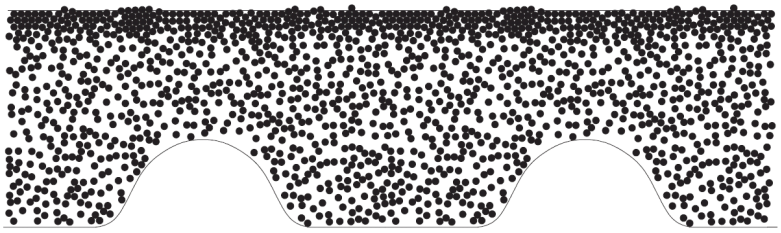

Figure 7. Skinning at the coating/ air interface caused by evaporation (Toivakka 1997).

2.3.3 Binder migration

Binder migration is the redistribution, or, preferential accumulation of binder particles to some region of the consolidating coating layer. The phenomenon was studied as early as 1965 by Heiser and Cullen, who concluded that binder migration depend on the dry solids content of the coating slurry as well as the drying intensity during hot air drying. Kline (1993) also found binder mobility to depend on the coating system particle size distribution. At a relatively early stage, computer simulation was used to study the mechanisms of binder migration (Nowicki et al. 1991). Experimental work using advanced analytical methods such as SEM coupled with Osmium staining (e.g. Pöhler et al. 2006) or Cryo-SEM (Luo et al. 2008; Cardinal et al. 2009) has been reported in more recent years.

The distribution of binder has an influence on the print quality of coated paper as well as the mechanical properties of the coating layer (Engström et al. 1991; Engström 1994; Matsubayashi et al. 1992). The influence on print quality relates mostly to unevenness in the physical and chemical surface properties of the coated paper, resulting from a heterogeneous distribution of binder. The mechanical properties of the coating layer are related to the ability of the binder to glue pigment particles into a coherent structure, without significant variations in lateral or vertical direction mechanical properties (Whalen-Shaw 1993). The

presence and mechanism of binder migration is, despite extensive research, still under debate in the scientific community.

2.4 Analysis of Governing Forces and Interactions

The interactions and forces described above can be evaluated in order to determine which models are relevant to include in simulations. This is done by calculating the forces based on variables and parameter values typical for coating processes. By forming ratios between these forces, it is possible to identify the forces that dominate under specific process conditions.

The mutual relevance of hydrodynamics, thermal motion and colloidal interactions are commonly described by the particle Reynolds and Peclet number. Similarly, a dimensionless expression can be formulated to assess the relative importance of the viscous (hydrodynamic) forces and the colloidal interaction forces.

Though these numbers indicate the relative influences of the three dominating force models, hydrodynamic, Brownian and colloidal forces, their values should only be considered as indicative. As a simulation is composed of a fairly limited number of interacting particles in a complex system with constantly changing conditions, many of the variables of the equations above will be particle pair specific and may also change with time. Considering that the particle system is generated with a size distribution, all other parameters being the same, the ratios will still be different for different particle size fractions.

2.4.1 Hydrodynamics

The impact of the hydrodynamic forces of the suspending liquid on the particles can be described using the particle Reynolds number, Re_p. The particle Reynolds number can be calculated using the equation

$$\mathrm{Re}_p = \frac{\rho_l a_{char} u_{char}}{\mu}, \tag{2}$$

where ρ_l is the density of the continuous (liquid) phase, a_{char} the characteristic particle size, u_{char} the characteristic velocity of the particles relative to the liquid and μ the viscosity of the suspension (Brady et al. 1988). In the simulation technique used in this work, the particle Reynolds number plays an important role due to the lubrication approximation, which assumes particles to react instantaneously to the flow of liquid. This assumption is only valid, however, for small particle Reynolds numbers (also see 3.1). In pigment coating processes, it is possible to estimate the particle Reynolds number given the size scale of the suspended particles, the properties of the suspending liquid and the flow field. During typical consolidation processes, the particles are within the nm to µm size range. The suspending liquid phase is water and the flow rate of the liquid relative to the particles does not exceed a few tens of µm/s. Under these conditions, the particle Reynolds number will be in the order of 10^{-7} to 10^{-11}. Thus, viscous forces will completely dominate over inertial forces and the low particle Reynolds number condition applies. The above analysis applies for consolidation of coating colour after the metering process. Under and in the vicinity of the coating blade, the situation might be different due to high velocities and diverging streamlines in the flow.

2.4.2 Brownian forces

The Peclet number, Pe, is used to compare the convective effect with the effect of particle diffusion. It can thus be utilised to in estimating the relative influence of hydrodynamic forces to diffusion. Convection in this work is driven by liquid absorption into the substrate and evaporation from the free surface, while diffusion results from the Brownian motion. For the current problem, the Peclet number can be expressed as

$$Pe = \frac{6\pi\mu a_{char} H u_{char}}{kT}, \tag{3}$$

where μ is the viscosity of the liquid phase, H is the characteristic length scale of the system (coating layer thickness), k is the Boltzmann constant and T is temperature. u_{char} is the velocity of the particles relative to the liquid, but can in the case of evaporation also be the velocity of the receding free surface. The Peclet number can therefore be used both in predicting filter cake formation and skinning (Cardinal et al. 2009, 2010). Peclet numbers larger than one indicate that the effect of diffusion is negligible (Hiemenz 1986).

The calculation of the Peclet number is not straight-forward in pigment coating consolidation simulations, since many of the conditions change during the consolidation process. However, when considering values relevant to the simulations of the present work, it can be concluded that the Peclet number can vary significantly during the course of a simulation. For instance, its value can be close to 10,000 at the early stages of consolidation, and for large particles experiencing rapid dewatering/ evaporation. On the other hand, it can be below one for the smallest particles during minimal dewatering/ evaporation. The calculated ratios results from the parameters; a_{char} = 2 µm, H = 5 µm,

u_{char} = 30 µm/s, T = 298 K and a_{char} = 0.2 µm, H = 1 µm, u_{char} = 1 µm/s, T = 353 K, respectively. The characteristic length scale above need to be chosen such, that movement of particles over this length scale would have a significant effect on the microstructure of the coating layer and its properties. The consideration above indicates that the effect of Brownian motion in simulations is mostly insignificant. However, it could possibly have an effect for the smallest particle size fraction at the late stages of consolidation. As previously discussed, pigment coating formulations can also include polymeric additives and soluble binders, for which the Peclet number would be even smaller. It should also be noted that the Brownian motion may have an effect on the structure formation by helping particles to rearrange and move past one another.

2.4.3 Colloidal interactions

The relative impact of hydrodynamics in relation to colloidal interactions can be formulated by an expression similar to the Peclet number. The expression, here termed K_{coll}, can be written

$$K_{coll} = \frac{a_{char}\mu u_{char}}{F_{el}^{P} + F_{vdw}^{P}}, \tag{4}$$

where values below 1 indicate a higher relative influence of colloidal forces. Estimating from the parameters of the simulations in this work, it can be concluded that this ratio can vary from 0.15 towards infinity. Typically, the relative influence of colloidal forces can be expected to dominate at the latter stages of consolidation while the hydrodynamics dominate at the beginning.

2.5 Simulation Methods

There are a multitude of different particle dynamics methods available for investigating various particle systems. The selection of method is made depending on the type of system intended for simulation, where the size of the particles, the dominating forces and the properties of the system must be taken into consideration. For example, molecular and Brownian dynamics is commonly used in systems of nano-sized particles where molecular or atomic-scale forces and Brownian forces dominate respectively. Granular dynamics is suitable for centimetre to metre-sized particle systems where mechanical forces and friction dominates. At the other end, planetary dynamics is utilised in simulating the transition of celestial bodies. Stokesian dynamics is used in simulating the behaviour of nm to μm sized particles suspended in a high-viscosity (liquid) medium. Stokesian dynamics is similar to Brownian dynamics, with the exception that the hydrodynamic interactions in the latter are highly simplified. In the current section, different simulation methods that have been utilised in studying pigment coating are discussed. Emphasis is put on a qualitative discussion of the Stokesian dynamics technique and its applicability to pigment coating research.

2.5.1 Simulation of pigment coating

There are several factors which have necessitated the development and application of modelling and simulation methods as a means of studying coating processes. It is important to understand the behaviour of pigment coating systems in order to control both, the rheological properties of the slurry during application and the structure formation during drying. However, in industrial-scale paper coating processes, the coating layer consolidates very

fast, typically within one second. The short consolidation time in combination with the small size scales (µm to nm) and the complexity of the process, has rendered it difficult or impossible to conduct purely experimental studies of coating process dynamics. Conventional experimental studies on coating structures have focussed on the structure of already consolidated coatings (e.g. Engström et al. 1991; Engström 1994; Pöhler et al. 2006). The many theories on formation mechanisms reveal the need for phenomenological modelling (Watanabe, Lepoutre 1982; Lohmander et al. 2001). Despite the difficulties, some studies have made progress through experimental investigation of the dynamics of coating layer formation (Sheehan et al. 1993; Ming et al. 1995; Stanislawska, Lepoutre 1995; Ma et al. 2004).

Recent overviews of the development and progress of various particle methods for investigating pigment coating on the microscopic scale are reported by Vidal and Bertrand (2006) and Pianet et al. (2008). It can be differentiated between two basic types of models; probabilistic and deterministic. Probabilistic methods have traditionally been the basis of different types of random particle deposition methods, which have commonly been applied in the generation of model pigment packings or in simulating coating layer consolidation. Such methods include steepest descent deposition (SDD), Monte-Carlo deposition (MCD), Hiorns and Nesbitt's deposition (HND), Lyons and Iyer's deposition (LID) (Eksi, Bousfield 1997; Vidal et al. 2003a, b; Hiorns, Nesbitt 2003; Lyons, Iyer 2004). Deterministic models utilise physical models such as force balances and Newton's laws of motion. The most commonly used deterministic models for simulation of particle systems include Stokesian dynamics (SD), the discrete element method (DEM), granular dynamics and the Lattice-Boltzmann method (LB) (Cundall, Strack 1979; Bilodeau, Bousfield 1998; Barbesta et al. 2001; Ladd, Verberg 2001; Raiskinmäki et al. 2001; Lyons et al. 2003; Bertrand et al. 2004; Bertrand et al.

2005; Hyväluoma et al. 2005; Pianet et al. 2008). There are also some examples of methods, e.g. dissipative particle dynamics (DPD), which can be considered as being semi-deterministic. These methods utilise deterministic laws of motion, but require non-deterministic elements in tuning the particle interactions to allow for larger timesteps (Hoogerbrugge, Koelman 1992; Koelman, Hoogerbrugge 1993; Nopola 2004; Martys 2005).

2.5.2 Stokesian dynamics

Stokesian dynamics (from Georges Gabriel Stokes, 1819-1903) was introduced by Brady and Bossis (Bossis, Brady 1984; Brady, Bossis 1988; Bossis et al. 1988), partly using convergence expressions developed by e.g. Koliha (1973) and O'Brien (1979), as a simulation technique for studying many-body interactions in non-equilibrium suspensions. Already in 1987 it was presented by Barnes et al. as a potential tool for computer simulation of the behaviour of particle suspensions.

Since its development, the technique with various modifications has been applied in the study of particle systems and their properties (Brady et al. 1988; Durlofsky, Brady 1989; Lovalenti, Brady 1993a,b; Chang, Powell 1994; Jones, Kutteh 1999; Ball, Melrose 1997; Melrose, Ball 2004; Kulkarni, Morris 2009). Improvements to the Stokesian dynamics method have during later years enabled the simulation of ever more complex systems. These systems include colloidal dispersions and the influence of temperature (Phung et al. 1996; Jones 2001), as well as simple cases of non-spherical particles (Ziler, Bousfield 1991; Ziler, Bousfield 1992; Clayes, Brady 1993; Hase, Bousfield 1994; Meng, Higdon 2008a,b). A timeline showing some key developments and practical applications of the Stokesian dynamics technique is presented in Figure 8.

PRE-STOKESIAN DYNAMICS		
1973	Koliha	Convergence expressions and their generalisation
1979	O'Brien	Absolute convergent expressions for particle interactions
1984	Bossis, Brady	Method for simulation of hydrodynamic and non-hydrodynamic interactions in particle suspension
1987	Durlofsky, Brady, Bossis	General method for computing hydrodynamic interactions of N suspended particles
STOKESIAN DYNAMICS		
1987	Barnes, Edwards, Woodcock	Describes Stokesian dynamics as a potential tool for the simulation of particle suspensions
1988	Brady, Bossis	First introduction as simulation method
1988	Brady, Phillips, Lester, Bossis	Method for calculating hydrodynamic interactions in infinite suspensions
1989	Durlofsky, Brady	Solid planar boundaries
1990	Bousfield	First application to coating of paper, introduction of lubrication approximation
1992	Toivakka, Eklund, Bousfield	Surface-particle interaction, Mechanical interactions in 2D
1993	Lovalenti, Brady	Force on single particle in small-amplitude oscillating and time-dependent low-Re flow fields
1993	Claeys, Brady	Simple non-spherical objects (ellipsoids)
1996	Phung, Brady, Bossis	Brownian motion/ Peclét numbers
1997	Toivakka	Further modification of lubrication approximation. Colloidal, steric and Brownian forces
1997	Toivakka, Salminen, Chonde, Bousfield	DLVO and steric forces
2000	Foss, Brady	Monodisperse hard spheres
2001	Jones	Linear shear flow
2001	Sierou, Brady	Accelerated Stokesian Dynamics (ASD)
2001	Barbesta, Bousfield, Rigdahl	Boundary roughness in SD model
2002	Sierou, Brady	Application of ASD
2004	Nopola	Modifications to 3D, differently sized particles
2008	Pianet, Bertrand, Vidal, Mallet	Stokesian dynamics/ DEM application for fluid flow feedback

Figure 8. Some key events in the development and application of the Stokesian dynamics technique.

Several improvements have been made to the traditional Stokesian dynamics technique in order to achieve greater computational effectiveness and to increase the size of the particulate systems. While the original technique allowed the simulation of no more than a few hundred particles, current

developments allow for efficient simulation of thousands to tens of thousands of particles (Sierou, Brady 2001).

Bousfield (1990) introduced the lubrication approximation in combination with a Stokes drag contribution from the liquid. This assumed that the long range hydrodynamic force could be approximated by Stokes law based on the bulk or base flow field without particles present. Conversely, the original Stokesian dynamics method subtracts the long range lubrication forces from the long range hydrodynamic interactions. Further modification was made to the lubrication approximation by Toivakka (1997), who applied algorithmic techniques common in molecular dynamics such as particle neighbour lists and a sparse matrix solver to further improve efficiency. An alternative approach towards reducing the computational cost of hydrodynamic force models was demonstrated by Sierou and Brady (2001). The method, named Accelerated Stokesian Dynamics (ASD), avoids the calculation of the far-field mobility matrix (see 2.2) by direct calculation of the far-field hydrodynamic force and utilisation of preconditioning schemes to reduce the cost of iterative matrix inversions. The ASD technique has been successfully utilised in several applications, e.g. studies on rheology and microstructure in non-colloidal suspensions (Sierou, Brady 2002) as well as in the implementation of Brownian motion (Banchio, Brady 2003).

The estimation of computational expense as function of the number of particles is not straight-forward. It depends on which Stokesian dynamics approach is used, and which other improvements it may include. Alterations to the traditional technique, using preconditioning schemes and omitting interactions between distant particle pairs will radically change the computational effort. In fact, the concentration of particles in the system, or interparticle distances, will be more of a limiting factor than the number of particles simulated. The forces in the system, boundary conditions and the size

of particles, also play a role. The steepness of interparticle forces of neighbouring particles slows down time integration due to a small Δt. Simulation of polydisperse systems subjected to consolidation, sedimentation or other particle agglomeration effects need to be planned with care. Even though the number of particles simulated is the same, both memory consumption and computational expenses can vary significantly over the time of a simulation. Nevertheless, some estimations are available in the literature, as summarised in Table 2 and graphically illustrated in Figure 9.

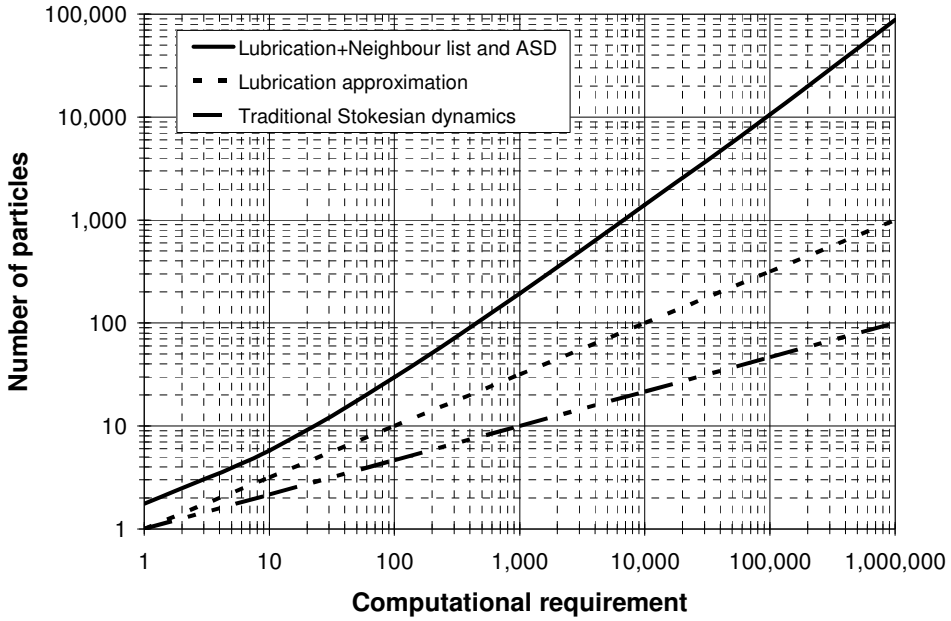

Figure 9. Approximate scaling between number of particles simulated and estimated computational requirement (unitless) for different SD approaches.

Table 2. Comparison in computational expense using different modifications to the traditional Stokesian Dynamics technique

Stokesian Dynamics Method	Source	Computation scaling
Traditional Stokesian Dynamics	Brady, Bossis 1988	$O(N^3)$
Lubrication approximation	Bousfield 1990	$O(N^2)$
Lubrication technique + Neighbour list	Toivakka 1997	O(N log (N))*
Accelerated Stokesian Dynamics (ASD)	Sierou, Brady 2001	O(N log (N))**

* Additional computation time is needed to generate and update the neighbour list.
** Additional computation time is needed to generate preconditioning scheme.

2.5.3 Stokesian dynamics simulation of pigment coating

Bousfield was the first to apply Stokesian dynamics in the simulation of pigment coatings (Bousfield 1990). Later on, a method for simulating the 2D microstructure development and levelling of coating at different drying rates was presented by Toivakka et al. (1992). The most common fields of pigment coating studies using Stokesian dynamics has been on rheological properties of pigment slurries and the motion of pigment particles (Toivakka et al. 1995; Toivakka, Eklund 1996; Toivakka 1997). The models developed by Toivakka et al. included hydrodynamic interactions and also contained a free surface model, electrostatic and van der Waals (DLVO) forces, steric forces, the Brownian motion and mechanical interactions (Toivakka 1997). The work of Toivakka et. al. was continued by Nopola (2004), who extended the simulation domain to three dimensions and adaptated the interaction models to allow for simulation of particle size distributions. The hydrodynamic interaction models were compared to results of finite element analysis (FEM) in order to obtain more accurate expressions for particles with large size differences and interactions with planar boundaries. The modifications by Nopola were furthered in this work, e.g. by applying minor model adaptations and the inclusion of non-linear dewatering profiles.

3. METHOD

The Stokesian dynamics technique provides a versatile means of studying the motion of particles subjected to various forces and torques. These can be defined by models and be progressively included into the calculation. The model is suitable for simulating colloidal suspensions, since colloidal particles are comparably much larger than the molecules of the surrounding liquid and the particle Reynolds number is less than one.

The main constraint to the original Stokesian dynamics technique is the computing power required to calculate long-range particle interactions. With the full range of possible particle interactions taken into account, the number of particles simulated has been, at maximum, in the order of a few hundred. Given the types of colloidal systems required for representatively simulating pigment coatings, this constraint is unacceptable. Both accurate representation of particle size distributions and the linking of micro-level mechanisms to macroscopic suspension behaviour require particle systems to comprise several thousands of particles. Modifications and simplifications to the original Stokesian dynamics technique are consequently needed in order to simulate larger system sizes.

In this chapter, the basic principles, interaction models and governing equations of the simulation technique is described. Time discretisation is briefly discussed, followed by a description of force and torque models deemed relevant to pigment coating processes.

3.1 Time Integration

The motion of particles in a fluid can be described by the coupled N-body Langevin equation (Brady, Bossis 1988)

$$\mathbf{m}\frac{d\mathbf{U}(t)}{dt} = \mathbf{F}^H + \mathbf{F}^P + \mathbf{F}^B. \quad (5)$$

The equation is a variant of Newton's second law of motion and simply states that mass, $\mathbf{m}$, times acceleration, which is given by the translational and rotational velocity vector $\mathbf{U}(t)$, is the arithmetic sum of all forces and torques exerted on the particle. These can include hydrodynamic forces and torques, $\mathbf{F}^H$, external or internal deterministic non-hydrodynamic forces and torques, $\mathbf{F}^P$, and stochastic forces and torques giving rise to the Brownian motion, $\mathbf{F}^B$. Given a small particle Reynolds number (Toivakka 1997; Nopola 2004), defined as

$$\mathrm{Re}_p = \frac{\rho_l a_{char} u_{char}}{\mu} << 1, \quad (6)$$

a simplification can be made to equation (5). For small flow rates or for small particles, the inertia of particles can be considered insignificant as the time needed for the particle momentum to relax is much shorter than the time scale for any significant movement of particles (Kim and Karrila 1991). Therefore, if the particle Reynolds number is small, the left hand side of equation (5) can be set equal to zero (assuming that $\mathrm{Re}_p = 0$). For pigment coatings, the liquid medium is most often water and the suspended particles are in the nm to µm size range. As the velocity of particles relative to the liquid typically does not exceed a few tens of µm/s, the small particle Reynolds number condition applies. Consequently, the hydrodynamic forces will balance the external forces and the total net force on a particle becomes zero. As the particle Reynolds number approaches zero, Equation (1) can be rewritten

$$\mathbf{RU} = -\mathbf{F}^P - \mathbf{F}^B, \tag{7}$$

where the hydrodynamic force and torque vector, $\mathbf{F}^H$, is determined by the resistance matrix $\mathbf{R}$ and the velocity vector $\mathbf{U}$ (Toivakka 1997). The forces that are determined by both particle velocities and positions are defined in $\mathbf{R}$. The external particle forces independent of particle velocities are defined in $\mathbf{F}^P$ and the Brownian motion is defined in $\mathbf{F}^B$. Long range interactions are included as drag forces and torques according to Stokes law along the diagonal of the resistance matrix $\mathbf{R}$. The Stokes drag contribution is used to take into account the influence of the liquid flow, when calculating the movement of particles. As the motion of particles does not influence the flow of the liquid, phenomena such as hindered settling (Yin, Koch 2007) are not taken into account. This can be a cause of inaccuracy especially in sedimentation-type simulations, but also to some extent when simulating drying. However, in consolidation simulations where the dominating mechanism of dewatering is liquid absorption into a base substrate, the induced error is expected to be small. As a result of this simple division of forces and torques it becomes relatively straight-forward to include additional interaction models, capturing new aspects of the physics of the systems under investigation.

During time integration for a particular simulation, first the right side of equation (7) is determined, after which the translational and rotational particle velocities are solved using Gaussian elimination or an iterative procedure. The particle positions can then be integrated in time with a small timestep, dt. The interparticle distances and magnitude of the forces and torques working on particles determine the timestep, dt, to be used.

3.2 Hydrodynamic Interactions

The resistance matrix in the original Stokesian dynamics method (Brady, Bossis 1988) is calculated as the sum of the reciprocal mobility matrix and the two-body resistance matrix,

$$\mathbf{R} = \left(\mathbf{M}^{\infty}\right)^{-1} + \mathbf{R}_{2B} - \mathbf{R}_{2B}^{\infty} \ , \tag{8}$$

in which the far-field many-body interactions are included in the mobility matrix $\mathbf{M}^{\infty}$ and two-body interactions in the resistance matrix $\mathbf{R}_{2B}$ (Toivakka 1997). The far-field two-body interactions, $\mathbf{R}_{2B}^{\infty}$, must be subtracted to avoid double counting.

In paper coating applications, the particle concentration in suspension, the volume fraction, is typically high, usually $0.4 \leq \phi \leq 0.6$. Thus, the two-body interaction forces are much greater than the forces resulting from far-field many-body interactions. Consequently, the resistance matrix can be approximated with short-range lubrication type interactions as

$$\mathbf{R} = \mathbf{R}_{2B} \, . \tag{9}$$

An alternative approach to reducing the computational cost of hydrodynamic force models has been demonstrated by Sierou and Brady (2001). The expensive calculation of the far-field mobility matrix was avoided by a direct calculation of the far-field hydrodynamic force and the utilisation of a preconditioning scheme to reduce the cost of iterative matrix inversions.

The method applied in this work considers four basic types of hydrodynamic interactions; forces and torques imposed on a single particle,

between a pair of particles, between a particle and a solid boundary and between a particle and a free surface. Each of these interactions is addressed separately.

3.2.1 Force and torque on a single particle

The hydrodynamic drag force on a single spherical particle in a Newtonian fluid can be approximated according to Stokes' law as

$$\mathbf{F} = -6\pi\mu a\mathbf{u} \tag{10}$$

where μ is the viscosity of the liquid phase, a the particle radius and $\mathbf{u}$ the particle velocity relative to the liquid surrounding it (Toivakka 1997). Similarly, the hydrodynamic torque influencing the particle can be approximated as

$$\mathbf{T} = -8\pi\mu a^3\boldsymbol{\Omega}, \tag{11}$$

where $\boldsymbol{\Omega}$ is the rotational velocity of the particle relative to the surrounding liquid.

3.2.2 Pairwise interactions

Pairwise forces and torques between nearby particles are calculated using near-field lubrication approximation type expressions. Thus, the net force and torque exerted on a particle result from the summation of hydrodynamic interactions with each of the nearby particles.

The relative 3-dimensional motion of a pair of spherical particles can be described by four different types of relative motion; squeezing, shearing,

pumping and twisting (I; Nopola 2004). For each of these modes of relative motion, the interparticle force models can be derived from Kim and Karrila (1991). However, when comparing the expressions of Kim and Karrila (1991) with numerical simulation results from finite element analyses (I; Nopola 2004) the differences were in some cases found to be significant. This was typical for particle pairs with large size differences, $\beta < 0.1$, which is not covered by the expressions presented by Kim and Karrila (1991). Furthermore, several of their expressions did not asymptotically approach zero for large particle separations, which enables accurate representation of interactions only in systems comprising high solids concentration.

The model described in the current work alleviates the constraints of Kim and Karrila (1991) by modifying the expressions where there were significant differences in the results. Thus, the theoretical expressions were modified to yield expressions in agreement with numerical results. The results of this work are presented in detail by Nopola (2004) and the expressions in combination with comparative examples are published by Sand et al. (I).

3.2.3 Particle/ boundary interactions

The hydrodynamic interaction between a particle and a boundary differs depending on the nature of the boundary. A free surface boundary at the particle suspension/ air interface allows for almost unconstrained lateral movement of liquid, while significant friction can be expected between the liquid and a solid boundary. The resulting differences in the liquid flow profile as result of the hydrodynamic interactions are illustrated in Figure 10. Two different cases of particle/ boundary interaction are described below.

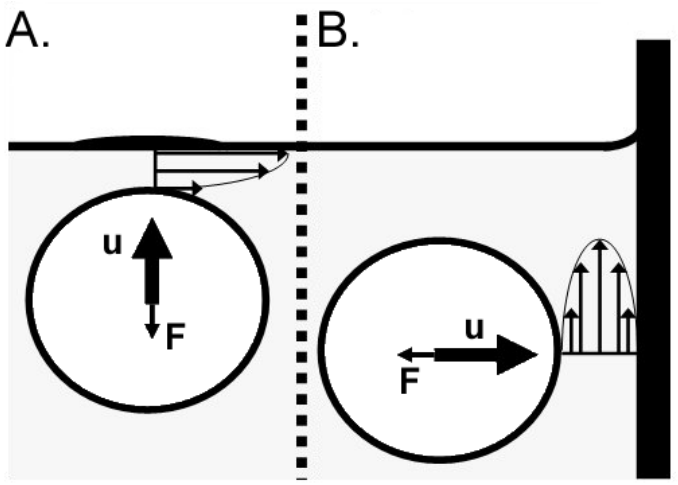

Figure 10. Comparison between particle/ free surface (A) and particle/ solid boundary (B) liquid flow profiles.

The hydrodynamic force on a particle moving towards a solid boundary can be obtained using the lubrication approximation (Toivakka 1991) as

$$F_{p-sb}^{H} = -12\pi\mu a u\left(\frac{\beta}{2} - \frac{\beta^2}{2(\beta-1)} - \frac{1}{4\beta} - 1 + \frac{3}{2}\beta\ln\left(\frac{\beta}{\beta-1}\right)\right), \tag{12}$$

where β is the non-dimensional distance between the sphere centre and the free surface, made dimensionless by the particle radius. This approximation is in good agreement with Brenner (1961), who provided an analytical solution to the problem. The relationship between the analytical solution and the lubrication approximation has previously been shown e.g. in Toivakka et al. (1991) and Toivakka (1997). Similarly, Goldman et al. (1967a; b) derived expressions for the forces and torques on a spherical particle suspended in liquid and moving parallel to or rotating in the vicinity of a plane wall.

In this work, the hydrodynamic forces and torques between a particle and a solid boundary are modelled using virtual spheres as boundaries and calculating the pairwise forces accordingly. A virtual sphere is placed at the

point of minimum distance from the particle to the boundary, while ensuring that the virtual sphere surface coincides with the local gradient of the boundary. If the boundary object is a wall, the virtual sphere radius is defined as one hundred times greater that that of the suspension particle for which the interaction is calculated. Similarly, a corner is represented by a virtual sphere of radius equal to $1/10 \times a$, where a represents the radius of the suspension particle. This moreover allows for the simulation of non-planar boundaries.

The interaction between a particle and the free surface of the liquid medium was modelled using a hydrodynamic force for submerged particles which was transformed to a surface tension force for particles penetrating the surface, as shown in Figure 11. This approach is only an approximation, since the free surface boundary is in reality able to deform. The interaction between a particle and a deformable free surface has been analysed by Geller et al. (1986), and is relatively complex. The interaction can be simplified by assuming the boundary to be non-deforming and enforcing of a transition between the particle-boundary interaction and the surface tension force.

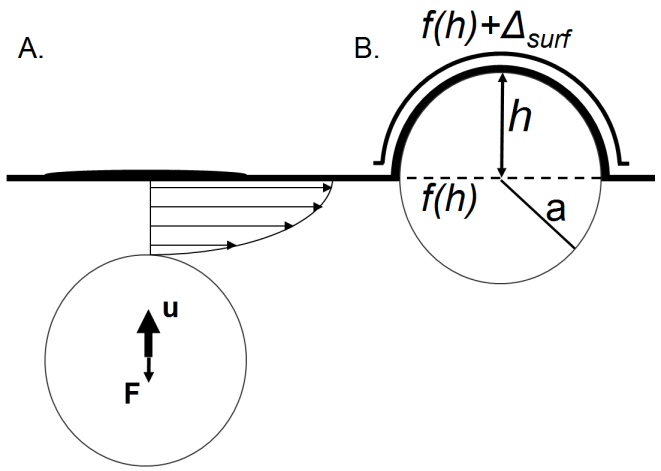

Figure 11. The free surface model, comprised of the hydrodynamic interaction (A) and surface tension model (B). B shows the increase in surface length caused by the particle penetrating it.

Assuming a non-deforming boundary, the hydrodynamic force component can be modelled according to the lubrication analysis of a sphere approaching the free surface. The free surface hydrodynamic force can be described as

$$F_{p-fs}^{H} = -3\pi\mu a u_{surf}\left(\frac{\beta}{2} - \frac{\beta^2}{2(\beta-1)} - \frac{1}{4\beta} - 1 + \frac{3}{2}\beta\ln\left(\frac{\beta}{\beta-1}\right)\right), \tag{13}$$

where F_{p-fs}^{H} is the hydrodynamic force on the particle caused by the free surface, μ is the viscosity of the liquid phase, a particle radius and u_{surf} the velocity at which the particle approaches the free surface. The free surface hydrodynamic force (13) differs from the solid boundary expression (12) by a factor of four, due to the assumption that liquid is allowed to flow freely at the free surface. Contrarily, a non-slip condition is assumed to apply in the solid boundary case (Toivakka et al. 1992; Toivakka 1997).

The surface tension force is modelled as a spring force, which is a function of the increase in particle surface above the liquid as the particle deforms the surface. The surface tension force is generally expressed by a capillary force, which requires the radius of curvature of the liquid film to be known. Due to the high concentration of particles, determination of the radius of curvature is not trivial. Therefore a spring force approach was used instead. The surface tension force is thus given by the equation

$$F_{ST} = \sigma\Delta_{surf}\,, \tag{14}$$

where σ is the surface tension component and Δ_{surf} the elongation of the free surface by the particle deforming it (Toivakka 1997). The elongation can be expressed as

$$\Delta_{surf} = 2a \arccos\left((a-h)/a\right), \tag{15}$$

where a is the radius of the particle and h the distance the particle has penetrated above the free surface (also see Figure 11). The relationship between the surface tension and hydrodynamic forces is exemplified in Figure 12. Since the free surface hydrodynamic force is both velocity and position dependent and the surface tension force only depends on position, combining the models is not straight-forward. In this work, a fit between the hydrodynamic and surface tension force is obtained by assuming a particle surface roughness. Thus, the free surface hydrodynamic force is used until the distance to the surface corresponding to the given particle surface roughness. At this point, the force is transferred to correspond to the surface tension force. The procedure is also described by Toivakka et al. (1991).

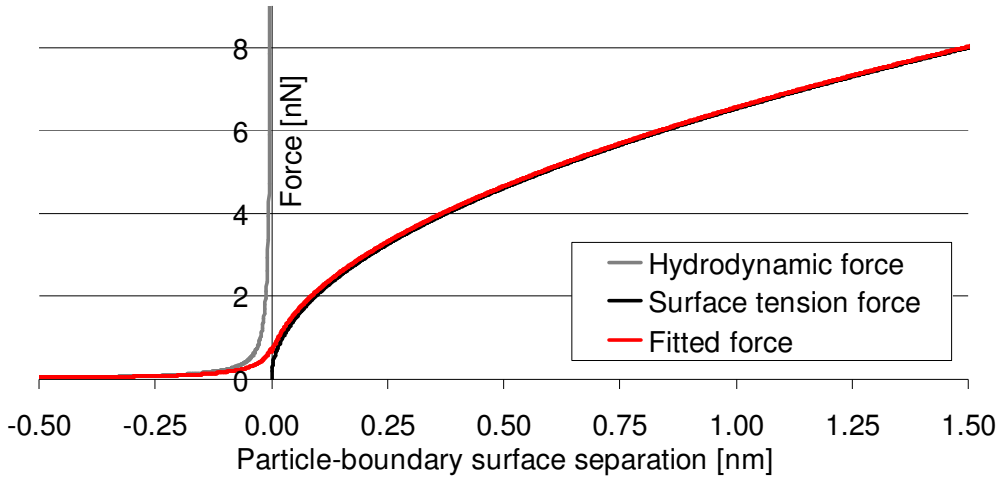

Figure 12. The free surface force on a particle of radius 1 µm, approaching and penetrating the liquid/ air interface at a velocity of 10 µm/s.

3.3 Non-Hydrodynamic Interactions

Accurate simulation of pigment coating systems necessitates the application of several different types of non-hydrodynamic interaction forces between particles. The background of each interaction phenomenon is described in brief. Each is followed by separate description of the interaction models including their constituent equations.

The interaction between charged particles at the nm - μm scale in an electrolyte-containing suspension requires the inclusion of colloidal interaction models of DLVO (Derjaguin-Landau-Verwey-Overbeek) type. An additional mechanical interaction model for particles at close contact, mimicking Born repulsion, is needed to prevent particles from overlapping (Lyklema 2005b; Shaw 2003).

Polymer-based components are commonly added to the coating system in order to promote steric stabilisation, which is obtained through polymer adsorption onto pigment particles. The resulting steric barrier between particles can be described by a steric repulsion model. Pigment-polymer interactions are nevertheless not trivial, and attractive forces between particles have been known to arise as a result. Such attractive forces can be produced, for example by polymer bridging between pigment particles or depletion flocculation due to the presence of non-adsorbing free polymer in the suspension (Napper 1983; Shaw 2003). Attractive forces resulting from polymers are, however, not taken into account in the current model.

Brownian motion is needed to describe diffusion and particle redistribution phenomena taking place as result of the thermal vibration of particles, random collisions with molecules of the suspending medium, other particles and system boundaries (Shaw 2003). A Brownian motion model enables the simulation of sedimentation processes and diffusion phenomena

taking place in consolidating coatings, including its effects on the structure development of the particle systems.

Depletion flocculation and bridging can be of importance in particle systems containing liquid-suspended and adsorbed polymer. Despite the substantial influence these phenomena can have on the constitution of particle suspensions (Tadros 1987; Melrose, Heyes 1993; Fellows, Doherty 2006), they were not included as constituent models in this work. For consolidation-type applications, there is currently a lack of suitable models or difficulties in finding appropriate parameters.

3.3.1 Colloidal interactions

The colloidal interaction model can be expressed by a combination of electrostatic repulsion and van der Waals attraction forces. The resulting net colloidal force, F_{coll}^{P}, is of DLVO type, given by

$$F_{coll}^{P} = F_{el}^{P} + F_{vdw}^{P}. \tag{16}$$

The attractive and repulsive components are given in (17) and (19).

The electrostatic repulsion component is expressed as a pairwise short-range repulsive force (Dabros and van de Ven 1992; Suzuki et al. 1969),

$$F_{el}^{P} = 4\pi\kappa\varepsilon_r\varepsilon_0\psi_1\psi_2 \frac{a_1 a_2}{a_1 + a_2} \frac{e^{-\kappa\Delta}}{1+e^{-\kappa\Delta}}, \tag{17}$$

where κ is the reciprocal electrostatic double layer thickness, ε_r is the dielectric constant of the continuous phase, ε_0 the permittivity of vacuum, ψ_1 and ψ_2 the surface potentials of the interacting particles and Δ the surface

separation distance. a_1 and a_2 are the radii of the particles. The reciprocal double layer thickness can, for a symmetric and asymmetric electrolyte, respectively, be approximated as

$$\kappa = \begin{cases} 3.29\times10^{9}|z|\sqrt{c} \\ \\ 2.32\times10^{9}|z|\sqrt{\sum z_i^2 c_i} \end{cases}, \tag{18}$$

where z is the valence and c the concentration of the ions (Hiemenz 1986).

The van der Waals attraction component can be estimated using an expression derived from Suzuki et al. (1969) (Dabros and van de Ven 1992; Toivakka 1997; Nopola 2004) as

$$F_{vdw}^{P} = -A_H \frac{\beta}{1+\beta} \frac{\lambda(\lambda + 22.232\Delta)}{6\Delta^2(\lambda + 11.116\Delta)^2}, \tag{19}$$

where A_H is the Hamaker constant and λ the London characteristic wavelength (Hogg et al. 1966). The colloidal interaction model is demonstrated in Figure 13, where the resulting force curves are shown for a few combinations of electrostatic double layer thicknesses and particle surface potentials.

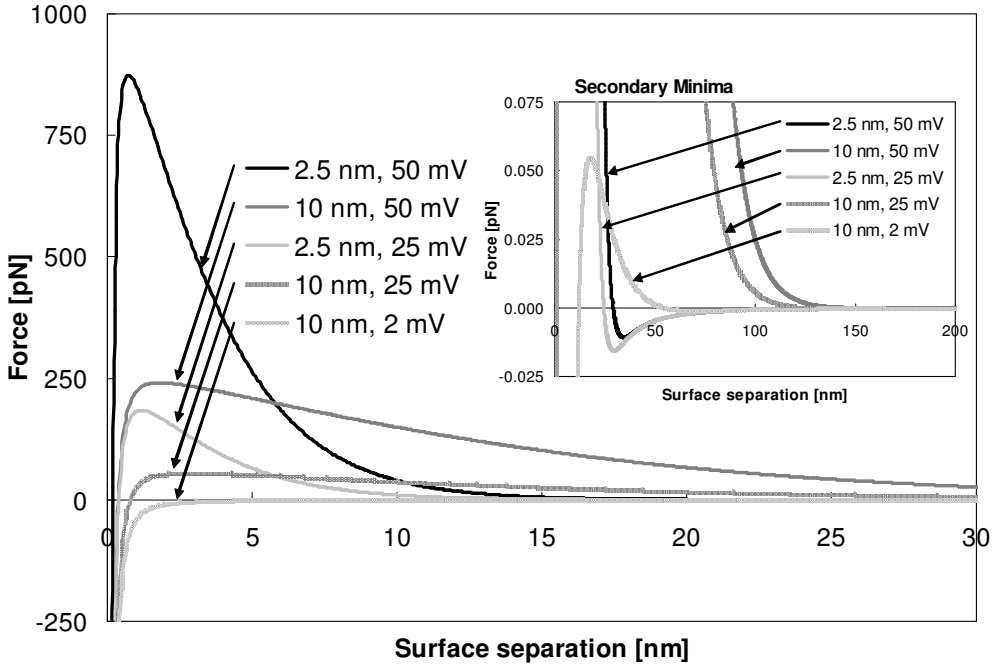

Figure 13. Colloidal interaction forces between two particles of 1 µm in diameter at a few cases of different double layer thicknesses and surface potentials. The zero interparticle force corresponds to the secondary minimum of the particle interaction energy curve calculated by the DLVO theory.

It is worth noting that a Born repulsion model, although not defined as a colloidal interaction, is needed to prevent particles from overlapping at close contact. A few considerations also need to be mentioned regarding the colloidal interaction model. In describing the surface potential of calcite in aqueous suspensions, the zeta potential, ζ, is traditionally used (Madsen 2002). The zeta potential measures the potential at a certain distance from the particle surface, it does not correspond directly to the surface potential, ψ. The surface potential and zeta potential relationship can be derived using the Stern model of the double layer. This model for charge distribution is, however, somewhat crude and not necessarily suitable for calcite surfaces in water (Hiemenz 1986; Eriksson et al. 2007).

3.3.2 Steric forces

Steric forces between particles are modelled as an osmotic pressure difference for surface separation distances less than twice the thickness of the adsorbed polymer layer. If the distance is less than the thickness of the polymer layer, an additional elastic force comes into play. This additional force is assumed to result from the compression of polymer chains, if the steric boundary layers overlap. Thus, the steric force is described as

$$F_{st}^{P} = F_{osm}^{st} + F_{el}^{st}, \tag{20}$$

the osmotic, F_{osm}^{st}, and elastic, F_{el}^{st}, components are calculated as

$$F_{osm}^{st} = \begin{cases} 0 & \Delta \geq 2\delta_{ster} \\ K_1 a\left(\Delta - 2\delta_{ster}\right) & \delta_{ster} < \Delta < 2\delta_{ster} \\ K_1 a\left(\delta_{ster} - \dfrac{2\delta_{ster}^2}{\Delta}\right) & \Delta \leq \delta_{ster} \end{cases} \tag{21}$$

$$F_{el}^{st} = \begin{cases} 0 & \Delta \geq \delta_{ster} \\ K_2 a \delta_{ster} \ln\left(\dfrac{4\delta_{ster}^3}{\Delta\left(\Delta - 3\delta_{ster}\right)^2}\right) & \Delta < \delta_{ster} \end{cases}, \tag{22}$$

where Δ is the surface separation, δ_{ster} the polymer layer thickness. K_1 and K_2 are constants that depend on the effective volume fraction of polymer in the adsorbed layer and density, molecular weight and solvency of the adsorbed polymer (Vincent et al. 1980, 1986; Einarson and Berg 1993).

3.3.3 Brownian motion

The Brownian motion model is based on the Einstein equation for calculation of the mean Brownian displacement, $\bar{x}$, of a particle as function of time, t, as

$$\bar{x} = \sqrt{2Dt} \,. \tag{23}$$

Particle diffusivity, D, is calculated as

$$D = \frac{RT}{6\pi\mu a N_A}, \tag{24}$$

where T is the system temperature, μ the viscosity of the continuous phase, R the universal gas constant and N_A Avogadro's constant (Shaw 2003).

A force of random direction was applied to each particle at each timestep. The R250 random number generator (Vattulainen et al. 1994) was used in order to accelerate the generation of random numbers. The direction of the Brownian force was represented by a unit vector generated by uniformly distributed points on the surface of a unit sphere according to the algorithm

(a) Choose z uniformly distributed in $[-1,1]$

(b) Choose t uniformly distributed in $[0,2\pi]$

(c) Let $r = \sqrt{1-z^2}$

(d) Let $x = \sqrt{r\cos(t)}$

(e) Let $y = r\sin(t)$.

When the unit vector, $\overline{a^0}$, is determined by the algorithm, the random force is calculated as

$$\overline{F} = K_{Brown}\overline{a^0}\sqrt{a}\,, \tag{25}$$

where a is the particle radius and K_{Brown} an iteratively determined, system specific parameter that can be used in taking into account the system temperature and particle size range. The K_{Brown} parameter is derived from a fitting curve to provide such weight to the force equation that the resulting displacement distribution of a single particle in infinite dilution will be in agreement with the Einstein equation (23), coupled to (24). An example of such a curve is shown in Figure 14, where K_{Brown} is plotted against temperature.

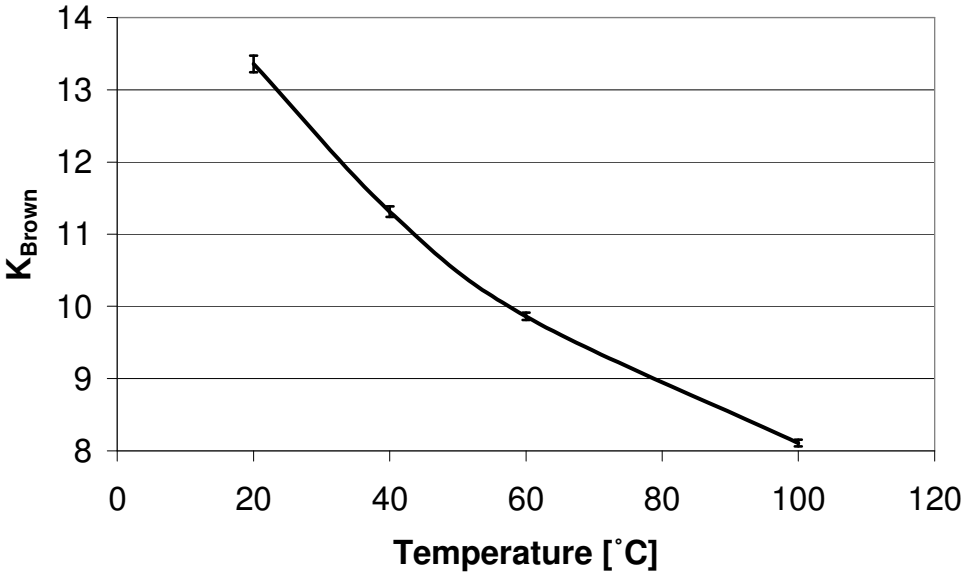

Figure 14. K_{Brown} parameter values as function of system temperature.

The curve is non-linear due to the viscosity of the liquid phase being non-linearly dependent on temperature. K_{Brown} decreases at increasing temperatures, since it corrects the force to correspond to the correct displacement. As the viscosity of the liquid phase rapidly decreases with rising temperature, less force is needed to obtain the theoretical displacement. Equation (25) scales the force to particle size. Thus, K_{Brown} should work over the full particle size range. It was noted, however, that the Brownian displacements will start to deviate from their theoretical values the more the particle size differs from the size at which K_{Brown} has been calibrated. However, over a narrow particle size range, this effect is insignificant. As this work considers particle systems where the size difference between the largest and smallest particles is 1:10, the error is expected to be less than 3 %. The parameter in Figure 14 is calibrated for a d = 2 µm particle. Each of the four data points shows the average and standard

deviation of 25 simulations, with 45,000 particle displacements in each simulation.

The model was tested and showed good compliance with analytical results, as shown in Figure 15. The left hand figure compares a displacement distribution of 49,900 individual displacements with a Gaussian and log-Gaussian distribution. The right hand side shows the displacement of an individual particle calculated at different time intervals. The total simulation time was 50,000 s. Thus, the data point at 5 s is an average of 10,000 displacements while the point at 480 s is an average of 100 displacements.

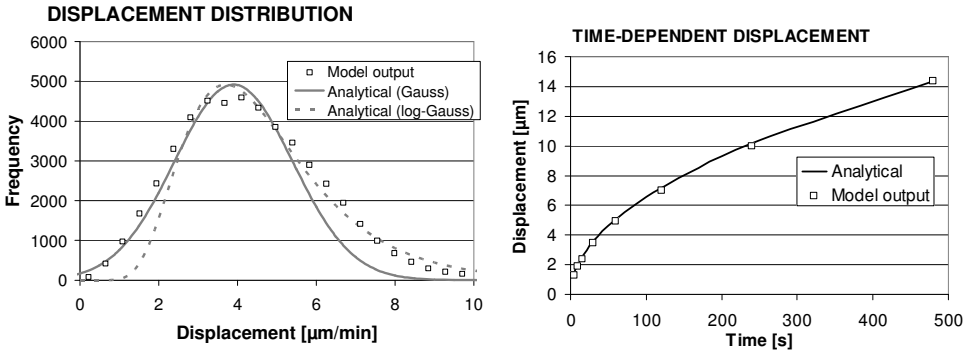

Figure 15. Comparison of analytical and model-produced Brownian displacements.

3.4 Algorithmic Techniques

There are several algorithmic techniques that allow reduction of the computational expense of costly particle dynamics simulations. The current application implements two of these methods; the neighbour list and sparse matrix techniques.

When the solid particle concentration in the suspension is high, particles are predominantly influenced by the interactions with their closest neighbours. If the interparticle separation distance is high however, the pairwise interaction

forces between particles approach zero. Consequently, a regularly updated nearby neighbour list for each particle is produced and only the corresponding interactions with listed particles are calculated. The computational expense can in this way be greatly reduced. The expense of updating the neighbour list is in most cases easily outweighed by the savings to avoid calculating interactions between distant particles.

The sparse matrix technique can be used due to the properties of the resistance matrix (Toivakka 1997). It was estimated by Nopola (2004) that the fullness ratio of the matrix is in the order of $37N^{-1}$. Particulate systems composed of thousands of particles, will thus result in a resistance matrix predominantly habituated by zero-elements. Furthermore, the symmetrical properties of the matrix require only half of the elements and their positions to be stored. Consequently, the current model utilises the HUTI iterative sparse-matrix solver (Malinen 1997), provided by the Finnish Centre for Scientific Computing (CSC), in solving equation (25).

3.5 Particle System Analysis

Post-processing of the results of particle dynamics simulations is essential in gaining understanding of both consolidation dynamics and the development of macroscopic properties of the particle system. The output of Stokesian dynamics simulations is extremely versatile in the sense that the mesh free position and velocity of each individual particle is known at every timestep, thus giving vast opportunities for data analysis. The analysis methods include e.g. microstructure analysis both through filtered visualisations and calculated solids concentration and displacement distributions. The current section briefly describes the different possibilities for particle system analysis employed in this work.

3.5.1 Microstructure Analysis

In this work, the microstructure is commonly considered as z-direction dry solids concentration profiles. The dry solids content is calculated by integrating the simulation domains into z-direction slices, for which the amount of solids measured in volume percent is calculated. The volume percent is then recalculated to weight percent assuming the liquid phase to have the density of pure water (1000 kg/m^3) and the solids density to be that of calcium carbonate (2700 kg/m^3). The monitoring of dry solids profile development during coating layer consolidation illustrates filter cake formation, skinning mechanisms and their time dependence. By filtering out and focusing on specific particle size fractions, phenomena such as small particle migration can be studied. Similarly, the distribution of large particles might be useful in detecting size segregation effects. Direct 3D visualisation of the particle system can in some cases aid in studying the above-mentioned effects, but is seldom productive in observing solids concentration gradients and their development in time.

Regarding binder migration, it is important to note that the simulation software does not distinguish between binder and pigment particles neither in terms of surface properties nor density. However, given the low volume of small particles relative to their larger counterparts along with the inherent principles of the simulation method, such as the assumption of zero particle Reynolds number, this cannot be considered a critical drawback. Furthermore, the direction of gravity in pigment coating processes is not constant and the time scale is too short to allow for a significant sedimentation of particles. Thus, the results can also to some extent be regarded as valid for binder-pigment systems.

3.5.2 Particle Motion

Particle motion is commonly presented using trajectories, illustrating the displacement of a particle during a given time interval. As trajectories typically do not illustrate the velocity and dynamics of particle movement, mobility distributions of individual or batches of particles can also be useful. Mobility distributions generate normal distribution-type results for consolidating particle systems under the influence of Brownian motion. These can be calculated both as absolute displacements or divided into their lateral and vertical components. Another useful tool in understanding the movement of particles within a particle system is to colour particles depending on their velocities. It is possible to utilise either local or global velocity, where local velocity compares the relative velocities of particles within the same timestep while global velocities are calculated over the time interval of the entire simulation.

3.5.3 Particle Agglomeration

A simple indication of particle agglomeration can be obtained by calculating interparticle surface separation distances. In its most simple form, the surface distances can be calculated between all particles of a simulation and surface separation distributions can be calculated. As we are only interested in the closest neighbours of any given particle, the diameter of the smallest particle can be used as limit for expanding the separation distribution. In this manner, we can ensure that we only include neighbouring particles which do not have intermediary particles between them. Otherwise we can expect to obtain multiple peaks, as often experienced when using for example, radial distribution functions (RDFs). Radial distribution functions are common in metallurgical and crystalline matter applications (Gacsi et al. 2002), but are ill-conditioned for polydisperse particle systems such as GCC coatings.

It is possible to identify clustered regions of particles within the consolidating layers by using a relatively simple cluster calculation algorithm in conjunction with visualisations of particle system configuration. The algorithm calculates interparticle distances and generates clustered regions from groups of particles which in proximity are closer to each other than an input threshold value. The threshold values must be selected with care, as known from image analysis utilising manual single-point thresholding as separation schemes (e.g. Russ 1995; Chinga 2002). Therefore, this type of cluster visualisation should be used with an appropriate knowledge on particle separation distributions and interparticle energy potentials. Furthermore, they should preferably be introduced in conjunction with data such as dry solids concentration or particle distribution profiles.

In visualisation, particles are thus identified as clustered or non-clustered. Futhermore, particle clusters are assigned cluster identities, allowing the separation of one cluster from another using colour codes. The particle clustering tool is useful in illustrating the development of the skin and filter cake regions of consolidating coatings, as well as particle agglomeration mechanisms within the layer.

3.5.4 Visualisation

Particle structures simulated using the Stokesian dynamics technique were visualised using the MDGraph (Ala-Viikari 2004) and PiMP++ software, which were both programmed using the OpenGL platform. MDGraph originates from 1998-2004, while PiMP++ was developed 2008-2009 during the course of and in response to the specific needs of the current work. Figure 16 shows a screen output of a consolidating polydisperse particle system.

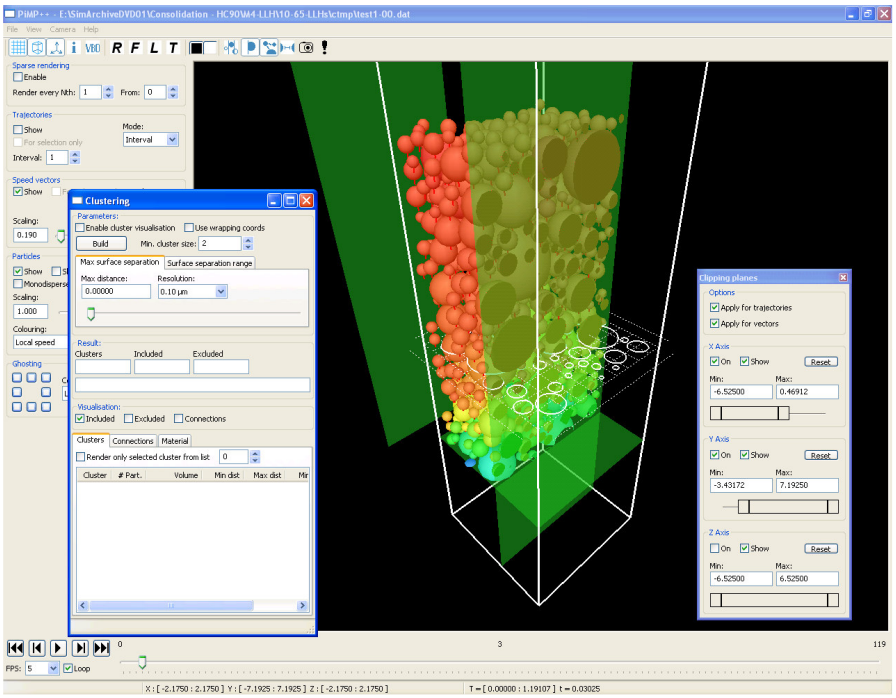

Figure 16. Visualisation of particle layer in PiMP++. Particles are coloured according to their local velocity. Cutting planes can be used to illustrate cross-sections of the particle laye

4. SUMMARY OF RESULTS

The simulation technique described in section 3 was applied in several theoretical and phenomenological investigations related to coating consolidation. These included filter cake formation, structure formation of consolidating coating layers, particle mobility and migration mechanisms during coating as well as the influence of colloidal properties on structure formation.

Efforts were made to make the simulation setup as realistic as possible, and moreover relevant to industrial coating processes. In some cases, however, it was found useful to also include model cases. Such cases are beneficial in promoting the fundamental understanding of behavioural mechanisms that are not trivial to identify in complex systems of interacting models and parameters. Parameter values were obtained from either pilot scale coating trials, laboratory measurements or the literature. In some cases, combinations of macroscopic modelling data and theoretical models were applied. These may include for example with respect to drying strategies.

The modelling and simulation work presented herein constitutes an effort to replicate industrially relevant parameters and study their influence on different coating layer properties. However, it is also acknowledged that a full understanding of the model and parameters is not trivial and that a completely accurate representation of the process is not possible. Modelling and simulations should be considered a means of testing the feasibility of suggested theories and hypotheses. They can be useful in explaining the relative influence of different mechanisms and give a possibility for theoretical prediction how changes to process parameters can influence the macroscopic properties of the coating layer.

A schematic illustration of the principal simulation setup and boundary conditions is shown in Figure 17. This setup is valid for all consolidation simulations performed in this work, however, not in the study of filter cake stability. The simulation domain is restricted by a planar boundary at the bottom, which allows liquid to permeate while particles are deposited at the surface (i.e. impermeable for particles). It should be noted that this work assumes particles to be subjected to a long range Stokes drag force as a result of the absorption flow of liquid by the base substrate. Thus, since particles are subjected to a uniform flow field, the model underestimates percolation flow. In reality the flow would also have components directed towards any local pore openings, or would vary due to heterogeneities in the absorptive properties of the base substrate. This effect was not considered in this work. On the upper side of the domain, there is a receding free surface, which is permeable by particles but applies a surface tension force (see free surface model). As the simulations are not valid for particles fully permeating the surface, roughly referred to as FCC/ SCC in many experimental studies, some caution should be exercised when interpreting the results beyond the point of FCC/ SCC. Furthermore, when air enters the coating structure, capillary forces created by the liquid menisci result in large contracting forces, the modelling of which is also outside the scope of the present work. Both the free surface evaporation and base substrate absorption boundary conditions are determined by a time-dependent dewatering profile and are not directly coupled to the solids concentration at the interfaces. Periodic boundary conditions are applied in the lateral directions.

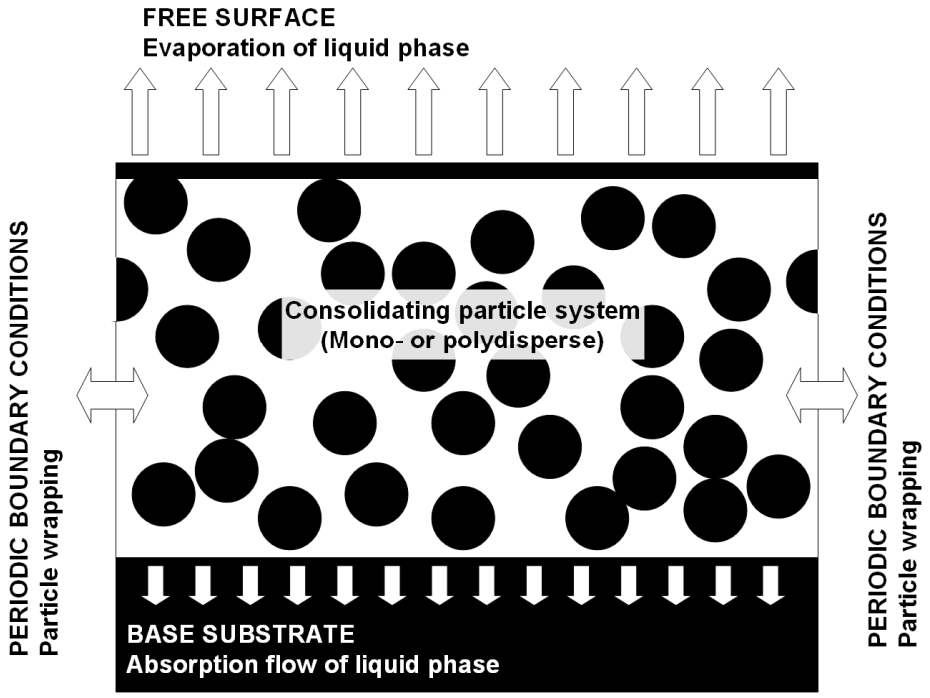

Figure 17. Schematics of consolidating particle system, including boundary conditions.

4.1 Filter Cake Stability and Structure

The structure of the filter cake influences the final structure of the coating layer and thereby also determines many physical and functional properties of the coated paper. The understanding of its formation, structure and stability under different conditions is therefore of importance for the control of coating layer properties.

The dynamic structures of filter cakes were characterised depending on the particle system properties and on externally applied conditions such as the dewatering rate and temperature. The study of filter cake stability and of structural properties takes a different approach as compared to the experimental studies presented in section 2 (e.g. Eklund, Salminen 1986; Letzelter, Eklund 1993; Lohmander et al. 2001; Engström 1986). By studying the stability of

already consolidated filter cakes instead of their formation, their dynamic behaviour and stability can be characterised (Sand et al. 2006). Thus, the interplay between the absorption flow of the base substrate and particle diffusion can be linked to the structure of the filter cake.

Monodisperse and polydisperse particle systems were simulated under the influence of Brownian motion and an absorption flow of continuous (liquid) phase into a base substrate. The absorption was a result of both capillary absorption and externally applied pressure. Filter cakes were formed through a strong initial absorption flow, which was applied to the particle-liquid suspension. The simulation time was 300 s, of which strong initial flow was applied for 20 s after which the parameters were changed and the simulation continued for another 280 s. This time scale is long compared to typical industrial paper coating processes. However, it was selected to be comparable to the experimental conditions of the laboratory-based work referenced in section 2.3.1 and above. A planar boundary was used to represent a base substrate, which provided a barrier to particles while allowing liquid to absorb. The influence of colloidal forces was not of interest here, but some electrostatic repulsion was applied to prevent the effect of particle agglomeration ($1/\kappa = 5$ nm, ψ = -25 mV). Following the formation of the filter cake, the flow rate was reduced to values in the range between 1 and 10 g/m^{2}s. The structure development of the filter cakes was subsequently investigated at different temperatures and for various particle systems. Monodisperse particle size distributions, with particle diameters ranging between 200 nm and 2 µm were simulated. The size range was selected to cover particle sizes comparable to binders and calcium carbonate pigment particles. A polydisperse system with a particle size distribution resembling fine-grade GCC was also simulated.

In the monodisperse system with d = 500 nm particles, Figure 18, the solids concentration gradient in the z-direction is illustrated at different

dewatering rates. The results show that the absorption rate had a significant influence on the structure of the filter cakes. Both mechanisms proposed in the literature; filter cake formation and thickening (also see Figure 6); were found to be realistic. However, they appeared to depend greatly on the simulation parameters. This might also be the reason for the contradictions found between different experimental investigations.

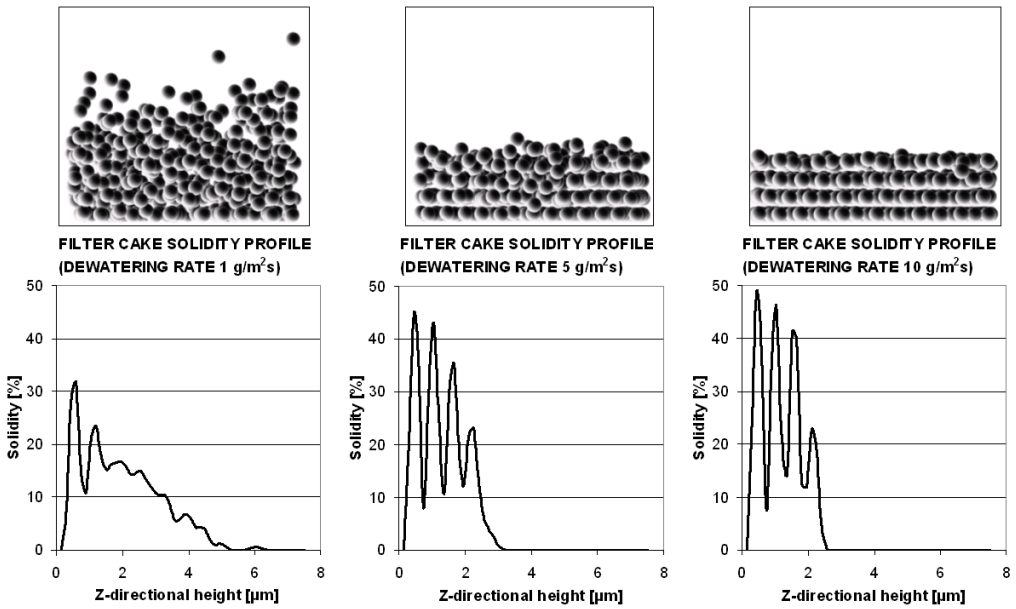

Figure 18. Filter cake structures illustrated at dewatering rates of 1, 5 and 10 g/m^{2}s after 280 seconds.

The filter cake structure and its deterioration was influenced by the size of the particles in the monodisperse systems, Figure 19. It was shown that the smallest particles, d = 200 – 400 nm, were able to diffuse against the base substrate absorption flow even at dewatering rates of 10 g/m^{2}s. This dewatering rate can according to the macroscopic modelling results, be considered normal in industrial coating processes (Timofeev et al. 2006). Thus, in practice, it can be possible for small pigment particles or binder to migrate against the absorption flow of the base substrate, if given sufficient time to do so.

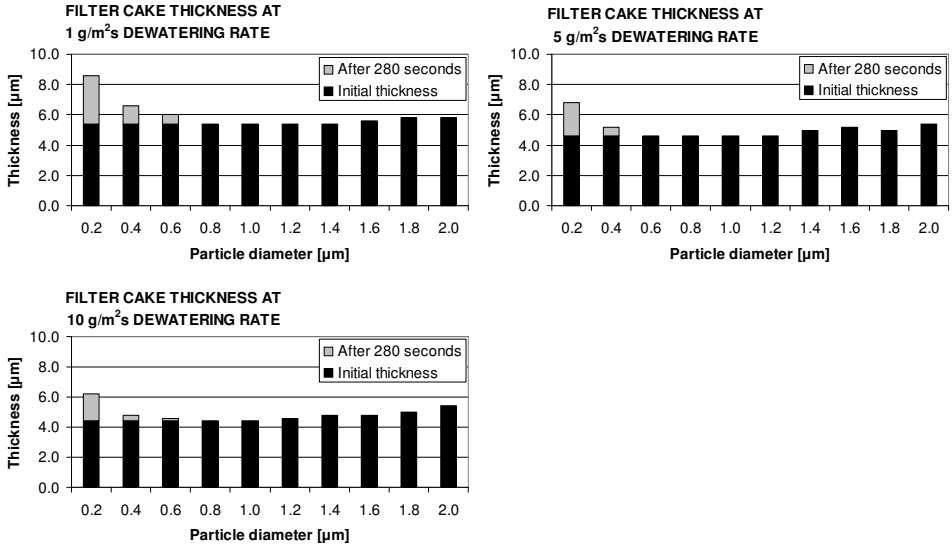

Figure 19. Filter cake thicknesses at different particle sizes, studied at different dewatering rates. Comparison between initial thickness and after 280 seconds illustrates the rate of filter cake deterioration.

Studies of the polydisperse particle size distribution, Figure 20, showed that the structure of the filter cake could be influenced by particle segregation effects and to some extent also small particle migration. As can be seen in the figure, size segregation effects take place at higher dewatering rates. It was also found that solids concentration gradients in some cases may arise as a result of filter cake surface roughness rather than the proposed thickening mechanism. This is also supported by later investigations on clustering effects in consolidating particle suspensions (see article VI and Sand et al. 2009a).

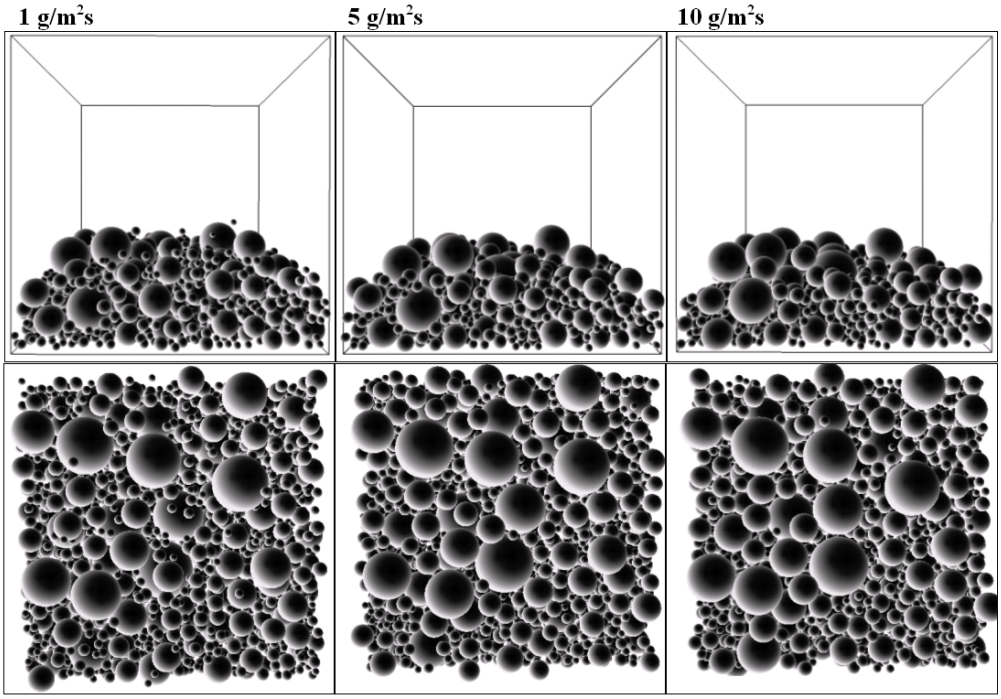

Figure 20. Side (above) and top (below) view of the polydisperse particle size distribution filter cake, with absorption rates of 1, 5 and 10 g/m²s. Situation after 280 s of simulation.

Increasing the temperature of the system promotes the Brownian motion of particles both by increasing the kinetic energy of the particles and by reducing the viscosity of the continuous phase (see Equation 24). It can thus be expected that an increase in temperature will reduce the density of the filter cake and promote the formation of concentration gradients.

The impact of temperature on the structure of the filter cake was examined for two different particle sizes and under temperatures ranging from 20 to 80 °C. The results are shown in Figure 21.

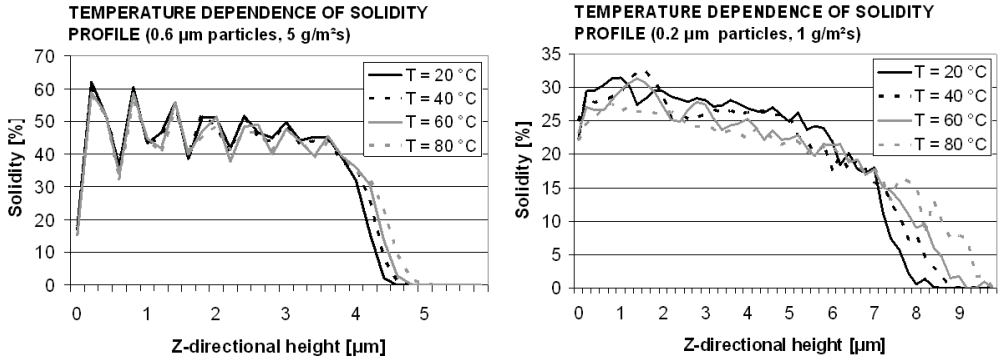

Figure 21. The influence of temperature on filter cake solidity profiles (after 280 s of simulation).

It was concluded that temperature had a rather small influence on large particles at high absorption rates. However, there was a notable effect on the filter cake structure in the monodisperse system with the smallest particle size, d = 200 nm, and at the lowest liquid flow rate.

The results show that the structure of the filter cake depends both on the properties of the particle system and on external conditions, such as dewatering flow and temperature. Ambiguous results published in the literature regarding the mechanisms controlling its structure, could be explained in the light of this study. For conditions that are close to typical industrial paper or board coating processes, a sharp filter cake structure can be expected. During the consolidation of the coating layer, this effect is expected to be most visible in situations where the applied amount of coating is high and the dry solids content of the coating suspension is low. Given the experimental setup and the selection of system properties, both thickening and sharp-solids concentration filter cake structures could be observed in simulations. The results provide a deeper understanding of coating process mechanisms.

4.2 Drying Strategy

The microstructure of the coating layer has been shown to have a strong impact on print quality, as well as many other properties related to the physical and functional attributes of the coated paper. This study aims to provide fundamental knowledge on the dynamics of microstructure development during consolidation. The investigation of consolidation at different drying strategies is useful in linking post-application process parameters to their impact on coating layer structure.

In order to investigate the influence of drying strategy on the structure formation and consolidation, a set of dewatering strategies (defined as time-dependent drying and base paper absorption profiles) were tested. Particle dynamics simulations were coupled with external data input from macroscopic modelling using VTT/Coatman and pilot coating trials performed at KCL, Espoo (Timofeev et al. 2007). Liquid evaporation rates, calculated from the coated and uncoated sides of the paper were used to generate dewatering profiles that were subsequently used as boundary conditions for simulations. Two drying strategies based on these preferences were investigated. A High-Low-Low case (HLL), which included intense initial drying followed by mild drying at the later stages, and a Low-Low-High case (LLH) with mild initial drying followed by more intense later stage drying. In addition to the macroscopic modelling-based dewatering strategies, two theoretical dewatering strategies were used in the comparison; pure absorption without evaporation (ABS) and pure evaporation without absorption (EVA). All the drying strategies were planned so as to produce the same amount of liquid dewatered, albeit at different rates versus time and with different a relationship between absorption and evaporation. The drying strategies are illustrated in Figure 22.

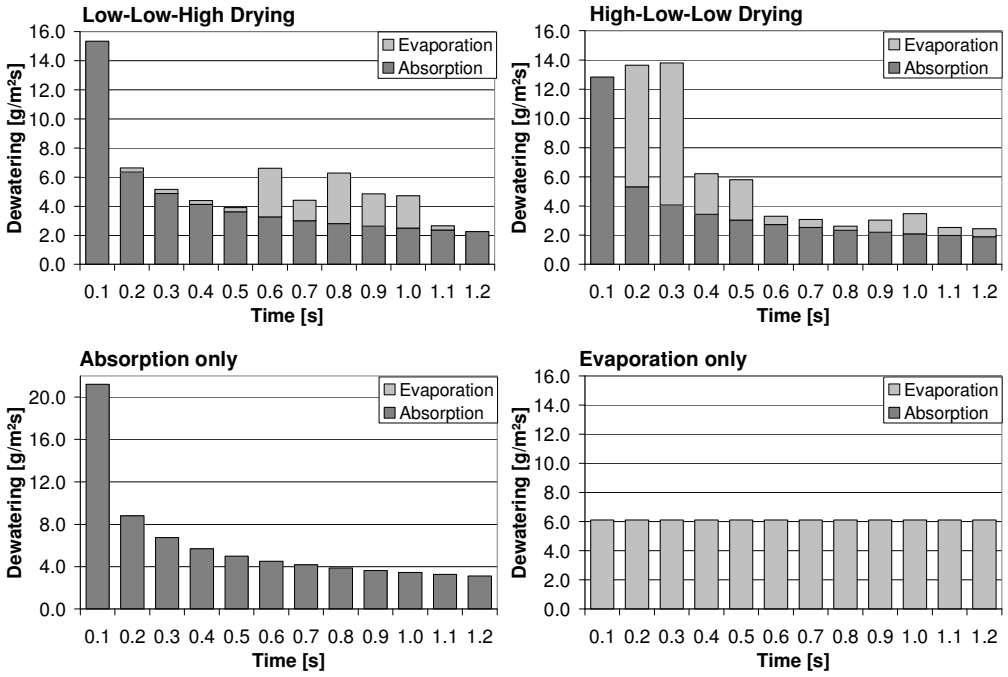

Figure 22. Drying strategies produced from macroscopic modelling (Timofeev et al. 2006) and simplified model cases (II).

In the simulations, paper coating temperature was estimated by adjusting the Brownian motion of particles and the viscosity of the liquid phase. To closely replicate the conditions typically found in industrial coating processes, a polydisperse particle size distribution resembling a fine-grade ground calcium carbonate was used (CoverCarb-75, Omya, Switzerland). The distribution satisfied the log-normal distribution described by the equation

$$p(d) = \frac{1}{\sigma_d \sqrt{2\pi}} \exp\left[\frac{-(d-\mu_d)^2}{2\sigma_d^2}\right], \tag{26}$$

where the mean particle diameter, μ_d, was 1.5 µm and the standard deviation, σ_d, 10.0 µm. Limitations in computation time and memory consumption disallowed a quantitative representation of the full binder-sized particle

fraction. However, roughly 50% of the particles simulated were represented by particles smaller than 300 nm in diameter and were thus comparable to the size of binders. A size fraction cut-off was applied for particles below 0.25 and above 2 µm in diameter. A comparison between the simulated and an experimental size distribution is shown in Figure 23, where normalisation is obtained by the size fraction cut-off described above.

The initial dry solids concentration of the slurry was 65 wt-% and the post-metering thickness of the coating layers was set between 10 and 30 µm. This covers a typical thickness range between LWC and double or triple coated paper (e.g. board coating). Colloidal suspension properties were selected based on experimental measurements by Eriksson et al. (2007) and parameters reported in the literature (II; Ackler et al. 1996; Vanni, Baldi 2002). The electrostatic double layer thickness, κ^{-1}, was set to 5 nm, the Hamaker constant, A_H, estimated as $1.0 \cdot 10^{-21}$ J and the surface potential of interacting particles, ψ_1 and ψ_2 was set to -25 mV.

The base substrate was described by a boundary-plane which allowed liquid absorption. The boundary does not allow penetration of solid particles, thus assuming a complete coating holdout.

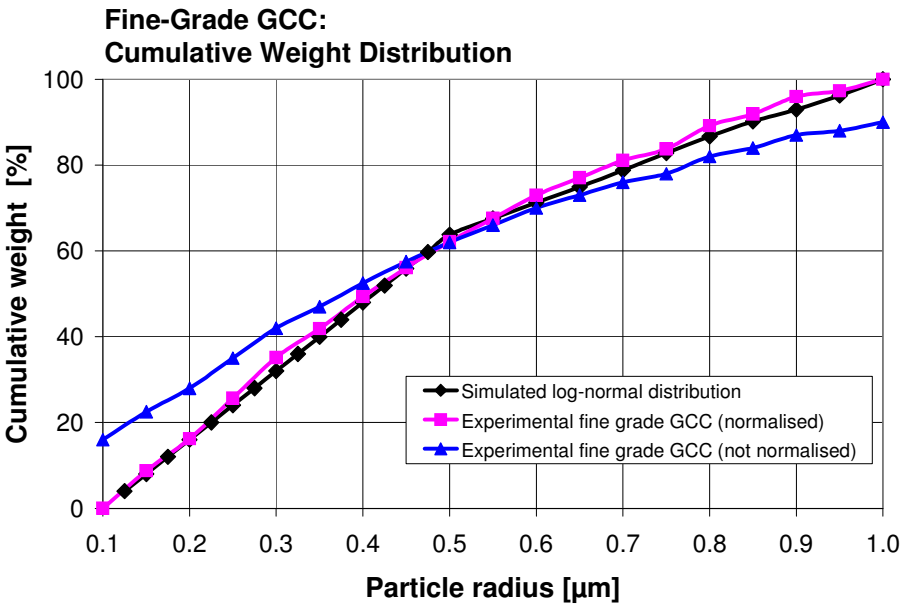

Figure 23. Simulated and experimentally measured cumulative weight distribution of fine-grade GCC (Sand et al. 2008b).

Based on consolidation simulations and using the different drying strategies described previously, the solids concentration profile development and coating layer formation could be monitored in time. Additionally, it is possible to track the redistribution of the binder-sized particle fraction and coating layer shrinkage. Coating layer immobilisation times could be identified by observing the stabilisation of the coating layer mass distribution, as exemplified in Figure 24. Depending on their thickness and the drying strategy, the coatings were typically immobilised within 0.3 to 0.5 seconds at around 85 wt-% dry solids, Figure 25.

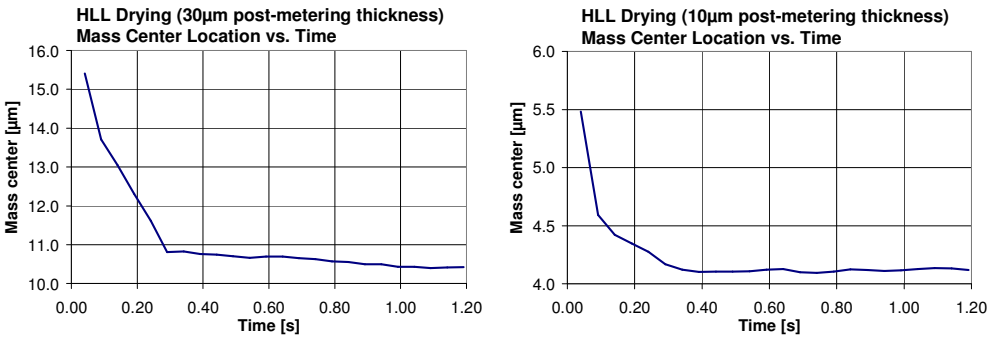

Figure 24. Mass centre location versus time for two different coating layer thicknesses. Results can be utilised in estimating immobilisation time.

The immobilisation point is traditionally defined as the point when water begins to form menisci on the coating layer surface (Lepoutre 1989), and is also known as the first critical concentration (FCC). This view on immobilisation naturally originates from a difficulty in monitoring internal structure formation of the coating layer during experimental studies on consolidation. The simulation-based approach does not experience these constraints. Thus, the definition of coating immobilisation used in this work differs from the traditional one (Lepoutre 1989). Immobilisation is here assumed to take place when the mass displacement within the layer evens out.

As is already suggested in Figure 24, the thinner coating layer consolidated more rapidly as compared to the thicker coating. To gain an understanding of the structure formation, the dry solids concentration profile was monitored in the z-direction for the same case as reported above. The results are presented in Figure 25. Thus, the structure formation is compared at different coating layer thicknesses but for the same drying strategy. The thinner coating layers consolidated very rapidly, and were typical in that there were no significant cross-structural solids concentration gradients arising as result of filter cake formation or skinning. The thicker coating layers on the other hand, showed a clear filter cake formation during the early stages of consolidation.

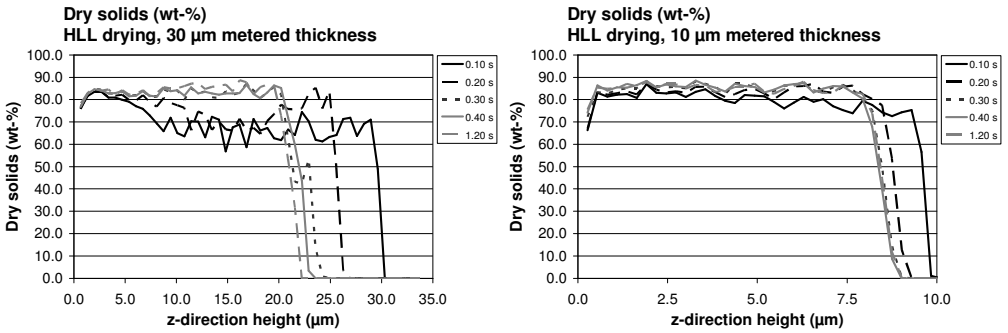

Figure 25. Structure formation in the 30 µm and the 10 µm layer, compared at the same drying strategy.

The difference in structure formation varied significantly as a function of the drying strategy, Figure 26. In all the cases except that of pure evaporation, filter cake formation initially dominated. Immobilisation was very fast in the HLL and pure absorption cases, while being significantly slower in the LLH and pure evaporation cases.

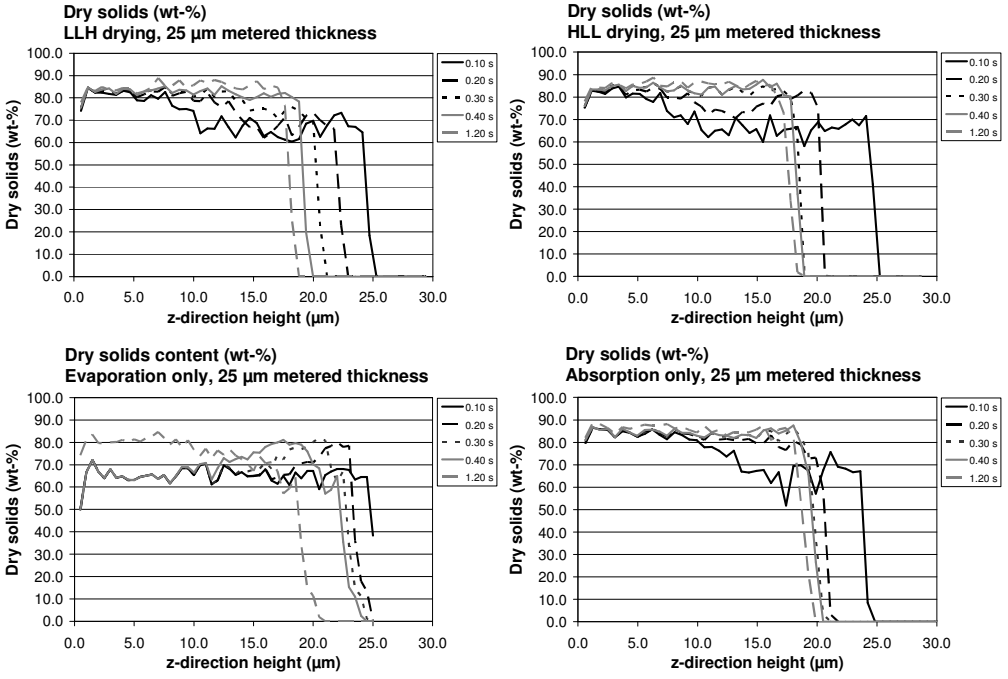

Figure 26. Solids structure development of the 25 µm coating layers compared at different drying strategies.

The drying strategies with strong initial evaporation, exhibited clearly observable skinning. The effect was significant in the HLL drying strategy, but also existed to some extent in the EVA case. In the mild initial drying case (LLH), the coating layer was already sufficiently dewatered at the initiation of the more intense drying stage to not allow skin formation. Z-direction concentration gradients arising as result of the drying strategy used, normally persisted up until several tenths of a second before immobilisation, at which point the concentrations evened out.

Particle distribution in consolidating coating layers was characterised by the number distribution and volume fractions of particles as a function of the z-direction position in the coating layer. The number distribution is the relative number of particles of a given size range in a specific position interval of the coating layer. The volume fraction, on the other hand, reports on the volume of particles of a certain size range divided by the total volume of solids within the specified position. Thus, the volume fraction is a way of normalising the particle distribution to the total solids concentration.

It can be assumed that in absorption-dominated dewatering profiles, with the prerequisite of at least some degree of coating holdout, there will be a gradual accumulation of small particles at the coating/ base substrate interface. Normalised to the higher solids content, it becomes less evident that there would be preferential accumulation of any particular size fraction in the filter cake region. However, it can also be expected that some particles are able to penetrate through voids between larger particles to generate a higher relative concentration of small particles. This should also be put in context with the particle size segregation that typically takes place in dynamic polydisperse particle systems (e.g. Williams 1976; Rosato et al. 1986). Similarly, evaporation dominated drying strategies can be expected to produce small

particle accumulation at the top of the coating layer. The distribution of particles in the 25 µm coating layers, reported as particle fraction, is shown in Figure 27.

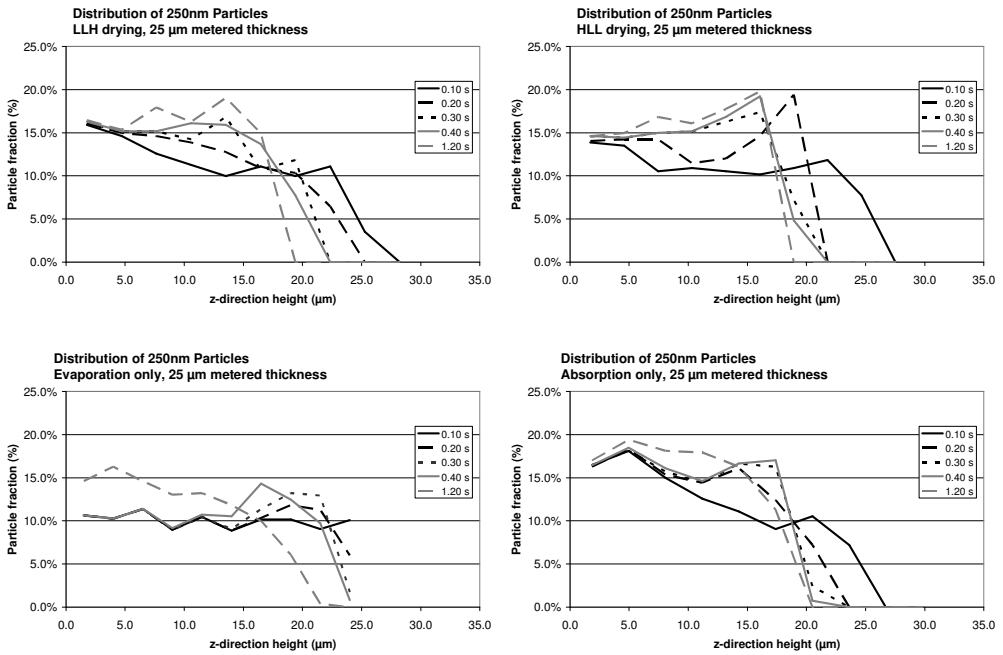

Figure 27. Redistributions of 250 nm particles over time, represented as particle fractions.

As was predicted theoretically, small particles accumulated in the filter cake when dewatering strategies including base substrate absorption was applied. Therefore, if the base substrate has an open structure, a loss of small pigment particles and binder to the base substrate can be expected. This has been reported for low solids content spray coating colours (Hämäläinen et al. 2002). In strategies where evaporation dominated, especially in the HLL case, there was a strong accumulation of small particles close to the surface of the coating. Such effects result when the surface tension and free surface hydrodynamics accumulate pigment particles faster than the Brownian motion allows them to redistribute in the coating layer. It was observed, however, that slowly dewatering coating layers had sufficient time to allow particle redistribution and

obtain a relatively even distribution profile in the z-direction. This was the case for the LLH and evaporation drying strategies. As the evaporation also causes local accumulation of larger particles, normalisation to the total dry solids is necessary for elucidating any preferential redistribution of small particles. When normalising the particle distribution to the dry solids concentration to show small particle distribution as volume fractions, Figure 28, the distribution profile was found to be almost constant throughout the layers. The even profiles are a sign of that small particles distribute according to the overall distribution of solids, without any significant deviations.

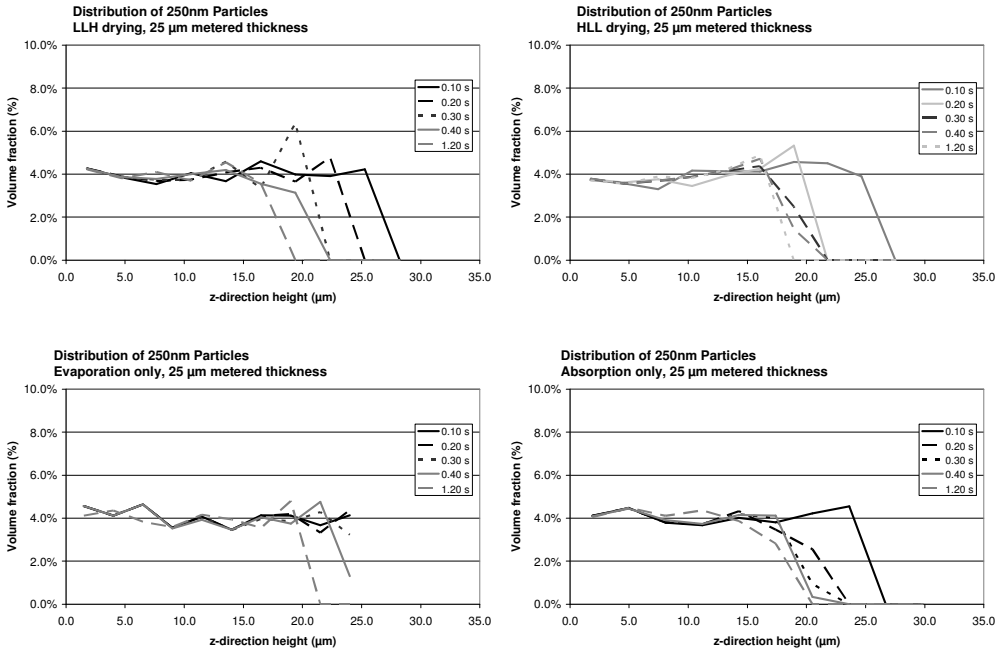

Figure 28. Redistributions of 250 nm particles over time, represented as volume fractions.

An accumulation of small particles could be observed when using HLL or evaporation drying, some 25% more than in the LLH and absorption cases. This might indicate that drying strategies including strong initial dewatering through evaporation can have an influence on the redistribution of binder-sized particles

in consolidating coating layers. Conversely, small particle accumulation was not observed in the filter cake region, even if the dewatering strategy would be dominated by absorption. Additionally, filter cake formation takes place much faster than skinning, and does not allow sufficient time for the particles to rearrange to any preferred location.

The drying strategy was concluded to have a clear influence on the dry solids concentration profile during consolidation. The solids profiles did, however, not persist until full immobilisation. It should also be noted that the use of thickeners or other additives to the coating suspension might lead to earlier immobilisation. This could in turn "freeze" solids concentration gradients into the structure. Consequently, regions of low porosity could result at either the base substrate or top of the coating, or both. Conversely, a region of high porosity would be formed in the bulk of the coating. The findings regarding the small particle distributions were ambiguous, though there were some signs of preferential accumulation either to the filter cake or skin side of the coating.

This part of the work furthers existing knowledge on coating consolidation mechanisms and structure formation during drying. The results can aid in the tuning of the drying strategy depending on the desired microstructure. By example, controlling the porosity of the top of the coating can be useful in obtaining a coated paper with desired printing properties. The distribution of small particles in the coating layer depending on drying conditions, might improve current understanding of binder migration.

4.3 Particle Mobility

Understanding of particle mobility in consolidating coating layers is paramount for the study of displacement mechanisms, which could explain phenomena such as particle migration and redistribution. The dynamics of particle motion in consolidating coating layers was tracked for various dewatering strategies and complements the study performed on the influence of drying strategy on coating layer structure formation.

The configuration of particle systems and simulation conditions are equivalent to that of the structure formation study at different drying strategies (II). This study however, focuses only on the mobility of small particles ($D \leq 300$ nm). This size is roughly comparable to the size of binders, although it should be noted that limitations in computation time and memory usage disallowed a quantitative representation of the binder fraction in a typical coating formulation. Direct visualisation of particle systems, including colouring either by their local (relative to each other at a given timestep) or global (relative to each other as calculated over the entire simulation time) velocities, allows for a qualitative observation of particle mobility. Such an example is shown in Figure 29, where particles are coloured according to their global velocities.

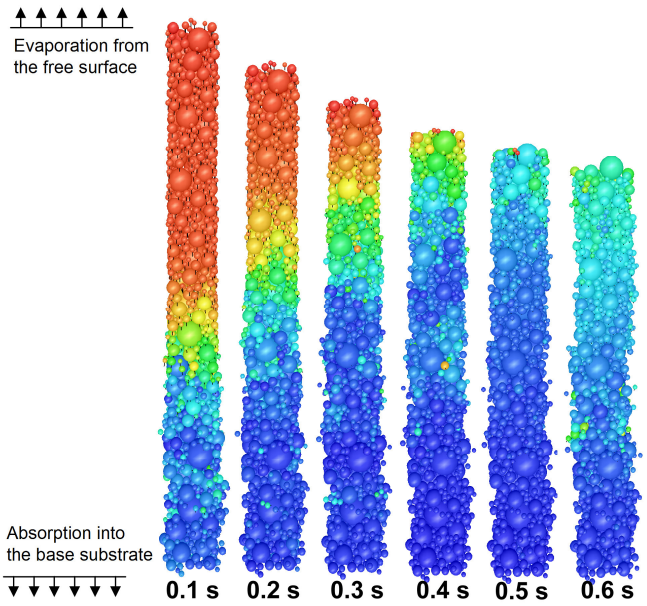

Figure 29. Visualisation of particle mobility utilising the LLH drying strategy (30 µm thickness, ψ = 50 mV, 1/κ = 5 nm). Particles are coloured according to their (global) velocity, where red is fastest and blue slowest.

Particle displacement distributions can be utilised as an indication of particle mobility and potential redistribution during consolidation. By reporting on separate displacements in the lateral and vertical directions, it is possible to distinguish between particle mobility in z-direction and the machine (MD) and cross directions (CD). In this work, movement in z-direction is referred to as vertical motion.

To illustrate the nature of particle mobility in various positions of the coating layer, the displacement distribution is illustrated at four different z-positions in Figure 30.

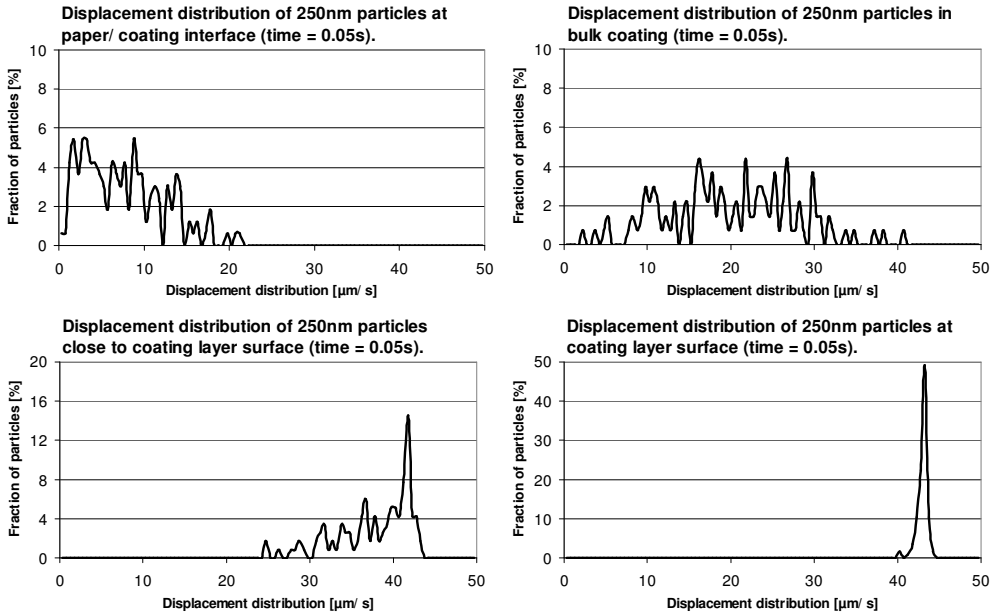

Figure 30. Displacement distributions of small particles at various z-direction positions utilising the HLL dewatering profile (10 µm coating thickness at 0.05 s).

A sharp peak of high displacement at the coating layer surface shows that the flow of liquid, both through absorption and evaporation, dominates over particle interactions and diffusion effects. Already somewhat below the surface level, the distribution can be seen to broaden as the interactions between particles increase. In the bulk suspension, the displacement distribution begins to resemble an undulating normal distribution, which indicates a strong influence of particle interactions as well as particle movement as result of Brownian motion. At the base substrate/ coating interface, the distribution is tilted towards shorter displacements. This is believed to result from a higher degree of particle pinning, either due to contact with the base substrate or within the high particle concentration region arising in the filter cake.

The displacement distributions were also separated into their x-, y- and z-direction components to enable an investigation of differences between the vertical and lateral motion of particles. The lateral motion of particles is defined

as the average between the x- and y-direction vectors. For instance, studying the directionwise displacement distributions of the 10 µm coating layer dried using the HLL strategy, lateral displacement dominated at the substrate/ filter cake boundary, Figure 31. This is believed to be a result of pinning of particles from movement in the z-direction, caused by the weak absorption flow of liquid into the base substrate.

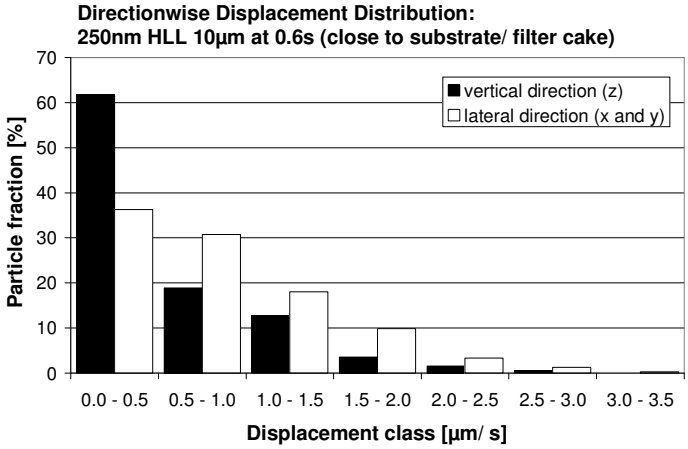

Figure 31. Displacement distribution for 250 nm particles in the 10 µm layer, separated into their vertical and lateral direction components.

The same effect could also be observed at the top of the coating layer during the early stages of consolidation. The z-direction displacement of particles was dominated by the absorption flow of liquid caused by hydrodynamic interactions with the free surface. When comparing the different drying strategies, Figure 32, it was found that particle mobility was enhanced in the drying cases, which resulted in higher solids concentration caused by skinning. For example, the HLL drying strategy produced skinning at the top of the coating and 82 wt-% solids, while the LLH case did not produce skinning and reached only 68 wt-% solids. Simultaneously, the lateral direction mobility was significantly higher in the HLL-case.

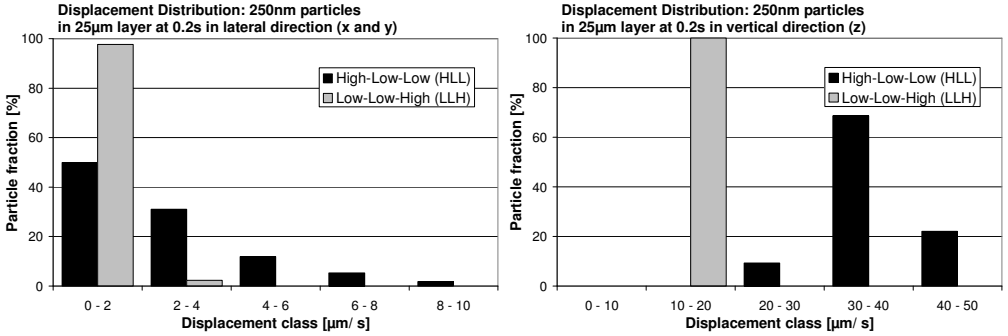

Figure 32. Directionwise (lateral and vertical, respectively) displacement distributions of 250 nm particles in the 25 µm layer close to the free surface after 0.2 s of consolidation.

This difference in lateral mobility between the drying strategies cannot be explained by similar z-direction pinning as is argued to be the case in the filter cake. Instead, it could possibly be a result of a laterally directed force on particles caused by the electrostatic repulsion component of the DLVO model. Another influential factor could be the hydrodynamic force between particles as the solids concentration is initially directionally dependent, due to the absorption and evaporation flows generating a denser layer in z-direction. The concentration difference between the lateral and vertical directions consequently needs to be evened out by lateral-direction redistribution of particles, as is illustrated schematically in Figure 33.

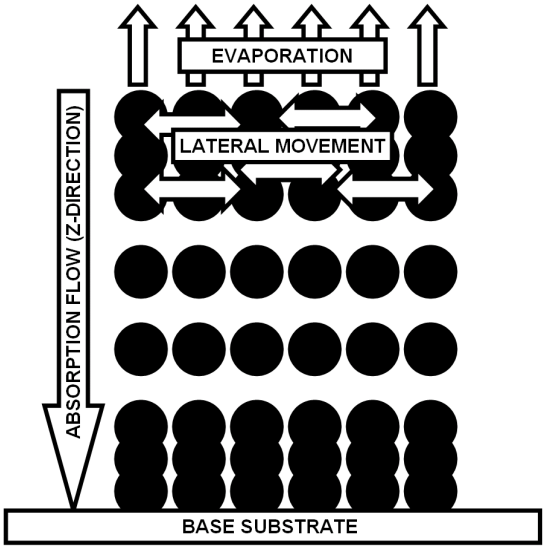

Figure 33. Schematic illustration of the lateral movement of particles in the top layer of the coating. Electrostatic repulsion and hydrodynamic interactions produce a laterally directed force.

Comparing the two model cases, pure absorption and pure evaporation, the mechanisms for consolidation are fundamentally different. As the absorption case entails rapid initial filter cake formation, the layer will dewater much faster than is the case in evaporation. Thus, following the same argument as in the discussion above, the absorption case can be expected to exhibit greater lateral mobility due to the higher solids concentration. This is confirmed by the results in Figure 34. The z-direction mobility is also higher, as result of the dewatering rate being higher in the absorption case and due to the absorption flow of liquid which does not take place during evaporation.

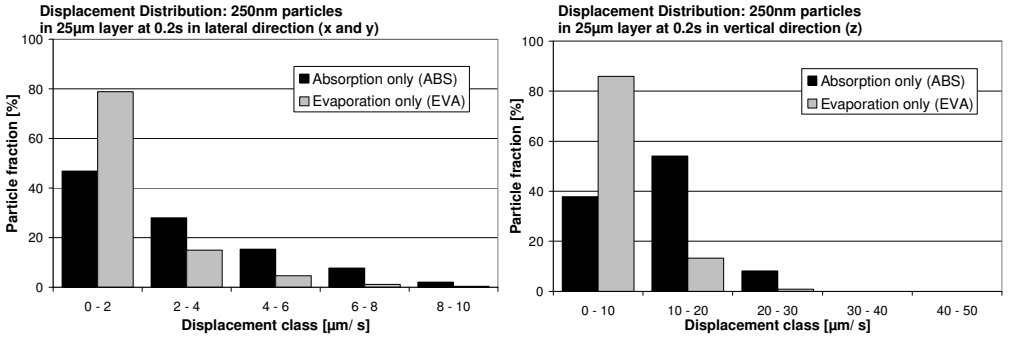

Figure 34. Directionwise (lateral and vertical, respectively) displacement distributions of 250 nm particles in the 25 µm coating layer close to the free surface (after 0.2 s of consolidation).

By studying the dynamics of particle mobility inside consolidating coating layers, the fundamental knowledge of phenomena related to particle migration is improved. Furthermore, some insight may also be provided regarding the vertical and lateral distribution of coating components. The results offer a deeper understanding of structure formation and particle distribution within the coating layer.

4.4 Colloidal Interactions

In order to understand the relevance of colloidal interactions on the structure formation of the coating layer, coating layer consolidation was simulated by including colloidal interaction models in conjunction with a range of different DLVO-parameters. The behaviour of colloidal suspensions is governed by the balance between the colloidal, external and hydrodynamic forces between particles. Given that the colloidal forces can be influenced by chemical additives, simulation of particle interactions can be useful in understanding and linking the microscopic and macroscopic behaviours of the suspensions. The objective of this study was to increase current understanding on how the

chemical properties of the pigment suspension influence the consolidation and microstructure of the coating layer. Furthermore, to give guidance as to how chemical additives may can be useful in producing a coating layer with desirable microstructural properties.

Colloidal interaction model parameters deemed realistic for coating suspensions, Table 3, were obtained from experimental measurements (Eriksson et al. 2007) and the literature (Vanni, Baldi 2002; Ackler et al. 1996). Coating layers of 20 to 30 µm were simulated, as these thicknesses were in the earlier studies found most useful in investigating cross-structural solids profile development (Sand et al. 2008a). The particle system setup was identical to the previous studies using polydisperse GCC-resembling particle size distributions.

Table 3. Colloidal interaction model parameters

Symbol	Value	Description
Electrostatic repulsion parameters		
ε_r	80	Continuous phase dielectric constant (water)
ε_0	8.85×10^{-12} C^2/Nm^2	Permittivity of vacuum
ψ_1, ψ_2	-50 to +50 mV	Surface potential of interacting particles
$1/\kappa$	2.5 to 10.0 nm	Double layer thickness
Van der Waals attraction parameters		
A_H	1×10^{-21} J	Hamaker constant
λ	100×10^{-9} m	London characteristic wavelength

Double layer thicknesses, $1/\kappa$, of 2.5 to 10 nm and surface potentials, ψ, between -50 and +50 mV were tested. It should be noted that the electrostatic repulsion model, which calculates the repulsive forces resulting from charged particle interactions, does not differentiate between positive and negative potentials.

Surface potentials of calcite in aqueous suspensions are, as also represented in Eriksson et al. (2007), typically described by the zeta potential, ζ. It can be measured by a number of different techniques (Madsen 2002), but as it measures the potential at a certain distance from the particle surface it does not directly correspond to the surface potential, ψ. The relationship between the surface potential and zeta potential can be derived using the Stern model of the double layer. However, given the surface potential range of this study, it is believed that the results are well applicable to calcite/ water dispersions.

The dielectric constant of the continuous phase (water/ electrolyte) was estimated to be constant, although other studies have reported variations depending on electrolyte concentration. As the solubility of calcite in water is low at high pH, and the concentration of other ions is also expected to be relatively low, the influence of changes in the dielectric permittivity on electrostatic repulsion can be considered negligible (Navarkhele et al. 1998).

The influence of the continuous (liquid) phase viscosity on the structure formation of coating layers was studied for a few select cases. The viscosity of coating slurries can be altered by several different mechanisms, including bridging effects of adsorbed polymers, depletion flocculation, or simply by an increase of the viscosity of the liquid phase. The influence of increasing the viscosity of the liquid phase was illustrated by simulating consolidations at 3 different viscosities and comparing the differences in the microstructures, Figure 35.

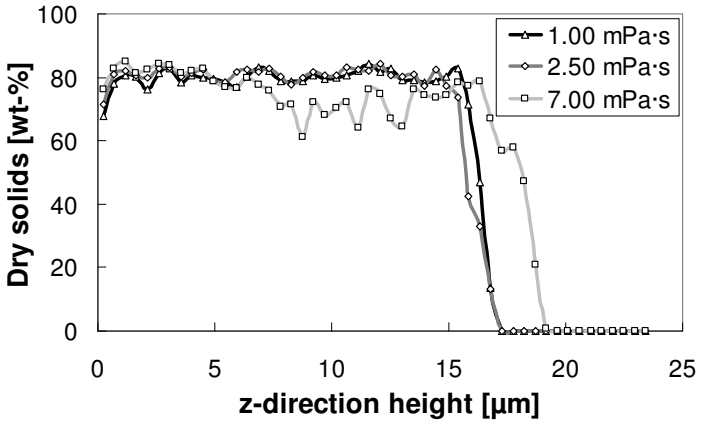

Figure 35. Solids structure depending on continuous phase viscosity (20 µm layer, $1/\kappa$ = 10 nm, ψ = -50 mV at 0.2 s).

An increase in viscosity slowed down the consolidation of the coating layer. If the immobilisation time is the same, a higher viscosity could thus hinder levelling of the solids concentration in the z-direction. This could also result in reduced shrinkage of the coating layer. A consequence of this would be a more porous coating structure along with persisting solids concentration gradients both towards the base substrate and, depending on drying strategy, also at the top of the coating layer.

As illustrated in Figure 36, the particle surface potential was shown to have a significant influence on the shrinkage of the coating layer. Particle surface potentials between 0 and 10 mV produced much thicker coating layers when compared to particle surface potentials above 10 mV.

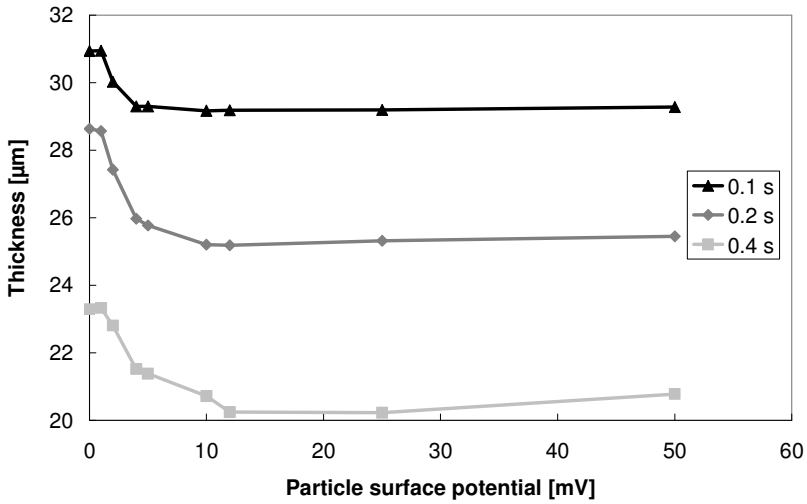

Figure 36. Coating layer thickness versus particle surface potential at different times (30 µm layer, $1/\kappa$ = 10 nm).

It was also noted that the particle surface potential did not have any significant systematic impact on the internal coating layer structure, Figure 37. Reduced electrostatic repulsion did thus not yield denser structures. This can be seen as somewhat counterintuitive, as the van der Waals attractive forces will increase in significance. The effect can be explained however, by the attractive forces that promote the generation of loosely packed particle aggregates (flocculation) that hinder particles from arranging into denser structures.

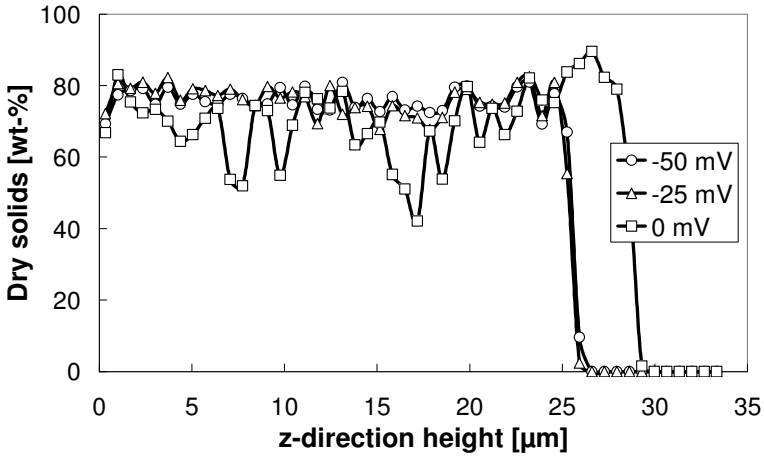

Figure 37. Solids structure in the z-direction of the 30 µm coating layer ($1/\kappa$ = 10 nm at 0.2 s) when applying different particle surface potentials.

As can be concluded from Figure 38, the consolidation and shrinkage of the coating layer proceeded at roughly the same rate regardless of the particle surface potential.

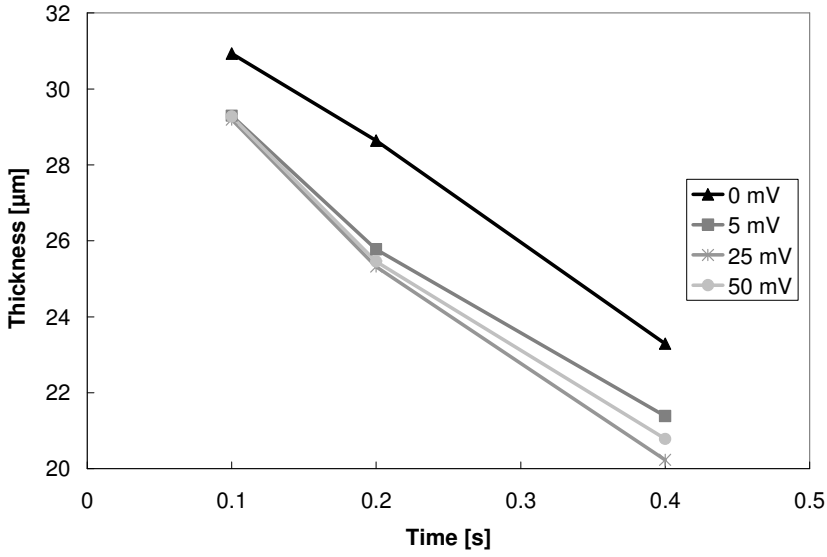

Figure 38. Coating layer shrinkage at different particle surface potentials (30 µm layer, $1/\kappa$ = 10 nm).

Particle arrangement within the coating layer can be quantified and illustrated using surface separation distributions as well as particle cluster visualisation. The radial distribution function is produced by calculating the surface separations from each particle to its nearby neighbours. The resulting probability distribution at the given colloidal parameter settings, is an indication of the average interparticle separation and its standard deviation. Strong particle clustering is revealed by a sharp peak at short interparticle separation, while more loose structures are seen as broad distribution regions at longer surface separation distances. The surface separation distribution in some simulations with different colloidal parameter selections are shown in Figure 39.

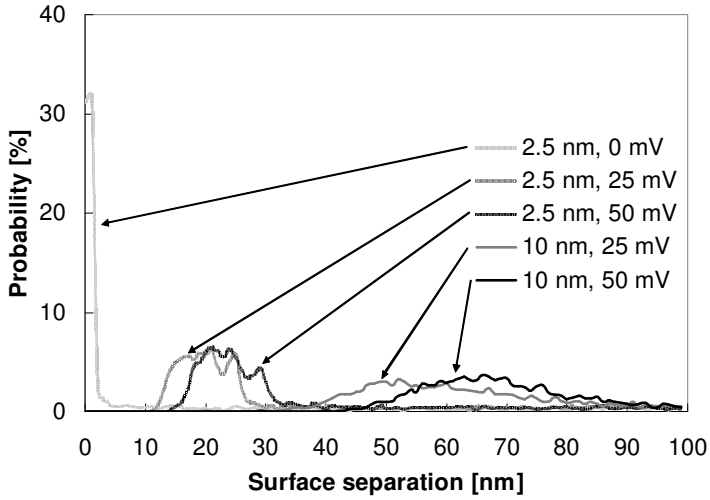

Figure 39. Surface separation distributions at different colloidal parameter settings.

It can be observed that the low particle surface potential is a strong promoter of particle agglomeration, while particles are more capable of moving and rearranging at high surface potentials and double layer thicknesses. Using cluster analysis, it is possible to confirm the effect of particle agglomeration in the low surface potential layers, as shown in Figure 40.

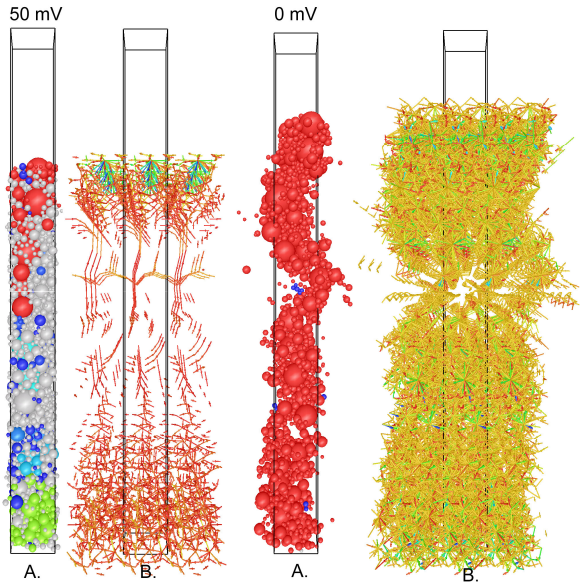

Figure 40. Cluster analysis of the 50 and 0 mV particle surface potential cases at 0.2 s. The clusters are shown in colour according to relative size (red=largest, blue=smallest), while non-clustered particles are grey. The A subfigures represent particle clusters, while the B subfigures show interparticle connections. The threshold value for clustering is 50 nm.

Figure 40 shows that even though a 0 mV particle surface potential produces a relatively thick coating layer, the particles are still strongly agglomerated. This is in contrast to the 50 mV case, which mainly exhibits clustering in the filter cake and the skin. Lateral redistribution of particles in the 0 mV layer (the visualisation does not include particle wrapping due to the periodic boundary condition) also illustrates the higher rigidness of this structure.

The impact of double layer thickness on structure formation was studied using values ranging from 2.5 to 10 nm in the simulations. The minimum double layer thickness was 2.5 nm due to the steepness of the interaction energy curve. Numerical difficulties and the exponential increase in computation time disallowed simulation at lower values. It has been reported however, that double layer thicknesses in calcite particle slurries can be expected in the 5 to 10 nm range (Hiemenz 1986). The solids structure of the 30 µm coating at different double layer thicknesses is shown in Figure 41.

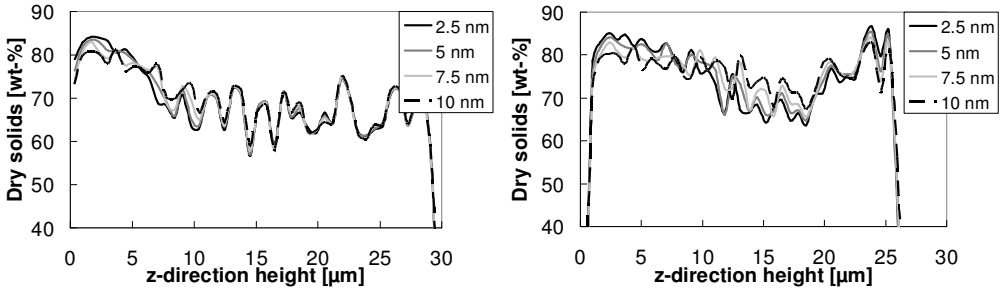

Figure 41. Dry solids structure in the 30 µm coating layer at different double layer thicknesses (ψ = 25 mV). At time 0.1 s left, and 0.2 s right.

The double layer thickness had only a slight influence on the thickness of the coating layer. Internally however, it appeared that lower double layer thicknesses strongly promoted the formation of z-direction cross structural solids concentration gradients. The effect was observed both in the filter cake formation and skinning at the top of the coating layer.

An alternative possibility for illustrating structural differences in the coating layer is to plot the cumulative dry solids content as a function of the z-direction position in the coating layer. This mode of illustration evens out solids concentration fluctuations and helps to accentuate and identify systematic differences in the structures. Figure 42 shows the cumulative solids content at 0.2 seconds, which corresponds to the illustration on the right side in Figure 41.

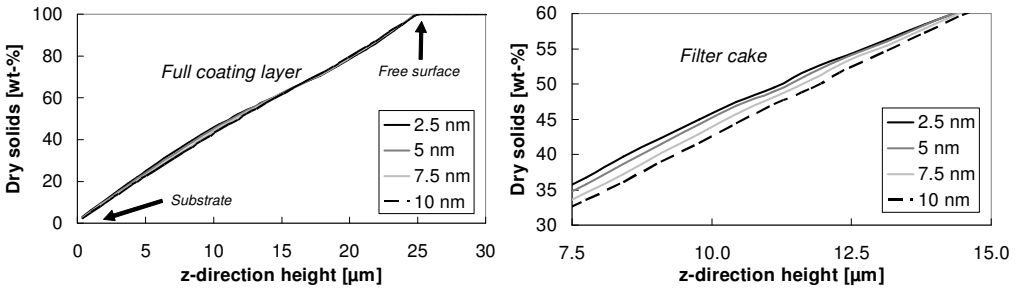

Figure 42. Cumulative dry solids content in the 30 µm coating layer (ψ = 25 mV). The full coating layer to the left and an enlargement of the filter cake region to the right.

Figure 42 shows the double layer thickness to mainly influence the structure development of the filter cake, but also to a lesser extent in the skin. The difference in dry solids concentration between the highest and lowest double layer thicknesses in the filter cake was about 5 wt-%, while being only around 2 wt-% in the skin. These differences are relatively small and do not necessarily have practical importance. It should nevertheless be noted that evaporation might help to decrease the thickness of the electrostatic double layer and possibly also aid in coagulating the system into the primary minimum of the interaction energy curve.

Similarly to the study on particle surface potentials, it is also possible to illustrate differences in the internal coating layer structure using cluster visualisation tools. For the same simulation as described above, coating layer formation and particle agglomeration mechanisms are illustrated in Figure 43.

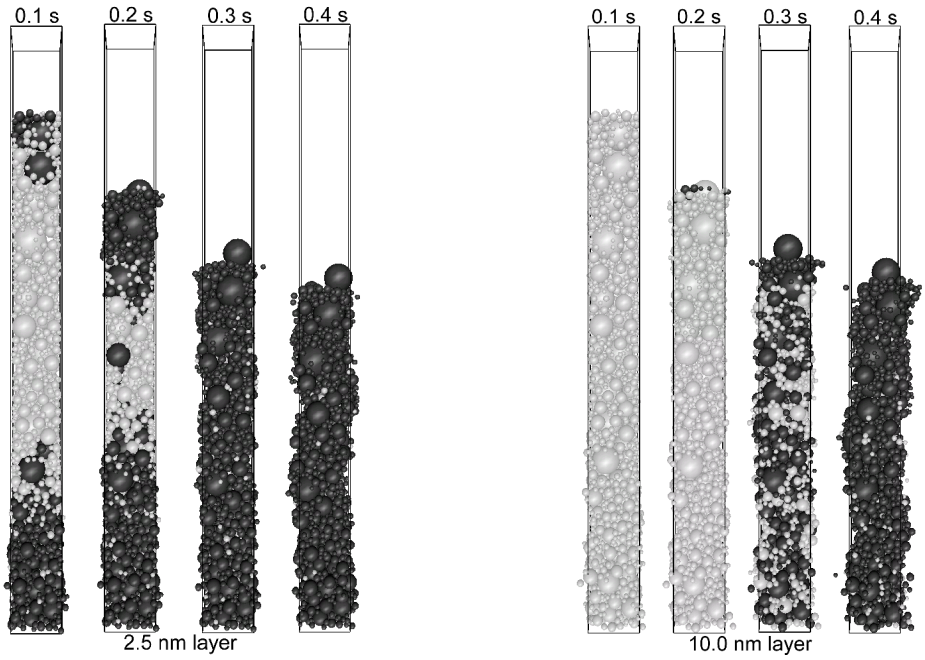

Figure 43. Consolidation visualisation at two different double layer thicknesses; 2.5 and 10 nm (ψ = 25 mV, HLL drying). The threshold for clustering is set to 20 nm.

Although the coating thickness is the same at corresponding simulation times in both cases, there is an observable difference in the internal coating structure development. For the 10 nm double layer thickness, the structure forms quite evenly, while tending to exhibit local particle agglomeration in the filter cake and skin in the 2.5 nm layer.

The colloidal interaction parameters had an influence on both the microstructure formation of the coating and its thickness. In coating suspensions, the particle surface potential of pigments is influenced by adsorbed chemicals on their surfaces and the double layer thickness is reflected by the ion concentration in the continuous phase. Thus, the results may aid in the dosing of chemical additives to control the properties of the coating suspension and producing coating layers of desired porosity and structural properties.

4.5 Particle Clustering Mechanisms

The same simulations as performed and analysed in terms of drying strategy, particle mobility and influence of colloidal interaction were further investigated using the particle clustering algorithm. Cluster analysis and visualisation of coating structures can be a useful tool in highlighting and explaining solids concentration differences and particle agglomeration in particle systems. It also enables a direct observation of clustering mechanisms that can have an impact on the macroscopic properties of the coating layer.

The consolidation process at LLH drying is illustrated at the 50 mV and 0 mV particle surface potentials, Figure 44. The results in this case show that no skinning takes place at the higher particle surface potential. This can also be concluded from the earlier studies on drying, Figure 26. The mild drying rate from the surface of the coating therefore allows the base substrate absorption to

dominate the dewatering of the coating layer. The more intense drying step at the later stages of consolidation takes place at a point where the layer is already fully clustered, which radically reduces the potential for skinning. Consequently, rapid filter cake growth continues until the layer is fully clustered at around 0.4 seconds. Note that even though the layer is fully clustered, shrinkage of the coating can still continue. However, the possibility for z-direction solids concentration gradients to be formed at this late stage in the consolidation is low. Identically to the HLL drying case in Figure 40, the absence of electrostatic repulsion between particles causes full agglomeration of the layer already at an early stage of consolidation. The inflexibility of the system due to attraction between particles impedes shrinkage. This can only proceed by a strenuous and relatively slow rearrangement in the lateral directions. In practical consolidation, adjustments to the surface potential might thus be useful in controlling the porosity of the coating layer. By adjustment of the drying strategy in combination with colloidal parameters, it is also possible to produce coating layers with desirable z-direction concentration profiles.

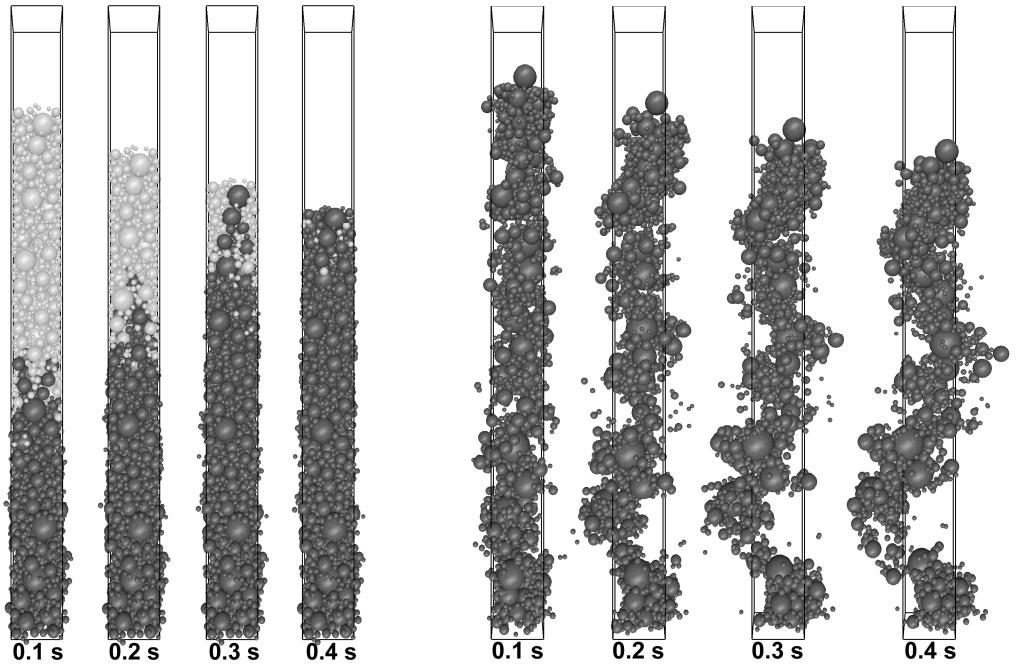

Figure 44. Consolidating particle layers at 50 mV particle surface potential (left) and 0 mV (right), applying the LLH drying strategy (1/κ = 5 nm, clustering threshold 50 nm).

The electrostatic double layer thickness has only a slight influence on the thickness development of the coating layer. However, the internal structure can be made to vary significantly by adjusting the double layer thickness. At the LLH drying strategy, consolidation proceeds by fast filter cake formation in the thin double layer thickness case. If the electrostatic double layer is thick, the consolidation proceeds uniformly over the layer, until a point is reached where the whole structure begins to cluster, as shown in Figure 45. Comparing the consolidation of 10 nm double layer coatings in two drying strategies based on experiments, Figure 43 and Figure 45, it appears that adjustments to the colloidal properties of the coating formulation can to some extent be used to offset the impact of the drying strategy.

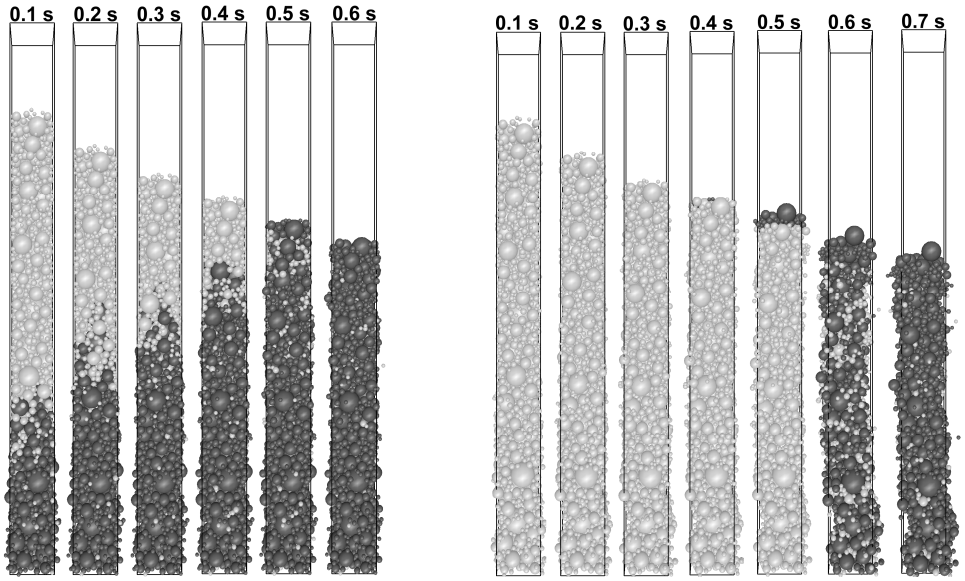

Figure 45. Consolidating particle layers (LLH drying) at 2.5 nm double layer thickness (left) and 10 nm (right). Clustered particles are dark, unclustered light (ψ = 25 mV, clustering threshold 20 nm).

By using filtering, as well as interparticle cluster connections, it becomes possible to study particle agglomeration mechanisms that take place during consolidation. One such observation from the simulations was the emergence of "fingered" structures in the un-concentrated bulk coating. It is possible that such structures provide skeletal support to the microstructure in more porous regions of the coating during consolidation. This can have an effect on shrinkage and may also limit lateral redistribution of particles. An example of the fingering effect is shown in Figure 46, where the effect can be noted at around 0.2 seconds. The effect, which has typically been observed in 2D-levelling of coating layers during drying (Toivakka et al. 1992) or rheological studies (Toivakka, Eklund 1994), therefore also seems to take place in 3D. The "fingered" structures arising in the coating layer could span over as many as 5-6 particles, accounting for a third of the coating layer. The typical growth direction was from the filtercake side due to the high relative volume of liquid dewatered by absorption. However, it is fully feasible to find such fingering

taking place also from the skin, given a very intense drying strategy or high levels of evaporation relative to absorption. In their nature, finger structures can be expected to be fairly sensitive to abrupt changes during the process of consolidation.

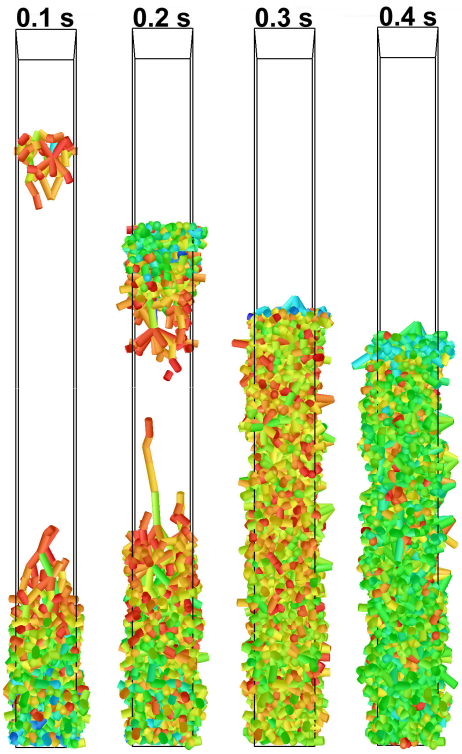

Figure 46. Consolidating of particle system, with arising "fingering" (HLL drying strategy, ψ = +25 mV, 1/κ = 2.5 nm, clustering threshold 20 nm). Visualisation of cluster connections (red = closer distance, blue = longer distance).

Cluster visualisation can be a useful tool in highlighting and explaining concentration differences and particle agglomeration in particle systems. Clustering mechanisms influencing the macroscopic properties of coating layers could also be identified. The work illustrates the interplay between the properties of the pigment suspension and the drying strategy in forming the structure of the coating layer. Furthermore, the work aids in the dosing of

chemicals and tuning of the drying process to produce coating layers of desirable microstructure.

5. CONCLUDING REMARKS

The current study employs a Stokesian dynamics-based technique in simulating the consolidation of particle systems that resemble pigment coatings. The model included full 3D particle motion, polydisperse particle size distributions, and interactions by hydrodynamics and colloidal forces. A novel Brownian motion model was included in the simulation technique. Particle dynamics simulations were performed, coupled to experimentally-obtained boundary conditions such as coating layer dewatering rates, colloidal interaction parameters and particle size distributions. The systems were designed to be relevant for practical coating processes, whilst still developing current theory on the mechanisms that take place. The focus was on the dynamical behaviour of coating suspensions during consolidation.

The stability of filter cakes was studied for a set of different base substrate absorption rates, particle sizes, size distributions and temperatures. It was found that the structure of the filter cake depended primarily on the absorption rate and particle size. The system temperature also appeared to have some impact. Filter cake concentration gradients in polydisperse systems were also found to be influenced by filter cake surface roughness as well as size segregation effects. Conflicting experimental results in the literature could in part be explained by differences in experimental conditions. In conditions typical for pigment coating of paper, a sharp filter cake can be expected.

The influence of the drying strategy on the structure formation and small particle distribution within coating layers was studied using 4 pilot trial and model based dewatering profiles. The z-direction dry solids profile was shown to vary significantly depending on the drying strategy and both filter cake formation and skinning could be observed. Dry solids profiles arising during the early stages of consolidation tended to even out over time, while the

small particle distributions also tended to persist after immobilisation. Furthermore, the fundamental mechanisms of particle movement and redistribution were studied. The most important findings were the correlation between local solids concentration and particle mobility, and the influence of the drying strategy on particle mobility.

The last part of the work investigated the influence of colloidal interactions on the consolidation of coating layers, including coating layer shrinkage, internal microstructure development, and particle agglomeration mechanisms (clustering). The particle surface potential was found to influence the thickness of the coating layer, while having a lesser effect on the internal microstructure. The thickness was influenced primarily by particle clustering phenomena that take place as a result of reduced electrostatic repulsion. Double layer thickness had a negligible influence on the shrinkage of the coating layer, but was found to impact the internal solids structure gradients of the coating layer. Both skinning and filter cake formation were accentuated at low double layer thicknesses. The results were also correlated with the drying strategy.

Since direct experimental verification of the simulation results in this work is difficult, if not impossible, caution should be exercised when drawing conclusions based on the simulations. The mechanisms identified should be interpreted in context of experimental observations of systems similar to those modelled in this work. Nevertheless, the work improves the current understanding of how processing conditions and suspension properties influence the consolidation of pigment coating layers. The results may find applicability both in tuning the drying strategy and chemical additives to the coating formulation, in order to produce a coated paper with a desirable porosity profile and cross-layer particle distribution.

6. SUGGESTIONS FOR FURTHER WORK

While this study takes an applied approach to particle dynamics simulation of consolidating pigment coatings, there are several possibilities for developing the simulation technique, its constituent models, and to apply the current technique in studying as yet uninvestigated coating related phenomena.

The limitations of the model are related to the lack of back-coupling between particle movement and the flow of the liquid phase, limitations in the number of particles and invalidity of the model as air starts to enter the coating structure. However, increased simulation capacity and computational systems based on parallel processing might relieve some of the limitations in the future. There are also uncertainties in colloidal force parameters, considering the complexity of pigment coating systems where parameters change during the consolidation process. Depletion and bridging forces resulting from liquid phase or adsorbed polymers could be included. Furthermore, there is a need to generate more complex base substrate structures and liquid flow profiles based on system geometry. This possibility has to some extent been explored using the Elmer software (Nopola 2004), but there is still a need for more advanced simulation schemes to take dynamic changes in the system geometry into account. The inclusion of different particle properties (e.g. density and surface properties) in simulations could provide a more accurate understanding of the behaviour of pigment/ binder systems. The currently available hydrodynamic pairwise interaction force models are limited to a maximum size ratio of 10 between particles. This does not allow simulation of nanoscale particles within the coating and thus leaves out particulate binders and thickeners smaller than 100 nm. Furthermore, the limitation to spherical particles could in future work be relieved by “gluing” spherical particles together to form more complex shapes.

Finally, there are still a wide range of simulations carried out in 2D, which with the current improvements to the simulation technique could also easily be carried out in 3D. Allowing 3D motion is essential, since it is otherwise impossible to capture percolation and filtration type phenomena. This is because small particles move in the porous network formed by the larger particles.

ACKNOWLEDGEMENTS

First of all, I would like to thank my supervisors, Professor Martti Toivakka at the Laboratory of Paper Coating and Converting, Åbo Akademi University, and Dr. Tuomo Hjelt at VTT (formerly KCL). Your help, encouragement and motivating discussions during the process of this work have been absolutely immeasurable! Thanks are also due to the numerous partners in the KCLCONS project. Although it is not possible to mention all of you, I would especially like to accredit Mr. Heikki Pajari and Ms. Hanna Koskela for their roles as project coordinators. I also recognise Dr. Ulla Forsström, who served as research director and kept an eye on the bigger picture.

There are several people who in their own way contributed either directly to my work or to my professional development in general. A lot of work was put in by Mr. Jani Kniivilä to improve our visualisation tools. Ms. Liisa Sinervo prepared and analysed pigment tablets for comparison with my own results. On the initiative of Mr. Tom Granqvist (DT Paper Science), Dr. Tamal Ghosh (formerly at Ciba) and Dr. Kaj Backfolk (Stora Enso), I had the opportunity to join in on their pilot trial at the Coating Technology Center (CTC, Raisio) back in 2004. Professor Luciano Beghello did not hesitate to take money out of his own pocket so that I could visit Karlstad University. A huge load of thanks also goes to Dr. Parvez Alam for helping me with my English.

I would also like to thank some of the people, whose work nobody sees but still is totally indispensable. I give credit to our excellent librarians, with Ms. Anita Forss in the pole position. I always felt you were on my side, helping me find those tricky references and sometimes even century old books. I think it is fair to say that behind every successful researcher, there is a devoted librarian. Then again, there are neither books nor librarians nor research without

sound financial administration in the background. For this, I would especially like to thank Ms. Agneta Hermansson.

Taking on the challenge of embarking on a multiple-year research project can be intimidating to say the least. However, as I found out, researching and writing a D.Sc. thesis can actually be quite enjoyable. This is possible if you are surrounded by a lot of nice and helpful people such as the staff at my home laboratory. Last but not least, I wholeheartedly appreciate the tireless support my family has given me since day one. Thank you all!

REFERENCES

Ackler, H., French, R. and Chiang, Y.-M. (1996): Comparisons of Hamaker Constants for Ceramic Systems with Intervening Vacuum or Water: From Force Laws and Physical Properties, Journal of Colloid and Interface Science 179, 460.

Ala-Viikari, J. (2004): MDGraph 1.1 – Technical Documentation, Åbo Akademi University, Turku, Finland.

Ball, R. and Melrose, J. (1997): A Simulation Technique for Many Spheres in Quasi-Static Motion under Frame-Invariant Pair Drag and Brownian Forces, Physica A 247, 444.

Banchio, A. and Brady, J. (2003): Accelerated Stokesian Dynamics – Brownian Motion, Journal of Chemical Physics 118(22), 10323.

Barbesta, F., Bousfield, D. and Rigdahl, M. (2001): Modeling of Rheological Properties of Coating Colors, Journal of Rheology 45(1), 139.

Barnes, H., Edwards, M. and Woodcock, L. (1987): Applications of Computer Simulation to Dense Suspension Rheology, Chemical Engineering Science 42(4), 591.

Bertrand, F., Gange, T., Desaulniers, E., Vidal, D. and Hayes, R. (2004): Simulation of the Consolidation of Paper Coating Structures: Should One Use Probabilistic or Deterministic Models?, Computers & Chemical Engineering 28, 2595.

Bertrand, F., Leclaire, L.-A. and Levecque, G. (2005): DEM-Based Models for the Mixing of Granular Materials, Chemical Engineering Science 60, 2517.

Bilodeau, R. and Bousfield, D. (1998): Shear-Thinning Predictions from Particle Motion Modeling, Journal of Rheology 42(4), 743.

Bossis, G. and Brady, J. (1984): Dynamic Simulation of Sheared Suspensions I. General Method, Journal of Chemical Physics 80(10), 5141.

Bossis, G., Brady, J. and Mathis, C. (1988): Shear-Induced Structure in Colloidal Suspensions I. Numerical Simulation, Journal of Colloid and Interface Science 126(1), 1.

Bousfield, D. (1990): The Simulation of Pigment Motion during Blade Coating, TAPPI Coating Conference, May 13-16, Boston, MA, 325.

Brady, J. and Bossis, G. (1988): Stokesian Dynamics, Annual Review of Fluid Mechanics 20, 111.

Brady, J., Phillips, R., Lester, J. and Bossis, G. (1988): Dynamic Simulation of Hydrodynamically Interacting Suspensions, Journal of Fluid Mechanics 195, 257.

Brenner, H. (1961): The Slow Motion of a Sphere through a Viscous Fluid towards a Plane Surface, Chemical Engineering Science 16, 242.

Cardinal, C., Jung, Y., Ahn, K. and Francis, L. (2009): Predicting and Characterizing Microstructure Development During Drying of Particulate Coatings, European Coating Symposium, September 7-9, Karlsruhe, Germany, 252.

Cardinal, C., Jung, Y., Ahn, K. and Francis, L. (2010): Drying Regime Maps for Particulate Coatings, AIChE Journal (accepted).

Chang, C. and Powell, R. (1994): The Rheology of Bimodal Hard-Sphere Dispersions, Physics of Fluids 6(5), 1628.

Chinga, G. (2002): Structural Studies of LWC Paper Coating Layers using SEM and Image Analysis Techniques, Ph.D. thesis, Department of Chemical Engineering, Norwegian University of Science and Technology, Trondheim, Norway.

Claeys, I. and Brady, J. (1993): Suspensions of Prolate Spheroids in Stokes Flow, Part 1, Dynamics of a Finite Number of Particles in an Unbounded Fluid, Journal of Fluid Mechanics 251, 411.

Cundall, P. and Strack, O. (1979): A Discrete Numerical Model for Granular Assemblies, Geotechnique 29, 47.

Dabros, T. and van de Ven, T. (1992): Surface Collisions in a Viscous Fluid, Journal of Colloid and Interface Science 149(2), 493.

Darcy, H. (1856): Les fontaines publiques de la ville de Dijon, Dalamont.

Durlofsky, L., Brady, J. and Bossis, G. (1987): Dynamic Simulation of Hydrodynamically Interacting Particles, Journal of Fluid Mechanics 180, 21.

Durlofsky, L. and Brady, J. (1989): Dynamic Simulation of Bounded Suspensions of Hydrodynamically Interacting Particles, Journal of Fluid Mechanics 200, 39.

Einarson, M. and Berg, J. (1993): Electrosteric Stabilization of Colloid Latex Dispersions, Journal of Colloid and Interface Science 155(1), 165.

Eiroma, E. and Huuskonen, J. (1983): Pigment Coating of Paper and Board, in Paper Manufacture Vol. 1, edited by Arjas, A., Teknillisten tieteiden akatemia, Turku, Finland.

Eklund, D. and Salminen, P. (1986): Water Transport in the Blade Coating Process, TAPPI Journal 69(9), 116.

Eksi, G. and Bousfield, D. (1997): Modeling of Coating Structure Development, TAPPI Journal 80(2), 127.

Engström, G., Rigdahl, M., Kline, J. and Ahlroos, J. (1991): Binder Distribution and Mass Distribution on the Coating Layer – Cause and Consequence, TAPPI Coating Conference, May 19-22, Montreal, Quebec, 169.

Engström, G. (1986): Die Entwicklung des Feststoffgehaltes in der Strichschicht zwischen Auftrag und Blade, Wochenblatt für Papierfabrikation 114(66), 195.

Engström, G. (1994): Formation and Consolidation of a Coating Layer and the Effect on Offset-Print Mottle, TAPPI Journal 77(4), 160.

Eriksson, R., Merta, J. and Rosenholm, J. (2007): The calcite/water interface I. Surface charge in indifferent electrolyte media and the influence of low-molecular-weight polyelectrolyte, Journal of Colloid and Interface Science 313, 184.

Fellows, C. and Doherty W. (2006): Insights into Bridging Flocculation, Macromolecular Symposia 231(1), 1.

Foss, D. and Brady J. (2000): Structure, Diffusion and Rheology of Brownian Suspensions by Stokesian Dynamics Simulation, Journal of Fluid Mechanics 407, 167.

Cardinal, C., Jung, Y., Ahn, K. and Francis, L. (2009): Predicting and Characterizing Microstructure Development During Drying of Particulate Coatings, European Coating Symposium, September 7-9, Karlsruhe, Germany, 252.

Gacsi, Z., Kovacs, J. and Pieczonka, T. (2002): Characterisation of Particle Arrangement using the Radial Distribution Function, 3rd International Powder Metallurgy Conference, September 4-8, Ankara, Turkey.

Geller, A., Lee, S. and Leal, L. (1986): The Creeping Motion of a Spherical Particle Normal to a Deformable Interface, Journal of Fluid Mechanics 169, 27.

Goldman, A, Cox, R. and Brenner, H. (1967a): Slow Viscous Motion of a Sphere Parallel to a Plane Wall – I Motion through a Quiescent Fluid, Chemical Engineering Science 22(4), 637.

Goldman, A., Cox, R. and Brenner, H. (1967b): Slow Viscous Motion of a Sphere Parallel to a Plane Wall – II Couette Flow, Chemical Engineering Science 22(4), 653.

Grön, J. (1998): Coating Suspension Structure and Rheology, Ph. D. Thesis, Laboratory of Paper Chemistry, Åbo Akademi University, Turku, Finland.

Hase, K. and Bousfield, D. (1994): Kaolin Pigment – Latex Interactions During Coating, TAPPI Coating Conference, May 1-5, San Diego, CA, 49, TAPPI Press, Atlanta, GA.

Heikkilä, P. (1993): A Study on the Drying Process of Pigment Coated Paper Webs, Ph. D. Thesis, Process Design Laboratory, Åbo Akademi University, Turku, Finland.

Heikkilä, L., Tømmerås, A., Engels, T. and Knudsen, E. (2000): In "Pigment Coating and Surface Sizing of Paper. Papermaking Science and Technology 11", edited by Lehtinen, E., Fapet Oy, Helsinki, Finland, 289.

Heiser, E. and Cullen, D. (1965): Effects of Drying Rates on Adhesive Redistribution and Coated Paper Properties, Tappi 48(8), 80A.

Hiemenz, P. (1986): Principles of Colloid and Surface Chemistry, 2nd edition, M. Dekker, New York, USA.

Hiorns, T. and Nesbitt, T. (2003): Particle Packing of Blocky and Platey Pigments – A Comparison of Computer Simulations and Experimental Results, TAPPI Advanced Coating Fundamentals Symposium, May 8-10, Chicago, IL, 152.

Hogg, R., Healy, D. and Fuerstenau, D. (1966): Mutual Coagulation of Colloidal Dispersions, Transactions of the Faraday Society 62(6), 1638.

Hoogerbrugge, P. and Koelman, J. (1992): Simulating Microscopic Hydrodynamic Phenomena with Dissipative Particle Dynamics, Europhysics Letters 19(3), 155.

Hyväluoma, J., Raiskinmäki, P., Koponen, A., Kataja, M. and Timonen, J. (2005): Lattice-Boltzmann Simulation of Particle Suspensions in Shear Flow, Journal of Statistical Physics 121(1-2), 149.

Hämäläinen, M., Grön, J. and Nissinen, V. (2002): A New Coating Method for Surface Treatment of Woodcontaining Paper Grades, TAPPI Coating and Graphic Arts Conference, May 5-8, Orlando, FL.

Hämäläinen, M. (2003): The Importance of Spray Coating Technology, PTS Symposium, September 16-19, Baden-Baden, Germany, 301.

Jones, R. and Kutteh, R. (1999): Sedimentation of Colloidal Particles Near a Wall: Stokesian Dynamics Simulations, Physical Chemistry Chemical Physics 1(9), 2131.

Jones, R. (2001): Stability of Colloidal Clusters in Shear Flow Near a Wall: Stokesian Dynamics Simulation Studies, Journal of Chemical Physics 115(11), 5319.

Kilmartin, J. (1990): Overview of Calendering and Supercalendering, in "Pulp and Paper Manufacture, Vol. 8. Coating, Converting, and Specialty Processes", edited by Kouris, M., Joint Textbook Committee of the Paper Industry, TAPPI/CPPA, 196.

Kim, S. and Karrila, S. (1991): Microhydrodynamics – Principles and Selected Applications, Butterworth-Heinemann, Boston, MA, ISBN 0-7506-9173-5.

Kline, J. (1993): Fundamental Aspects of Latex Mobility in Paper Coatings, TAPPI Advanced Coating Fundamentals Symposium, April 30-May 1, Minneapolis, MN, 93.

Koelman, J. and Hoogerbrugge, P. (1993): Dynamic Simulations of Hard-Sphere Suspensions under Steady Shear, Europhysics Letters 21(3), 363.

Koliha, J. (1973): Convergent and Stable Operators and Their Generalization, Journal of Mathematical Analysis and Applications 43(3), 778.

Kulkarni, S. and Morris, J. (2009): Ordering Transition and Structural Evolution under Shear in Brownian Suspensions, Journal of Rheology 53(2), 417.

Ladd, A. and Verberg, R. (2001): Lattice-Boltzmann Simulations of Particle-Fluid Suspensions, Journal of Statistical Physics 104(5-6), 1191.

Laudone, G., Matthews, G. and Gane, P. (2006): Modelling the Shrinkage in Pigmented Coatings during Drying: A Stick-Slip Mechanism, Journal of Colloid and Interface Science 304, 180.

Lehtinen, E. (2000): In "Pigment Coating and Surface Sizing of Paper. Papermaking Science and Technology 11", edited by Lehtinen, E., Fapet Oy, Helsinki, Finland, 14.

Lepoutre, P. (1989): The Structure of Paper Coatings: An Update, Progress in Organic Coatings 17, 89.

Letzelter, P. and Eklund, D. (1993a): Coating Color Dewatering in Blade Coaters. Part 1. Mathematical Model and the Influence of Color Parameters, TAPPI Journal 76(5), 63.

Letzelter, P. and Eklund, D. (1993b): Coating Color Dewatering in Blade Coaters. Part 2. The Influence of Machine Configuration, TAPPI Journal 76(6), 93.

Linnonmaa, J. and Trefz, M. (2000): In "Pigment Coating and Surface Sizing of Paper. Papermaking Science and Technology 11", edited by Lehtinen, E., Fapet Oy, Helsinki, Finland, 415.

Lohmander, S., Martinez, M., Lason, L., Rigdahl, M. and Li, T.-Q. (2001): Dewatering of Coating Dispersions – Model Experiments and Analysis, Journal of Pulp and Paper Science 27(6), 183.

Lovalenti, P. and Brady, J. (1993a): The Hydrodynamic Force on a Rigid Particle Undergoing Arbitrary Time-Dependent Motion at Small Reynolds Number, Journal of Fluid Mechanics 256, 561.

Lovalenti, P. and Brady, J. (1993b): The Force on a Sphere in a Uniform Flow with Small-Amplitude Oscillations at Finite Reynolds Number, Journal of Fluid Mechanics 256, 607.

Luo, H., Cardinal, C., Scriven, L. and Francis, L. (2008): Ceramic Nanoparticle/Monodisperse Latex Coatings, Langmuir 24(10), 5552.

Lyklema, J. (2005a): In "Fundamentals of Interface and Colloid Science I: Fundamentals", edited by Lyklema, H., Elsevier Academic Press, Amsterdam, The Netherlands.

Lyklema, J. (2005b): In "Fundamentals of Interface and Colloid Science IV: Particulate Colloids", edited by Lyklema, H., Elsevier Academic Press, Amsterdam, The Netherlands.

Lyons, A., Iyer, R. and Bousfield, D. (2003): Particle Motion Modeling for Particle Size Distributions in Blade Geometries, TAPPI Advanced Coating Fundamentals Symposium, May 8-10, Chicago, IL, 44.

Lyons, A. and Iyer, R. (2004): Use of Particle Packing Modeling with Lognormal Particle Size Distributions to Develop a Strategy to Improve Blade Coating Runnability, TAPPI Coating and Graphic Arts Conference and Exhibit, May 16-19, Baltimore, MD, 438.

Ma, Y., Davis, H. and Scriven, L. (2004): Microstructure Development in Drying Latex Coatings, Progress in Organic Coatings 52(1), 46.

Madsen, L. (2002): In "Encyclopedia of Surface and Colloid Science, vol. 4, Surface Charge of Calcite", edited by Hubbard, A., Dekker.

Malinen, J. (1997): HUTI-HUT Iter Library User's Guide, Center for Scientific Computing, Espoo, Finland.

Martys, N. (2005): Study of a Dissipative Particle Dynamics based Approach for Modeling Suspensions, Journal of Rheology 49(2), 401.

Matsubayashi, H., Saito, Y., Takagishi, Y., Miyamoto, K. and Kataoka, Y. (1992): The Influence of Coating Structure on Paper Quality, TAPPI Coating Conference, May 17-20, Orlando, FL, 161.

Melrose, J. and Heyes, D. (1993): Simulations of Electrorheological and Particle Mixture Suspensions: Agglomerate and Layer Structures, Journal of Chemical Physics 98(7), 5873.

Melrose, J. and Ball, R. (2004): "Contact Networks" in Continuously Shear Thickening Colloids, Journal of Rheology 48(5), 961.

Mendez, B. and Morita, H. (2001): Curtain Coating – A Novel Coating Technique for High-Precision Coating, Wochenblatt für Papierfabrikation 129(22), 1492.

Meng, Q. and Higdon, J. (2008): Large Scale Dynamic Simulation of Plate-Like Particle Suspensions. Part I: Non-Brownian Simulation, Journal of Rheology 52(1), 1.

Meng, Q. and Higdon, J. (2008): Large Scale Dynamic Simulation of Plate-Like Particle Suspensions. Part II: Brownian Simulation, Journal of Rheology 52(1), 37.

Ming, Y., Takamura, K., Davis, H. and Scriven, L. (1995): Microstructure Development in Latex Coatings, TAPPI Journal 78(11), 151.

Ming, Y., Davis, H., Scriven, L., Takamura, K. and Vodnick, J. (1995): Latex Particle Behaviour in Paper Coatings Examined by Low Voltage Scanning Electron Microscopy, TAPPI Coating Conference, May 19-20, Dallas, Texas, 391.

Napper, D. (1983): Polymeric Stabilization of Colloidal Dispersions, Academic Press, London, England.

Navarkhele, V., Agrawal, R. and Kurtadikar, M. (1998): Dielectric Properties of Electrolytic Solutions, Pramana Journal of Physics 51 (3&4), 511.

Nopola, T. (2004): Simulation of Particle Motion in Concentrated Colloidal Suspensions, Licentiate thesis, Department of Mathematics, University of Turku, Turku, Finland.

Nowicki, S., Davis, H. and Scriven, L. (1991): Drying and Binder Migration in Coated Papers, Tappi Coating Conference, May 19-22, Montreal, QC, 337.

O´Brien, R. (1979): Weakly Stable Operators, Journal of Mathematical Analysis and Applications 70(1), 170.

Parpaillon, M., Engström, G., Pettersson, I., Fineman, I., Svanson, S., Dellenfalk, B. and Rigdahl, M. (1985): Mechanical Properties of Clay Coating Films Containing Styrene-Butadiene Copolymers, Journal of Applied Polymer Science 30, 581.

Prall, K., Shaler, S. and Lepoutre, P. (2000): Pigmented Latex Coatings: Microstructure and Viscoelastic Mechanical Properties, Nordic Pulp and Paper Research Journal 15(5), 564.

Phung, T., Brady, J. and Bossis, G. (1996): Stokesian Dynamics Simulation of Brownian Suspensions, Journal of Fluid Mechanics 313, 181.

Pianet, G., Bertrand, F., Vidal, D. and Mallet, B. (2008): Modeling the Compression of Particle Packings using the Discrete Element Method, TAPPI Advanced Coating Fundamentals Symposium, June 11-13, Montréal, Canada, 278.

Pöhler, T., Juvonen, K. and Sneck, A. (2006): Coating Layer Microstructure and Location of Binder – Results from SEM Analysis, TAPPI Advanced Coating Fundamentals Symposium, February 8-10, Turku, Finland, 89.

Raiskinmäki, P., Shakib-Manesh, A., Jäsberg, A., Koponen, A., Kataja, M. and Timonen, J. (2001): Simulations of Particulate Suspensions with the Lattice-Boltzmann Method, American Physical Society – Annual Meeting of the Division of Fluid Dynamics, November 18-20, San Diego, CA.

Rajala, P., Häkkinen, H. and Berg, C.-G. (2002): The Effect of Intense Air Drying on Material Distribution and Quality in Coated Papers, 13th International Drying Symposium, August 27-30, Beijing, China, 1800.

Rajala, P. (2004): The Influence of New Drying Methods on the Quality of Blade-Coated Offset Paper, Ph. D. Thesis, Helsinki University of Technology, Espoo, Finland.

Rosato, A., Prinz, F., Standburg, K. and Swendsen, R. (1986): Monte Carlo Simulation of Particulate Matter Segregation, Powder Technology 49, 59.

Routh, A. and Russel, W. (1999): A Process Model for Latex Film Formation: Limiting Regimes for Individual Driving Forces, Langmuir 15(22), 7762.

Routh, A. and Zimmerman, W. (2004): Distribution of Particles during Solvent Evaporation from Films, Chemical Engineering Science 59(14), 2961

Russ, J. (1995): The Image Processing Handbook, CRC Press, Boca Raton, FL.

Salminen, P., Roper, J., Pollock, M. and Chonde, Y. (1995): Determining the Dynamic Water Retention Contribution of Various Cobinders and Thickeners, TAPPI Coating Conference, May 19-20, Dallas, Texas, 277.

Salminen, P. and Toivakka, M. (2000): In "Pigment Coating and Surface Sizing of Paper. Papermaking Science and Technology 11", edited by Lehtinen, E., Fapet Oy, Helsinki, Finland, 677.

Sand, A., Toivakka, M. and Hjelt, T. (2006): Investigation of Filter Cake Stability using Numerical Simulation Technique, TAPPI Advanced Coating Fundamentals Symposium, February 8-10, Turku, Finland, 279.

Sand, A., Toivakka, M. and Hjelt, T. (2007): The Application of Modified Stokesian Dynamics to 3D Particle Motion Simulations of Pigment Coating Colours, International Conference on Computational Methods, April 4-6, Hiroshima, Japan, 97.

Sand, A., Toivakka, M. and Hjelt, T. (2008a): Coating Layer Consolidation and the Influence of Drying Strategy – A Numerical Study, Progress in Paper Physics Seminar, June 2-5, Espoo, Finland, 65.

Sand, A., Toivakka, M. and Hjelt, T. (2008b): Small Particle Migration Mechanisms in Consolidating Pigment Coating Layers, TAPPI AdvancedCoating Fundamentals Symposium, June 11-13, Montréal, Canada, 289.

Sand, A., Toivakka, M. and Hjelt, T. (2009a): Colloidal Interactions and Particle Clustering in Consolidating Pigment Coating Layers, Papermaking Research Symposium, June 1-4, Kuopio, Finland, 39.

Sand, A., Kniivilä, J., Toivakka, M., and Hjelt, T. (2009b): Microstructure Development in Consolidating Pigment Coatings Studied by Numerical Simulation, European Coating Symposium, September 7-9, Karlsruhe, Germany, 69.

Santos, N. and Velho, J. (2004): Coating Structure with Calcium Carbonate Pigments and its Influence on Paper and Print Gloss, Pulp and Paper Canada 105(9), 43.

Sierou, A. and Brady, J. (2001): Accelerated Stokesian Dynamics Simulations, Journal of Fluid Mechanics 448, 115.

Sierou, A. and Brady, J. (2002): Rheology and Microstructure in Concentrated Noncolloidal Suspensions, Journal of Rheology 46(5), 1031.

Shaw, D. (2003): Introduction to Colloid and Surface Chemistry, 4th edition, Butterworth-Heinemann, Oxford, USA.

Sheehan, J., Takamura, K., Davis, H. and Scriven, L. (1993): Microstructure Development in Particulate Coatings Examined With High-Resolution Cryogenic Scanning Electron Microscopy, TAPPI Journal 76(12), 93.

Stanislawska, A. and Lepoutre, P. (1995): Consolidation of Pigmented Coatings: Development of Porous Structure, TAPPI Coating Conference, May 19-20, Dallas, TX, 67.

Suzuki, A., Ho, N. and Higuchi, W. (1969): Prediction of the particle size distribution changes in emulsions and suspensions by digital computation, Journal of Colloid and Interface Science, 29(3), 552.

Tadros, T. (1987): Solid/ Liquid Dispersions, Academic Press, London, Great Britain.

Toivakka, M. (1991): Simulering av partikelrörelse i bestrykningsskiktet under torkning, M.Sc. thesis, Laboratory of Paper Chemistry, Åbo Akademi University, Turku, Finland.

Toivakka, M. (1997): Simulation of Particle Motion in Pigment Coating Colors, Ph.D. thesis, Laboratory of Paper Chemistry, Åbo Akademi University, Turku, Finland.

Toivakka, M. and Eklund, D. (1994): Particle Movements during the Coating Process, Nordic Pulp and Paper Research Journal 9(3), 143.

Toivakka, M. and Eklund, D. (1996): Prediction of Suspension Rheology through Particle Motion Simulation, TAPPI Journal 79(1), 211.

Toivakka, M., Eklund, D. and Bousfield, D. (1995): Prediction of Suspension Viscoelasticity through Particle Motion Modeling, Journal of Non-Newtonian Fluid Mechanics 56, 49.

Toivakka, M., Eklund, D., and Bousfield, D. (1991): Pigment Motion during Drying, AIChE Forest Products Symposium, November 17-22, Los Angeles, CA, 159.

Toivakka, M., Eklund, D. and Bousfield, D. (1992): Simulation of Pigment Coating During Drying, TAPPI Coating Conference, May 17-20, Orlando, FL, 403, TAPPI Press, Atlanta, GA.

Toivakka, M, Salminen, P., Chonde, Y. and Bousfield, D. (1997): Consolidation of Particulate Suspension – Model Study with Plastic Pigments, TAPPI Advanced Coating Fundamentals Symposium, May 9-10, Philadelphia, PA, TAPPI Press, Atlanta, GA, 89.

Timofeev, O., Pajari, H., Koskela, H., Paaso, J. and Kiiskinen, H. (2007): Drying of Coated Paper; Simulation and Pilot Experiments, PAPTAC 93rd Annual Meeting, February 5-9, Montreal, Canada, A221.

Usher, S., De Kretser, R. and Scales, P. (2001): Validation of a New Filtration Technique for Dewaterability Characterization, AIChE Journal 47(7), 1561.

Van de Ven, T. (1989): Colloidal Hydrodynamics, edited by Ottewill, R. and Rowell, R., Academic Press, London, Great Britain.

Vanni, M. and Baldi, G. (2002): Coagulation Efficiency of Colloidal Particles in Shear Flow, Advances in Colloid and Interface Science 97, 151.

Vattulainen, I., Ala-Nissilä, T. and Kankaala, K. (1994): Physical Tests for Random Numbers in Simulations, Physical Review Letters, 73(19), 2513.

Vidal, D., Zou, X. and Uesaka, T. (2003a): Modeling Coating Structure Development Using a Monte-Carlo Deposition Method. Part I Modeling Methodology, TAPPI Journal 2(4), 3.

Vidal, D., Zou, X. and Uesaka, T. (2003b): Modeling Coating Structure Development Using a Monte-Carlo Deposition Method. Part II Validation and Case Study, TAPPI Journal 2(5), 16.

Vidal, D. and Bertrand, F. (2006): Recent Progress and Challenges in the Numerical Modeling of Coating Structure Development, TAPPI Advanced Coating Fundamentals Symposium, February 8-10, Turku, Finland, 241.

Vincent, B., Luckham, P. and Waite, F. (1980): The Effect of Free Polymer on the Stability of Sterically Stabilized Dispersions, Journal of Colloid and Interface Science 73(2), 508.

Vincent, B., Edwards, J., Emmett, S. and Jones, A. (1986): Depletion Flocculation in Dispersions of Sterically Stabilized Particles ("Soft Spheres"), Colloids and Surfaces 18, 261.

Watanabe, J. and Lepoutre, P. (1982): A Mechanism for the Consolidation of the Structure of Clay-Latex Coatings, Journal of Applied Polymer Science 27(11), 4207.

Whalen-Shaw, M. (1993): Binder Migration In Paper and Paperboard Coatings, TAPPI Press, Atlanta, GA.

Williams, J. (1976): The Segregation of Particulate Materials. A Review. Powder Technology 15, 245.

Yin, X. and Koch, D. (2007): Hindered Settling Velocity and Microstructure in Suspensions of Solid Spheres with Moderate Reynolds Numbers, Physics of Fluids 19(9), 93302

Ziler, Z. and Bousfield, D. (1991): Disk-Shaped Particle Motion in Shear Fields, AIChE Forest Products Symposium, November 17-22, Los Angeles, CA, 169.

Ziler, Z. and Bousfield, D. (1992): The Motion of Disk-Shaped Pigments in Transient Shear Flows, TAPPI Coating Conference, May 17-20, Orlando, FL, 373.

SWEDISH SUMMARY

Pigmentbestrykning är den vanligaste metoden för vidareförädling av papper. Genom applicering av ett tunt skikt av finfördelat mineralpigment på papperet, kan dess utseende och tryckbarhet förbättras avsevärt.

Utvecklingen av bestrukna pappersprodukter för nya ändamål, samt den tilltagande populariteten för nya applikationsmetoder för bestrykningssmeten, har gjort det allt viktigare att noggrant kunna kontrollera bestrykningsskiktets egenskaper. De styrande mekanismerna för mikrostrukturens dynamiska tillkomst i pigmentskiktet under konsolideringsfasen är dock fortfarande inte väl undersökta. Detta hänger samman med processens komplexitet; en storleksskala från µm- till nm-nivå, tidsperioder på under en sekund, samt extrema processförhållanden såsom höga temperaturer och tryckpulser. De svårigheter som uppstår i samband med experimentella undersökningar kan till stor del övervinnas genom tillämpning av numeriska modeller samt genom studier baserade på datorsimulering. Dessa metoder kan som sådana, eller i kombination med experimentella resultat, avsevärt öka förståelsen av de mekanismer som styr mikrostrukturens formation och pigmentskiktets makroskopiska egenskaper.

Målsättningen med detta arbete var att klargöra vilka mikroskopiska strukturer som uppkommer i bestrykningsskiktet under konsolideringen. Inverkan av den våta pigmentstrukturen, processförhållanden samt pigmentsuspensionens egenskaper på konsolideringen och mikrostrukturen hos bestrykningsskiktet undersöktes. Detta arbete syftar till att öka förståelsen för konsolideringsmekanismer, liksom kopplingen mellan pigmentsuspensionens egenskaper, processförhållanden och slutproduktens egenskaper. Resultaten kan även ge vägledning i valet och doseringen av tilläggskomponenter till bestrykningssmeten för att man ska uppnå ett bestrykningsskikt med önskvärda strukturella egenskaper.

En matematisk modell, baserad på en modifierad version av Stokesian dynamics-simuleringsteknik, vidareutvecklades och tillämpades i ett antal studier relaterade till bestrykningsskiktets konsolidering. Modellen beskriver tredimensionella partikelrörelser i polydispersa system. En sådan beskrivning är nödvändig för att man skall kunna förstå perkolationsfenomen och partikelmigrering som uppstår under konsolideringen. Partikelinteraktionerna omfattade partikelsuspensionens hydrodynamiska beteende, kolloidala interaktioner, Born repulsion, samt en sterisk repulsionsmodell för adsorberat polymert material. Den Brownska rörelsen samt en modell för den fria ytan, det vill säga gränsytan mellan pigmentsuspensionen och luften, inkluderades för att möjliggöra undersökning av konsoliderings- och torkningsfenomen.

Uppkomsten av en filterkaka, ett område av lokalt förhöjd partikelkoncentration, vid gränsytan mellan pigmentsuspensionen och bassubstratet, är ett grundläggande fenomen vid bestrykning av absorberande material såsom papper. Filterkaksstabiliteten undersöktes i ett flertal olika partikelsystem, på vilka applicerades varierande absorptionshastigheter för bassubstratet samt ett antal olika systemtemperaturer. Filterkaksstabiliteten påverkades främst av absorptionshastigheten samt partikelstorleken. Temperaturen visade sig även ha inflytande på filterkakans struktur. Konsolideringen av polydispersa partikelsystem undersöktes vid olika påläggsmängder, samt för ett antal torkstrategier baserade på pilotförsök och teoretiska avvattningsmodeller. Resultaten visade att torkningsstrategin inverkar kraftigt på mikrostrukturens utveckling, samt på fördelningen av små partiklar i bestrykningsskiktet. En tydlig koppling mellan torkstrategi och partikelrörlighet under konsolidering kunde även noteras. Pigmentsuspensionens kolloidala egenskaper hade ett starkt inflytande på bestrykningsskiktets krympning samt den interna fördelningen av fast material, det vill säga dess koncentrationsprofil i z-riktning. Visualisering av partikelsystemens konsolidering i tiden, samt jämförelser mellan system av

olika egenskaper och utsatta för olika processförhållanden, var användbart för illustration av olika strukturbildningsmekanismer.

Resultaten bidrar till förståelsen av de fundamentala mekanismer som driver konsolideringen av bestrykningsskikt. Vidare beskriver resultaten samband mellan processförhållanden och bestrykningssmetens inneboende egenskaper, samt dessa faktorers inverkan på bestrykningsskiktets mikrostruktur.

ISBN 978-952-12-2412-6

UNIPRINT
Åbo 2010